ANALYSIS ON THE ROLE OF BATTERY STORAGE SOLUTIONS IN THE OPTIMAL DESIGN OF DECENTRALIZED ENERGY SYSTEM STRUCTURES

MASTER THESIS

by

Gonzalo Falagan

Supervisor: Nils Körber, M.Sc., Thomas Offergeld, M.Sc.

Day of delivery: 25 May 2020

ANÁLISIS DE LA FUNCIÓN DE SOLUCIONES DE ALMACENAMIENTO ELECTROQUÍMICO EN EL DISEÑO ÓPTIMO DE SISTEMAS DE ENERGÍA DESCENTRALIZADOS

Autor: Falagan de la Sierra, Gonzalo.
Director: Nils Körber.
Entidad Colaboradora: Institut für Hochspannungstechnik (IFHT), RWTH Aachen.

RESUMEN DEL PROYECTO

En el contexto de la transición energética el paradigma de uso y consumo de energía está cambiando. El objetivo es mejorar la eficiencia global a la vez que se incrementa el uso de fuentes renovables. En este sentido ya se han implementado cambios en la legislación en Europa, y se espera que los cambios se multipliquen a medida que se introducen más medidas políticas. Para mejorar la eficiencia y autosuficiencia energéticas, el uso de sistemas de almacenamiento electroquímico (baterías) es una opción disponible que ofrece una gran flexibilidad. Sin embargo debido a sus altos costes, la decisión de adoptar no es inmediata.

Para aclarar esta decisión de inversión se ha desarrollado en este trabajo un modelo matemático de un sistema de baterías y se ha implementado en una herramienta de optimización existente para edificios y distritos. La herramienta se encuentra en desarrollo en el Institut für Hochspannungstechnik de la RWTH Aachen, y permite la optimización multicriterio en cuanto a costes y emisiones, considerando un gran abanico de opciones para la mejora de eficiencia. La aplicación resulta en un diseño de instalación y un plan de operación óptimos de una combinación de recursos energéticos distribuidos, como generadores renovables, así como renovaciones a los edificios. Para lograr un modelo más realista del sistema, se ha desarrollado e implementado un modelo de la red eléctrica de distribución. Esto permite evaluar los resultados técnica y económicamente no solamente a nivel individual de cada edificio, sino también el impacto de baterías en la flexibilidad de la red.

Los resultados muestran que el coste de baterías es demasiado alto para ser adoptadas de manera económica para autoconsumo. Por otra parte se valida la aplicación de baterías para aliviar sobrecarga de líneas cuando se usan de manera global por parte de un operador de red. Los resultados sugieren que sistemas de almacenamiento centralizados para apoyar la red eléctrica son una alternativa económicamente razonable a los sistemas domésticos.

Palabras clave: Baterías, MILP, distribuido, optimización

INTRODUCCIÓN

Desde hace varias décadas el paradigma de uso de la energía en Alemania está cambiando. En este proceso, se ha identificado que el sector de la construcción tiene un gran potencial

de optimización; la energía que se consume en los edificios representa por sí sola el 27% del uso anual de energía en el país. Esto ha llevado a la definición de la "transición energética integrada", como marco para el análisis y la racionalización del uso de la energía en edificios. Como se indica en [DEU18], sus principales objetivos son: la reducción de la demanda de energía primaria mediante el cambio a tecnologías de mayor eficiencia; el aumento del uso de energía renovable en todos los sectores de la economía y la flexibilización de las redes eléctricas mediante el almacenamiento de energía. Ejemplos de ello son la renovación de las cubiertas de los edificios para reducir las pérdidas de calefacción y refrigeración; el paso a tecnologías de calefacción eficientes, como las bombas de calor; y la instalación de almacenamientos de energía térmica o de baterías.

En relación con estos objetivos, el papel potencial del almacenamiento de energía electroquímica (Sistemas de Almacenamiento de Baterías, o BSS) se hace evidente. Pueden desempeñar un papel directo para permitir que la generación descentralizada se utilice más eficazmente; al mismo tiempo, pueden dar flexibilidad a la red eléctrica en situaciones de gran demanda. Estos objetivos divergen y pueden considerarse en conflicto mutuo. Por lo tanto, se justifica un análisis de la contribución de los BSS individuales a los objetivos divergentes.

Se ha realizado un estudio en profundidad de la literatura existente. El objetivo general de los trabajos citados en esta sección es el diseño eficiente de las instalaciones de Recursos Energéticos Distribuidos (REE). En este sentido, el problema se modela como un conjunto de demandas que deben ser cubiertas (principalmente electricidad y calor, además de refrigeración) y un conjunto de fuentes de energía de entrada con las que se pueden cubrir las demandas. La solución óptima viene entonces por una forma de elegir las formas más baratas de cubrir las demandas, reducir las demandas, aumentar la eficiencia de la conversión de entrada a salida, o una combinación de ambas. Se trata, por tanto, de una aplicación específica del problema genérico de la "localización de instalaciones capacitadas", un problema clásico de la investigación operativa.

El enfoque del problema y su solución pueden adoptar muchas formas. El modelo más extendido es el del *energy hub* [GEI07]. Su principal ventaja es su simplicidad, ya que su modelización de las tecnologías instalables se compone de una conversión de energía con una cierta eficiencia, limitada por las restricciones propias de cada tecnología (por ejemplo, potencia mínima, tiempo de arranque, etc.). Las tecnologías estándar incluyen la cogeneración eléctrica-térmica, calderas, bombas de calor, energía fotovoltaica y calefacción térmica solar. En otros trabajos se han incluido diferentes opciones de inversión: turbinas eólicas [OMU13], demanda flexible (DR) y vehículos eléctricos (EV) [BRA15]; medidas de renovación [STA14], [FAL16]; almacenamiento de calor y frío [LI16]; y tecnología combinada de refrigeración, calor y electricidad [DI 16]. Además, existen modelos de optimización multiobjetivo, que logran un equilibrio entre el costo y las emisiones de CO2 [DI 16], [FAL16].

Una característica común entre los trabajos citados es i) la limitación en el número de opciones tecnológicas consideradas, y/o ii) la optimización a través de métodos heurísticos. Para analizar el impacto de la BSS en los sistemas de energía descentralizados, encontrando el dimensionamiento y la operación matemáticamente óptimos para cumplir con los objetivos establecidos, se ha ampliado un modelo DER de programación lineal

entera mixta (MILP) para entornos residenciales y se ha aplicado a un caso de estudio utilizando datos del mundo real. Las dos cuestiones a probar son:

I. ¿En qué medida las BSS afectan al autoconsumo, y cuál es su óptimo dimensionamiento?

II. ¿En qué medida las BSS pueden contribuir a la gestión de la congestión de una red?

METODOLOGÍA

El modelo de optimización global consiste en una formulación MILP que se descompone en dos elementos: un problema de planificación de la expansión multimodal con variables enteras (binarias), y un problema de operación de un año con variables continuas. Debido a la estructura *bloque-angular* de las matrices de restricción del problema combinado, se justifica la aplicación de una metodología de solución conocida como Descomposición de Bender [BEN62] [VAN69]. Esto mejora la eficiencia de los cálculos con respecto a los métodos más comunes de *branch and bound*.

El consumo de energía dentro de un hogar se modela por medio de *energy hubs*. Para cada edificio, se impone un balance energético en el que las entradas y salidas totales de energía deben ser iguales. Dentro de los límites del centro de energía, se pueden adoptar varias tecnologías de conversión de energía, que se caracterizan por su eficiencia, así como por restricciones operativas como la potencia máxima/mínima, los tiempos de funcionamiento obligatorios, etc. Los costos se expresan mediante funciones lineales, cuyos coeficientes se han extraído de un amplio estudio de mercado previo. Las curvas de demanda se generan a partir de datos reales de consumo y meteorológicos, teniendo en cuenta las variaciones estocásticas. El modelo de BSS incorporado se describe en la Figura 1.

Para evaluar el impacto de las restricciones de la red en la instalación óptima de los edificios individuales, así como la interacción entre la red y la BSS, se utilizó una linealización de las ecuaciones de flujo de la potencia por medio del flujo de potencia de CC. Esta metodología permite determinar una matriz de factores de distribución de la transferencia de energía (PTDF), calculada en base a la topología y las impedancias de la red. Esta matriz relaciona las entradas/salidas de energía en los nodos con la variación de los flujos de potencia a través de las líneas. Esto a su vez permite formular las restricciones de flujo de las líneas, que a su vez restringen los intercambios de energía en los nodos de la red. La formulación de las restricciones específicas se describe en la Figura 2.

Una vez que se han considerado las relaciones de la red, el problema deja de ser una solución iterada sobre los edificios individuales; en cambio, se define un sistema compuesto de múltiples edificios interconectados. Para aplicar la metodología de solución de BD, se modificó la rutina de código a fin de reestructurar el problema: desde una optimización de inversión y operación iterada sobre múltiples edificios independientes, a una optimización global del sistema en su conjunto. Esto implicó la reestructuración de nuevas matrices de restricciones para ajustarse a la estructura requerida por el método de solución.

BSS Dimensioning and Operation model

Variables

$\boldsymbol{P}$	$\boldsymbol{C}$	$\boldsymbol{x_1}^{\boldsymbol{el_{in}}}$	…	$\boldsymbol{x_t}^{\boldsymbol{el_{in}}}$	$\boldsymbol{x_1}^{\boldsymbol{el_{out}}}$	…	$\boldsymbol{x_t}^{\boldsymbol{el_{out}}}$	$\boldsymbol{x_1}^{\boldsymbol{C\_SOC}}$	…	$\boldsymbol{x_t}^{\boldsymbol{C\_SOC}}$

Constraints

Change in SOC

$$\boldsymbol{x_t^{C\_SOC}} = \boldsymbol{x_{t-1}^{C\_SOC}} + \frac{\boldsymbol{x_t^{el_{in}}} * \vartheta_{el} - \boldsymbol{x_t^{el_{out}}} / \vartheta_{el}}{\frac{T}{8760}} \quad \forall\, t \in T$$

SOC limits

$$\boldsymbol{C} * SOC_{min} \leq \boldsymbol{x_t}^{\boldsymbol{C\_SOC}} \leq \boldsymbol{C} * SOC_{max} \quad \forall t \in T$$

Power limits

$$-\boldsymbol{P} \leq \boldsymbol{x_t}^{\boldsymbol{el_{in}}} \quad \forall t \in T$$

$$\boldsymbol{x_t}^{\boldsymbol{el_{out}}} \leq \boldsymbol{P} \quad \forall t \in T$$

Power/Capacity relation

$$\boldsymbol{C} \leq D_{max} * \boldsymbol{P}$$

Figura 1. Modelo matemático de batería.

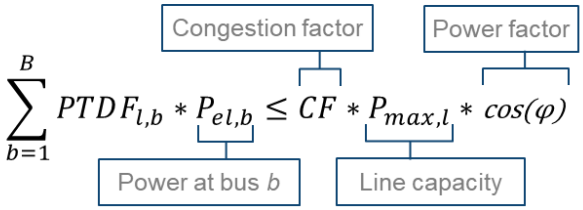

Figura 2. Modelo matemático de restricción de línea.

Para probar la validez de los métodos de modelado y solución, se creó un caso de prueba que empleaba datos de construcción del mundo real de un distrito residencial de Alemania. El caso de prueba incluía diferentes tipos de edificios residenciales, con diferentes comportamientos de demanda de energía y diferentes características físicas. En el caso de prueba se incluyó el cable de red características y topología también. El caso de prueba se seleccionó como representativo después de una serie de pruebas con casos de prueba de diferentes tamaños, logrando un equilibrio entre el tiempo de cálculo y la extrapolabilidad de los resultados. El caso de prueba se describe gráficamente en la Figura 3.

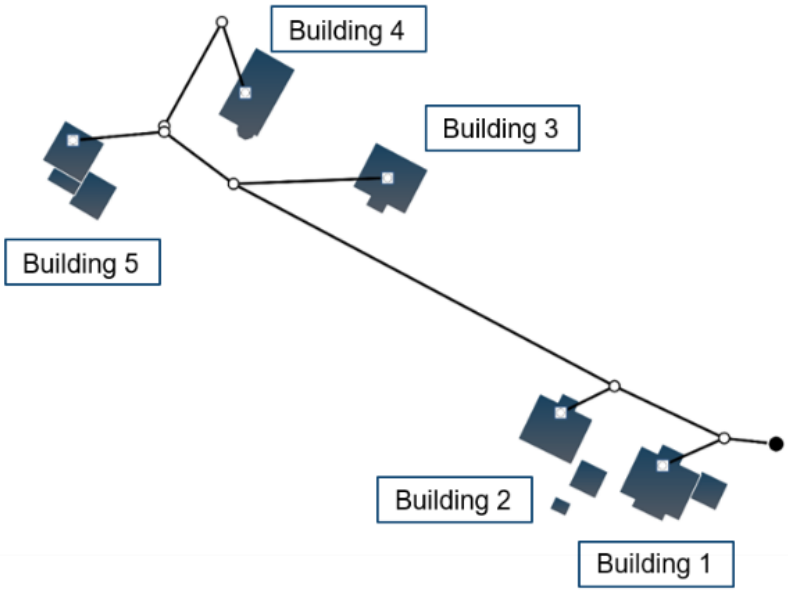

Figura 3. Representación gráfica del caso de prueba.

Las pruebas se realizaron de tres maneras. En primer lugar, se analizó el impacto de los BSS en edificios individuales sin la red, centrándose en la relación con las tecnologías de generación (principalmente fotovoltaicas) y realizando un análisis de sensibilidad de costes. En segundo lugar, se llevó a cabo un análisis de los edificios conectados, sin almacenamientos, para determinar el impacto de la red y el potencial de restricción real de sus límites de transporte de energía. Por último, se incluyeron tanto el BSS como el modelo de red, lo que obligó además a elaborar un escenario en el que se daría prioridad a las tecnologías de gran demanda eléctrica, como las bombas de calor. Este escenario se prevé realista en el corto plazo, a medida que aumenta la electrificación del transporte y de calefacción residencial.

RESULTADOS

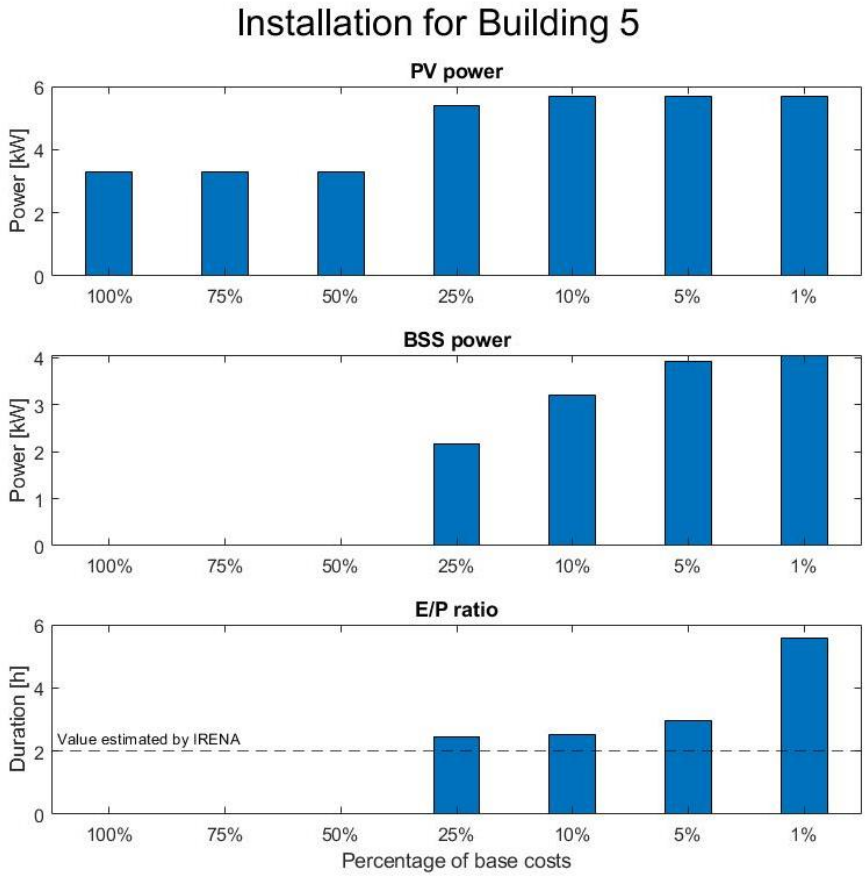

Figura 4. Potencia fotovoltaica instalada (arriba), potencia de BSS instalada (medio), relación energía potencia de BSSS (abajo)

Los resultados muestran modificaciones en el comportamiento de la inversión y la operación. Para la primera prueba, el análisis de sensibilidad de costos arrojó un costo umbral de adopción de alrededor del 25% de los costos originalmente considerados. Además, se demostró que las BSS permitían aprovechar más PV, aumentando el valor de ambas inversiones. Ambos efectos pueden verse como la potencia fotovoltaica instalada, la potencia del BSS y la relación energía/potencia del BSS representadas contra las reducciones en los costes del sistema BSS en la Figura 4.

La interpretación de estos resultados es la siguiente: en primer lugar, la mejora económica del BSS se produce al permitir cantidades más elevadas de generación fotovoltaica, más barata que la electricidad alimentada por la red. Ambas tecnologías aumentan de tamaño a medida que los costos del BSS disminuyen, hasta que la energía fotovoltaica alcanza el límite máximo de potencia instalable impuesto por la superficie disponible en el tejado. Por lo tanto, se valida la hipótesis de un mayor autoconsumo.

La segunda prueba arrojó un resultado previsible: sin la flexibilidad disponible de almacenamiento de energía, si la red es en algún momento incapaz de satisfacer toda la demanda, el problema se vuelve matemáticamente infactible.

La tercera prueba arrojó los resultados más matizados. El impacto de las limitaciones de la red es visible tanto en la inversión (colocación de la BSS, selección de la tecnología) como en el funcionamiento. Los resultados pueden resumirse en algunos puntos clave:

- Las BSS permiten flexibilidad de operación, aplanando los perfiles de flujo de potencia a través de las líneas de la red.
- Debido a las economías de escala, una optimización global tiende a almacenamientos centralizados. Las limitaciones de la red definen el grado de centralización del almacenamiento, antes de que se alcancen los límites de transferencia de energía, y también afectan a la ubicación del almacenamiento.
- Las restricciones de la red impulsan el cambio hacia tecnologías más eficientes, incluso si el costo de la inversión es mayor (por ejemplo, bomba de calor aire-aire a bomba de calor tierra-aire).
- El aumento de los costos derivados de la inversión y el funcionamiento restringidos de la red no se asigna proporcionalmente a todos los consumidores. Concretamente, algunos consumidores operan de manera individual más barata, pero menos eficiente desde el punto de vista energético, mientras que otros asumen el costo de optimizar el funcionamiento de la red, de modo que el costo neto sigue siendo mínimo.

CONCLUSIONES

El trabajo desarrollado amplió un modelo de optimización MILP para la inversión en recursos energéticos distribuidos, y lo utilizó para analizar la dinámica de costos de la instalación a nivel residencial de recursos de almacenamiento de baterías con respecto a la red. Se confirma la función de las BSS como facilitador de una mayor generación de renovables. Los resultados muestran que se logra un resultado óptimo a nivel global a través de una distribución desigual de los costos, y por lo tanto no está libre de discriminación. Además, la optimización del almacenamiento centralizado debe tenerse en cuenta al considerar la propiedad de los activos, posible a nivel de vecindario/comunidad, frente al almacenamiento a nivel de hogar. Cabe señalar que estos resultados son más pertinentes en un escenario con una alta electrificación del transporte y la calefacción, ambos previstos en el futuro próximo.

REFERENCIAS

[BRA15] Brahman, F.; Honarmand, M.; Jadid, S.: Optimal electrical and thermal energy management of a residential energy hub, integrating demand response and energy storage system. In Energy and Buildings, 2015, 90; S. 65–75.

[BEN62] Benders, J. F.: Partitioning procedures for solving mixed-variables programming problems. In Numerische Mathematik, 1962, 4; S. 238–252.

[DEU18] Deutsche Energie-Agentur: Energy efficiency in the building stock-statistics and analyses, 2018.

[DI 16] Di Somma, M. et al.: Multi-objective operation optimization of a Distributed Energy System for a large-scale utility customer. In Applied Thermal Engineering, 2016, 101; S. 752–761.

[FAL16] Falke, T. et al.: Multi-objective optimization and simulation model for the design of distributed energy systems. In Applied Energy, 2016, 184; S. 1508–1516.

[GEI07] Geidl, M. et al.: Energy Hubs for the Future. In IEEE Power & Energy Magazine, 2007.

[LI16] Li, L. et al.: Economic and environmental optimization for distributed energy resource systems coupled with district energy networks. In Energy, 2016, 109; S. 947–960.

[OMU13] Omu, A.; Choudhary, R.; Boies, A.: Distributed energy resource system optimisation using mixed integer linear programming. In Energy Policy, 2013, 61; S. 249–266.

[STA14] Stadler, M. et al.: Optimizing Distributed Energy Resources and Building Retrofits with the Strategic DER-CAModel. In Applied Energy, 2014, 132; S. 557–567.

[VAN69] van Slyke, R. M.; Wets, R.: L-Shaped Linear Programs with Applications to Optimal Control and Stochastic Programming. In SIAM Journal on Applied Mathematics, 1969, 17; S. 638–663.

ANALYSIS ON THE ROLE OF BATTERY STORAGE SOLUTONS IN THE OPTIMAL DESIGN OF DECENTRALIZED ENERGY SYSTEM STRUCTURES

Author: Falagan de la Sierra, Gonzalo.
Supervisor: Nils Körber.
Collaborating institution: Institut für Hochspannungstechnik, RWTH Aachen.

PROJECT SUMMARY

In the course of the energy transition the paradigm of energy usage is changing. The aim is to improve overall energy efficiency and to increase the share obtained from renewable sources. In this sense changes have already been implemented in legislation in Europe, and they will progressively increase as more measures are introduced into policy.

To achieve efficiency and self-sufficiency the use of Battery Storage Systems is an available option that offers a high degree of flexibility. However due to the high investment costs, the decision to adopt is not straightforward. In order to make such an investment decision transparent a mathematical model of BSS technology is developed and integrated in a larger energy optimization tool for buildings and neighborhoods in the present thesis. The tool, under development at the Institute for High Voltage Technology of RWTH Aachen, allows for multicriteria optimization in terms of costs and emissions, in consideration of a large portfolio of optional efficiency measures. The output is an optimal installation and operation of a combination of distributed energy resources, such as renewable energies, while also considering, building renovations.

To form a more accurate model of the system, an electric grid model is developed and implemented in the optimization tool. This additionally allows for a technical and economic analysis of BSS not only in behind-the-meter applications, but also as a tool for distribution grid level flexibility.

The results show that BSS systems are yet too expensive to be adopted, with the target of increasing self-sufficiency. Additionally they show that BSS can alleviate line overloading when owned and operated by the grid operator. The results suggest that central storage systems offer a sensible economic alternative to domestic storage systems for the purpose of relieving grid load.

Keywords: Battery, MILP, Decentralized, Optimization.

INTRODUCTION

For multiple decades the energy usage paradigm in Germany is changing. In this process, the building sector has been identified as having a large potential for optimization; energy consumed in buildings alone accounts for 27% of the annual energy usage in Germany. This has led to the definition of the “integrated energy transition”, as a framework for

analysis and rationalization of energy usage in buildings. As stated in [DEU18], its main goals are: the reduction of primary energy demand through a switch to higher efficiency technologies; the increase in use of renewable energy across all sectors of the economy and the provision of flexibility in electricity grids by means of energy storages. Examples of this are the renovation of building shells to reduce heating and cooling losses; the switch to efficient heating technologies such as heat pumps; and the installation of heat or battery energy storages.

In relation to these goals, the potential role of electrochemical energy storage (Battery Storage Systems, or BSS) becomes clear. They can play a direct role in enabling decentralized generation to be used more effectively; at the same time, they can provide flexibility to the electricity network in situations of high demand. These objectives diverge, and can be seen as standing in mutual conflict. Therefore an analysis on the contribution of unique BSS towards diverging goals is justified.

An in depth study of existing literature has been conducted. The overall objective of the works cited in this section is the efficient design of Distributed Energy Resource (DER) installations. In this sense the problem is modelled as a set of demands that need to be covered (mainly electricity and heat, additionally cooling) and a set of input energy sources with which the demands can be covered. The optimal solution then comes by a way of choosing the cheapest ways to cover the demands, reducing the demands, increasing the efficiency of input to output conversion, or a combination thereof. It is therefore a specific application of the generic "capacitated facility location" problem, a classic problem in operations research.

The approach to the problem and its solution can take many forms. With regards to the modelling of the buildings themselves, they are modelled as multi-energy systems. the most widespread model is the energy hub [GEI07]. Its main advantage is its simplicity, for its modelling of installable technologies is composed of an energy conversion with a certain efficiency, limited by restrictions specific to each technology (e.g. minimum power, maximum run time etc.). Standard technologies include CHP, boilers, heat pumps, PV and solar thermal generation. Subsequent works have included different investment options: wind turbines [OMU13], demand response (DR) and electric vehicles (EVs) [BRA15]; renovation measures [STA14], [FAL16]; heat and cold storage [LI16]; and Combined Cooling, Heat and Power technology [DI 16]. Additionally, multi-objective optimization models exist, that strike a balance between cost and CO2 emissions [DI 16], [FAL16].

A common feature among the cited works is either i) limitation in the number of technology options considered, and/or ii) optimization through heuristic methods. To analyze the impact of BSS in decentralized energy systems, finding the mathematically optimal dimensioning and operation to fulfill the goals stated, a mixed-integer linear programming (MILP) DER model for residential environments has been expanded and applied to a study case using real world data. The two hypotheses to be tested are:

I. To what extent do BSS affect self-consumption, and what is their optimal dimensioning.
II. To what extent can BSS contribute to congestion management of a network?

METHODOLOGY

The global optimization model consists of an MILP formulation which is decomposed into two stages: a multimodal expansion planning problem with integer (binary) variables, and a one-year operation problem with continuous variables. Due to the block-angular structure of the constraint matrices of the combined problem, the application of a solution methodology known as Bender's Decomposition [BEN62] [VAN69] is warranted. This improves computational efficiency with respect to more common branch-and-bound methods.

The energy consumption within each household is modelled by means of an energy hub. For each building, an energy balance is enforced in which the total energy inputs and outputs must be equal. Within the bounds of the energy hub, a number of energy conversion technologies can be adopted, which are characterized by an efficiency, as well as operational restrictions such as maximum/minimum power, obligatory run times, etc. The costs are expressed by means of linear functions, the coefficients of which have been previously extracted from an extensive market study. Demand curves are generated from real-world consumer and weather data, accounting for stochastic variations.

The incorporated BSS model is described in Illustration 1.

BSS Dimensioning and Operation model

Variables

$\boldsymbol{P}$	$\boldsymbol{C}$	$\boldsymbol{x_1}^{\boldsymbol{el_{in}}}$	…	$\boldsymbol{x_t}^{\boldsymbol{el_{in}}}$	$\boldsymbol{x_1}^{\boldsymbol{el_{out}}}$	…	$\boldsymbol{x_t}^{\boldsymbol{el_{out}}}$	$\boldsymbol{x_1}^{\boldsymbol{C\_SOC}}$	…	$\boldsymbol{x_t}^{\boldsymbol{C\_SOC}}$

Constraints

Change in SOC

$$\boldsymbol{x_t^{C\_SOC}} = \boldsymbol{x_{t-1}^{C\_SOC}} + \frac{\boldsymbol{x_t^{el_{in}}} * \vartheta_{el} - \boldsymbol{x_t^{el_{out}}} / \vartheta_{el}}{\frac{T}{8760}} \quad \forall\, t \in T$$

SOC limits

$$\boldsymbol{C} * SOC_{min} \leq \boldsymbol{x_t}^{\boldsymbol{C\_SOC}} \leq \boldsymbol{C} * SOC_{max} \quad \forall t \in T$$

Power limits

$$-\boldsymbol{P} \leq \boldsymbol{x_t}^{\boldsymbol{el_{in}}} \ \forall t \in T$$

$$\boldsymbol{x_t}^{\boldsymbol{el_{out}}} \leq \boldsymbol{P} \quad \forall t \in T$$

Power/Capacity relation

$$\boldsymbol{C} \leq D_{max} * \boldsymbol{P}$$

Illustration 1. Mathematical model of battery storage system.

To assess the impact of network restrictions on the optimal installation of individual buildings, as well as the interplay between network and BSS, a linearization of the power flow equations by means of DC power flow was utilized. This methodology allows the determination of a Power Transfer Distribution Factor matrix, calculated by means of the

network topology and impedances. This matrix relates the energy inputs/outputs at nodes with the variation in power flows through lines. This allows for line flow constraints to be formulated, which in turn restrict power exchanges at the nodes of the network. The specific constraint formulation is described in Illustration 2.

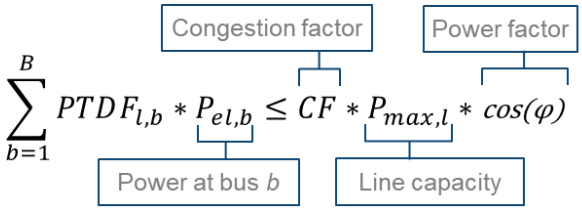

Illustration 2. Model of network constraints.

Once the network relations have been considered, the problem ceases to be solvable iteration over the individual buildings; instead, a system composed of multiple buildings is defined. To apply the BD solution methodology, the coded routine was modified in order to restructure the problem: from an investment and operation optimization iterated over multiple independent buildings, to a global optimization of the system as a whole. This involved restructuring constraint matrices in order to fit the structure required for the solution method.

To test the validity of the modelling and solution methods, a test case employing real-world building data from a residential district in Germany was created. The test case included different types of residential buildings, with different energy demand behaviors and different physical characteristics. Included in the test case were the network cable characteristics and topology as well. The test case was selected as representative after a series of tentative runs with test cases of different sizes, striking a balance between computation time and result extrapolability. The test case is described graphically in Illustration 3.

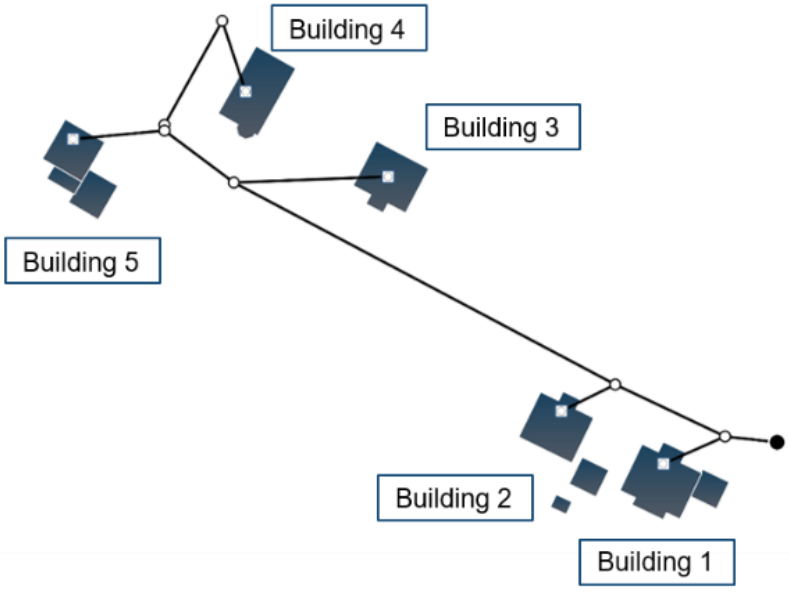

Illustration 3. Test case buildings and network.

The tests were performed in three ways. Firstly, the impact of BSS on individual buildings without the network was analyzed, focusing on the relation with generation technologies (primarily PV) and performing a cost sensitivity analysis. Secondly, an analysis of the connected buildings, without storages, was conducted, to determine the impact of the network and the real restriction potential of its power carrying limits. Finally, both BSS and grid model were included, additionally forcing a scenario that would prioritize electrically-demanding technologies, such as heat pumps.

RESULTS

The results show modifications in both investment and operation behaviors. For the first test, the cost sensitivity analysis yielded an adoption threshold cost of around 25% of originally considered costs. Also, the BSS were shown to enable more PV to be harnessed,

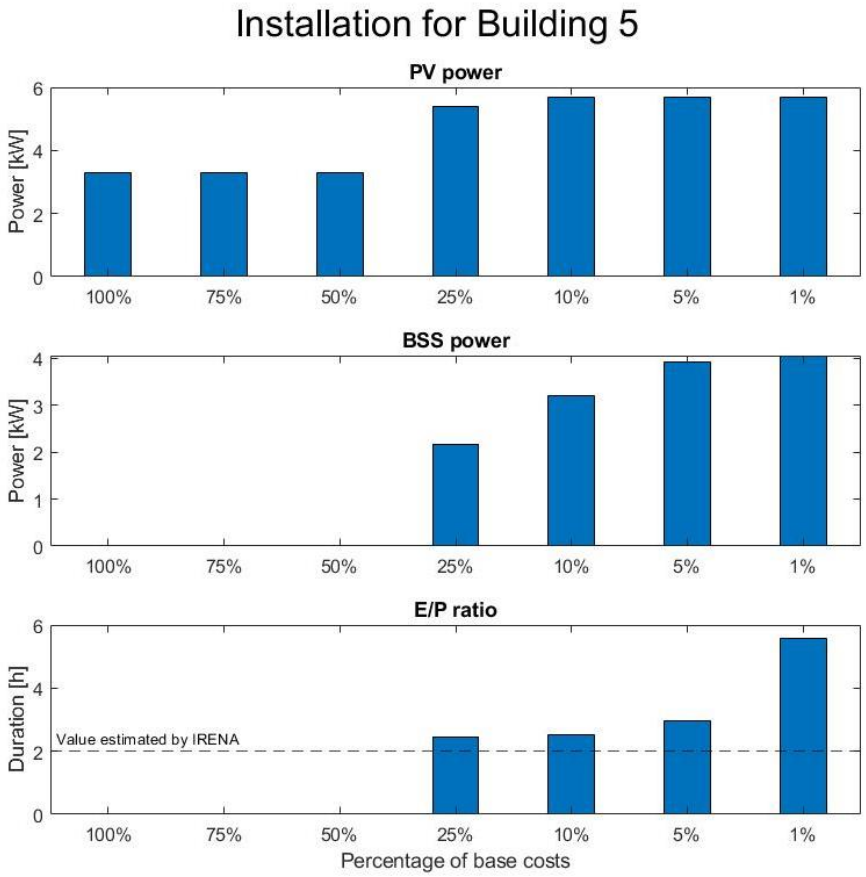

Illustration 4. Installed PV power (top) , BSS power (middle) and BSS energy/power ratio (bottom).

increasing the value of both investments. Both of these effects can be seen as installed PV power, BSS power and BSS Energy/Power ratio plotted against the reductions in BSS system costs in Illustration 4.

The interpretation of these results is as follows: first, the economic improvement of the BSS comes by way of allowing higher amounts of PV generation, cheaper than grid-fed

electricity. Both technologies increase in size as BSS costs decline, until PV reaches the maximum installable power limit imposed by the available roof area. The hypothesis of increased self-consumption is therefore validated.
The second test yielded a foreseeable result: without the available flexibility of energy storage, if the network is at some point incapable of supplying all demand, the problem becomes infeasible.
The third test yielded the more nuanced results. The impact of network constraints is visible in both investment (BSS placement, technology selection) as well as operation. The results can be summarized in some key points:

- BSS allow for flexibility of operation, flattening the power flow profiles through the network lines.
- Due to economies of scale, a global optimization tends towards centralized storages. Network constraints define how centralized the storage can be, before power transfer limits are reached, as well as affecting the placement of the storage.
- Network restrictions prompt the switch towards more efficient technologies, even if the investment cost is higher (e.g. air to air heat pump to ground to air heat pump).
- The increase in costs derived from the network-restricted investment and operation is not allocated proportionally to all consumers. Specifically, some consumers operate in an individually cheaper, but less energy-efficient manner, while others bear the cost of optimizing the network operation, so that the net cost is still minimized.

CONCLUSIONS

The developed work expanded an MILP optimization model for investment in distributed energy resources, and used it to analyze the cost dynamics of home-installation of battery storage resources with respect to the grid. The role of BSS as enabler of higher renewable generation is confirmed. The results show that a globally-optimal result is achieved through uneven distribution of costs, and is therefore not free of discrimination. Additionally, the optimality of centralized storage should be taken into account when considering asset ownership, possible at a neighborhood/community level, versus household-level storage. It is worth noting that these results bear more relevance in a scenario with high electrification of transport and heating, both of which are expected in the near future.

REFERENCES

[BRA15] Brahman, F.; Honarmand, M.; Jadid, S.: Optimal electrical and thermal energy management of a residential energy hub, integrating demand response and energy storage system. In Energy and Buildings, 2015, 90; S. 65–75.

[BEN62] Benders, J. F.: Partitioning procedures for solving mixed-variables programming problems. In Numerische Mathematik, 1962, 4; S. 238–252.

[DEU18] Deutsche Energie-Agentur: Energy efficiency in the building stock-statistics and analyses, 2018.

[DI 16] Di Somma, M. et al.: Multi-objective operation optimization of a Distributed Energy System for a large-scale utility customer. In Applied Thermal Engineering, 2016, 101; S. 752–761.

[FAL16] Falke, T. et al.: Multi-objective optimization and simulation model for the design of distributed energy systems. In Applied Energy, 2016, 184; S. 1508–1516.

[GEI07] Geidl, M. et al.: Energy Hubs for the Future. In IEEE Power & Energy Magazine, 2007.

[LI16] Li, L. et al.: Economic and environmental optimization for distributed energy resource systems coupled with district energy networks. In Energy, 2016, 109; S. 947–960.

[OMU13] Omu, A.; Choudhary, R.; Boies, A.: Distributed energy resource system optimisation using mixed integer linear programming. In Energy Policy, 2013, 61; S. 249–266.

[STA14] Stadler, M. et al.: Optimizing Distributed Energy Resources and Building Retrofits with the Strategic DER-CAModel. In Applied Energy, 2014, 132; S. 557–567.

[VAN69] van Slyke, R. M.; Wets, R.: L-Shaped Linear Programs with Applications to Optimal Control and Stochastic Programming. In SIAM Journal on Applied Mathematics, 1969, 17; S. 638–663.

Abstract

In the course of the energy transition the paradigm of energy usage is changing. The aim is to improve overall energy efficiency and to increase the share obtained from renewable sources. In this sense changes have already been implemented in legislation in Europe, and they will progressively increase as more measures are introduced into policy.

As the building sector alone accounts for 27% of total energy consumption, measures taken in this realm are expected to be one of the main sources of improvements in efficiency. Major leverage factors are the high potential for the rationalization of end energy usage and the utilization of local renewable energy sources.

To achieve energy- and self-sufficiency the use of Battery Storage Systems is an available option that offers a high degree of flexibility. However due to the high investment costs, the decision to adopt is not straight forward. In order to make such an investment decision transparent a mathematical model of BSS technology is developed and integrated in a larger energy optimization tool for buildings and neighborhoods in the present thesis. The tool, currently under development at the Institute for High Voltage Technology of RWTH Aachen, allows for multicriteria optimization in terms of costs and emissions, in consideration of a large portfolio of optional efficiency measures. The output is an optimal installation and operation of a combination of distributed energy resources, such as renewable energies, while also considering, building renovations.

To achieve a more accurate model of the system, an electric grid capacity model is developed and implemented in the optimization tool. This additionally allows for a technical and economic analysis of BSS not only in behind-the-meter applications, but also as a tool for distribution grid level flexibility.

The results show that BSS systems are yet too expensive to be adopted, with the target of increasing self-sufficiency. Additionally they show that BSS can alleviate line overloading when owned and operated by the grid operator. The results suggest that central storage systems offer a sensible economic alternative to domestic storage systems for the purpose of relieving grid load

Table of Contents

Page

Table of Figures

page

List of Tables

page

1 Introduction

1.1 Motivation

The impact of human activity on our natural environment is ever more present in the minds of European citizens and legislators. This has led to policies searching for minimization of carbon emissions being implemented on both European [BÖH09] and national level [BUN17], [IDA11]. A new paradigm in energy usage aims, among other things, at a more efficient use of energy, less dependency on non-renewable sources (fossil fuels and nuclear).

The path to the new energy usage paradigm has been called “energy transition” (*Energiewende* in Germany). A specific approach has been proposed by the German Energy Agency (DENA), called “Integrated energy transition”. It includes transformation of three of the most energy-intensive sectors of the economy: electricity, heating and transport. As stated in [DEU18], the main goals are: the reduction of primary energy demand through a switch to higher efficiency technologies; the increase in use of renewable energy across all sectors of the economy and the provision of flexibility in electricity grids by means of energy storages.

Within this framework, the building sector is recognized as a major area of leverage for the transition, as it represents 27% of the primary energy consumed yearly in Germany. Within the measures considered for buildings are insulation improvements, switch to more efficient and/or carbon neutral heating technologies and installation of distributed energy resources for self-consumption.

Approximately three quarters of the energy consumed in buildings in Germany is dedicated to space heating. Therefore improvements in this matter are expected to have a substantial impact on the overall consumption. However this change is not without its drawbacks: the cost of refurbishing old buildings is substantial, as is the cost of installing new heating technologies. Therefore the change must be done accounting for the measures that have the most impact at the least cost.

The same logic applies to the change towards renewable electrical generation. In a general sense, these technologies could be understood as replacements for the large-scale, centralized generation plants that exist today. This is in part true, as large installations of these technologies have been/are currently being deployed in certain parts of the world

[GJE05], [HAR11]. However, they require certain location-specific characteristics to offset the high investment costs associated. In the case of PV or wind for example this translates as enough hours of wind/sunlight per year to make the installation profitable. Furthermore, centralized generation requires power generated to travel large distances to the end customer, incurring in corresponding losses at all steps of the network (transmission and distribution lines, voltage transformation, etc.).

At the same time, small scale installations of these technologies are also growing at a fast pace [WIR19], driven by the concerns about emissions, as well as the search of consumers for increased freedom and flexibility. This has generated a feedback loop, by which a growing market attracts more buyers, driving technology development and reduction of prices. As can be expected, the change from old fuel burning heating technologies to new electrical heating technologies naturally involves a greater electricity demand from the buildings. The installation of distributed electrical generation can at times cause buildings to become net exporters, and inject power into the electrical grid. These two circumstances can potentially cause stress to the grid, and the optimal energy supply solution should take this into account.

The potential for feed-in on the side of the consumers stems from their desire to optimize their cost of energy supply. As the installation of DERs requires substantial investment costs, the consumer is willing to sell surplus generation as an additional income stream. This situation is bound to happen in the presence for example, of high solar irradiation. In these situations, large amounts of DER generation could lead to potential feed-in congestion problems.

The utility of energy storages in these situations is then cut out: energy storages can, on the one hand, serve for time arbitrage for the individual consumers, allowing them to make use of self-generated power generated at times of low demand. On the other hand, it allows for potentially large feed-in flows to be distributed as well to hours with conditions less demanding for the grid, avoiding potentially problematic situations for the grid operator. However, these two objectives (consumer cost optimization and optimal grid operation) can be seen as conflicting, as they require access to the same, limited resource: the storage capacity.

As is the case with generation options, there are several energy storage technologies available for installation by the consumers. These include hydrogen generation/storage (Power-to-Gas P2G) and electrochemical storages such as vanadium-redox, lead-acid

and lithium-ion batteries. Of these, the one that has experienced faster development and reduction in costs has been lithium-ion [GOL19]. Furthermore, this family of technologies displays high efficiencies and relatively long lifetimes. It is therefore seen in this thesis as a main option for small-scale energy storage.

To tackle the overall economic problem, it is useful to make use of mathematical optimization models to aid the investment decision making process.

1.2 Goals and Structure of the Thesis

The goal of this thesis is to analyze the impact of Battery Storage Systems (BSS) on the optimal energy investments of consumers. This includes the aspect of operation, for which a model of the distribution grid is to be developed. The main objective is therefore to analyze the optimal deployment and use of BSS at a neighborhood level, accounting for the operational limits imposed by the grid.

The theoretical basics needed to understand the implemented methodology are presented in chapter 2. This includes aspects of battery storage systems and grid power flows, as well as a detailed description of optimization methods and the particular algorithm employed in this work.

The methodology involves an existing model for distributed energy resource optimization, detailed in section 3, which is expanded to include both electrical storages and grid connections. Once the operating conditions have been implemented, the model is validated using a simplified study case. After validation, the model is tested using modified scenarios within the study case. The results generated are presented in chapter 4.

The analysis of results and derived conclusions are presented in chapter 5. This chapter incorporates a discussion on the validity of the model, as well as the implications of the results. Finally, in the same chapter, an outlook of future steps is introduced.

2 Theoretical Basics

In this chapter, the theoretical basics of the thesis are presented and explained. Firstly, the concept of Distributed Energy System (DES) is presented. The optimization problem it entails is discussed, drawing on previous research work to illustrate possible methodologies and perspectives. Secondly the specifics of Battery Storage Systems (BSSs) are described, from a general perspective as well as mathematical modelling. Then the modelling of grid operation is explored. Finally the last section describes the basics of convex optimization, linear programming and specifically of Mixed Integer Linear Programming (MILP), together with an extensive explanation of Benders' Decomposition (BD).

2.1 Distributed Energy Systems

In the wake of the energy transition, Distributed Energy Resources (DER) such as Combined Heat and Power units, Photovoltaic (PV) installations and Biomass heating gain in importance. As their system permeation is projected to accelerate in the coming years [DAV15], the topic of distributed energy system optimization has been the subject of several studies in the past decade. The approaches, scale and results vary substantially between publications, so it is warranted to establish a comparison between different existing methodologies in order to establish a state-of-the-art for the current thesis.

The overall objective of the works cited in this section is the efficient design of DER installations. In this sense the problem is modelled as a set of demands that need to be covered (mainly electricity and heat, additionally cooling) and a set of input energy sources with which the demands can be covered. The optimal solution then comes by a way of choosing the cheapest ways to cover the demands, reducing the demands, increasing the efficiency of input to output conversion, or a combination thereof. It is therefore a specific application of the generic "capacitated facility location" problem, a classic problem in operations research. Additionally, multi-objective optimization models exist, that strike a balance between cost and CO_2 emissions [DI 16], [FAL16].

The approach to the problem and its solution can take many forms. With regards to the modelling of the buildings themselves, they are modelled as *multi-energy systems*. the most widespread model is the *energy hub* [GEI07], explained more in detail in Section 3.1.1. Its main advantage is its simplicity, for its modelling of installable technologies is

composed of an energy conversion with a certain efficiency, limited by restrictions specific to each technology (e.g. minimum power, maximum run time etc.). Standard technologies include CHP, boilers, heat pumps, PV and solar thermal generation. Subsequent works have included different investment options: wind turbines [OMU13], demand response (DR) and electric vehicles (EVs) [BRA15]; renovation measures [STA14], [FAL16]; heat and cold storage [LI16]; and Combined Cooling, Heat and Power technology [DI 16]. The subject of energy storages, and particularly BSS is analyzed in section 2.1.1.

Variables to be optimized include design and operation, and the approaches vary widely between studies. Design, also known as *expansion planning*, can take the form of *greenfield* or *brownfield* expansion, depending on its incorporation of previously existing infrastructure (brownfield) [ZHA15] or not (greenfield).

Operation optimization refers to the dispatch decisions of a certain generation/conversion technology throughout a time frame. It takes different time horizons and resolutions, as well as different ratios of real world/approximated data. A common approach is to choose typical days for each season, with characteristic demands, and replicated them throughout the year, using different hourly resolutions [MOG16], [MEH13], [HAI13]. When available, real world data specific to a test case are used. If not, standard load profiles can be used. Alternatively, synthetic profiles generated through probabilistic methods are also an option. Environmental data, such as solar irradiation and temperature are used to calculate solar generation and heat demand time series. [FAL16]. The scale at which the energy hub concept is applied is also a point to consider. Many of the cited works apply the model to single buildings, be it residential or industrial/commercial ones. This implies that for clusters of buildings or districts, certain energy inputs are supplied via grids. The most recurrent are electricity grid, gas network an district heating networks, while occasionally the existence of district cooling networks is also considered. While some studies restrict the installation/operation of technologies based on existing grid structures [MOR16], others specifically address the network design problem within the optimization [MEH12], [FAL16], [ZHA15] (as an integrated generation, demand and network optimization). The modelling of grid operation is explained more in detail in section 2.1.2.

One way to expand the consumers' maneuverability within the grid limitations is the use of EST for a more flexible operation. The possibility of including EST in the optimization

is contemplated widely. Technologies such as heat and cold storage are a common element in DER installations [HAI13] [LI16] [MOR16]. BSS are less common, but have been considered in some studies [STA14] [FAL16].Since BSS directly connect with the electricity grid, they are of special importance in the work of this thesis.

2.1.1 Battery Storage System

The subject of BSS installation on a consumer level is still widely debated. Even though the profitability of home BSSs need more real-world experience to be consistently proven, it is considered a potential investment option for consumers by many of the cited studies, especially when installed together with PV generation [SCH18], [CUC16]. The objective of the BSS is to reduce dependency on the grid, take advantage of time-variable tariffs and maximize the use of in-house generation, such as PV or CHP units..

EST introduce an important aspect in the operation of an energy hub. They allow for time flexibility in the overall operation of an energy hub, which is a major advantage when dealing with time-varying resources such as PV or wind generation. The introduction of EST adds *time-coupling constraints*; essentially, decisions that were previously independent from one time step to the next now must be considered simultaneously, as the option exists to store excess energy from one period and use it in a later one. While this increased flexibility is positive from the point of view of the results, the problem becomes substantially harder to solve.

The specific technologies clustered under the term BSS are electrochemical energy storages. This includes Nickel metal hydride (NMH), Lead-acid and the dominant family of Lithium-ion technologies. Due to recent, vast improvements in performance and cost reduction, Li-ion technologies are considered the status-quo in the field of stationary BSSs, and though most of the operation and modelling aspects apply to all electrochemical batteries, this section focuses on said Li-ion technologies.

The main concern about the use of BSSs in energy applications is the problem of ageing. While technically all systems experience lifetime reduction due to operation decisions (e.g. friction induced degradation in mechanical systems, temperature induced degradation of insulation in electrical systems), this is especially notable in BSSs. Because of their internal characteristics, variables such as charge/discharge power, depth of discharge (DOD), state of charge (SOC) and especially cycling can induce rapid degradation of a BSSs [MUE15], effectively shortening its lifetime and potentially rendering a

possibly profitable investment unprofitable. Therefore the investment lifetime is directly influenced by the operation decisions.

The ageing processes of Li-ion batteries are extremely complex and not yet fully understood. However elaborate models have been established based on theoretical and empirical data to understand and predict the impact of different stress factors [XU18a]. These can be broken up into *environmental factors* and *operation factors*. Environmental factors include temperature [MIL10] and calendrical ageing (time induced degradation). While the latter is inevitable, the former is of relatively low importance, due to most large BSSs being installed in places with a stable temperature and/or incorporating temperature control systems.

The operation factors present a complicating circumstance, namely that their effect is likely not independent. This means that the impact of a given discharge/charge power decision can be increased by, for example, the SOC at the given moment. This leads to highly non-linear, possibly non-convex functions, which are not well suited to optimization algorithms.

The optimization of BSSs in grid connected schemes has been studied extensively during recent years. Figure 2-1 shows a classification of BSS ageing models based on their approach [MAH18].

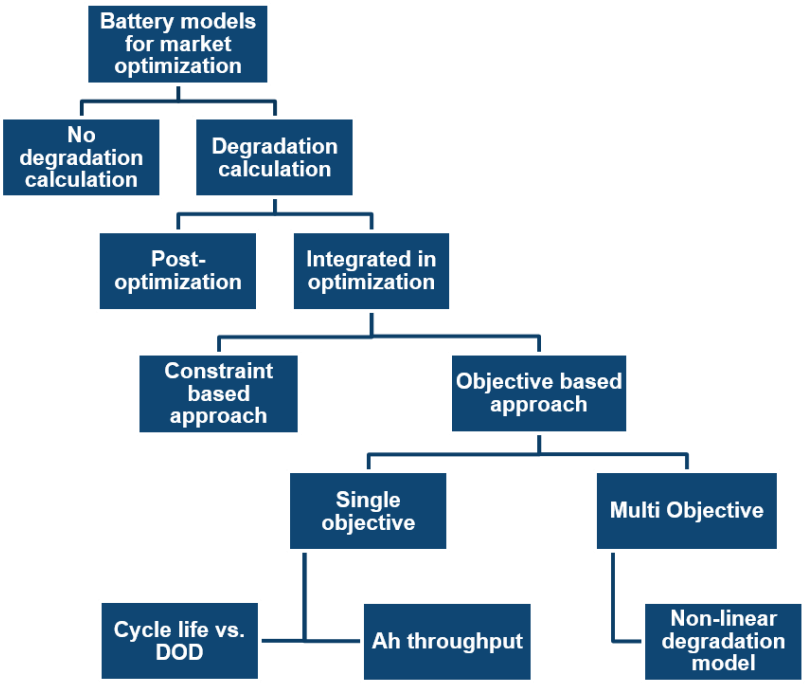

Figure 2-1: Battery Storage System ageing modelling approaches [MAH18].

Of all the options reviewed, the simplest is to ignore the degradation, and have the battery operate freely. This implies a fixed lifetime for the BSS, independent of operation. While convenient from a modelling point of view, it does not faithfully represent real internal processes or operation of the BSS. When considering the degradation of the battery, it can be done *ex post* to calculate the degradation of the system *without influencing the optimal operation decision*, or it can be intrinsically part of the optimization, conditioning the optimal operation decisions.

Within this subgroup, the integration can be done in two ways, or a combination of both. The simplest one is to establish constraints on the degradation inducing variables. This can include limits on cycles (introducing a replacement cost after *n* number of cycles) [SED16]; time windows for charge/discharge decisions throughout the operation period [GAB12] [GAB13], limits on SOC [ABD18], and limits on charge/discharge power. However these limits are always establish *a priori*, such that they are not adapted to the problem at hand. Furthermore, in the case of cycling limits, the difficulty in determining actual cycles is especially problematic.

A lot of attention has been paid to *cycling effects*. This is relevant from the manufacturers' point of view, as it is used a measure of estimated lifetime that can imply guarantee

periods. Cycling of batteries is generally discussed in terms of number of cycles and depth of discharge (DOD), as the relation between these two factors has been observed to behave as in Figure 2-2.

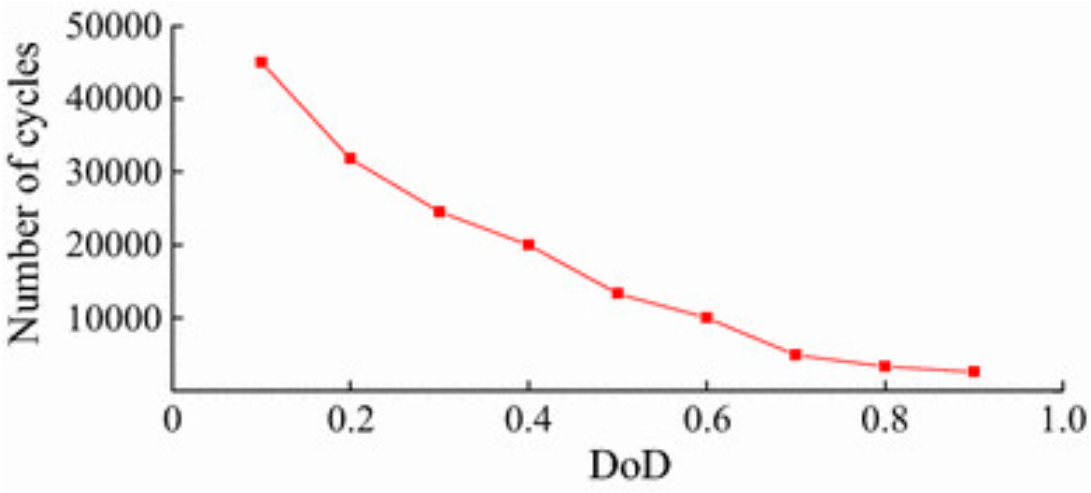

Figure 2-2: Cycle lifetime of Li-ion NMC battery as a function of cycle depth [WAN16].

The problem of cycling impact has been successfully addressed by applying the *Rainflow* counting algorithm, originally developed for fatigue calculation in materials engineering [END74][MUS12].With this method, subsequent charge/discharge decisions are grouped forming charge/discharge *half cycles*. These cycles can then be counted and provide an accurate total lifetime calculation. However this algorithm cannot be transformed into a linear function, and therefore presents severe challenges to its integration in optimization solvers. The other option is to consider the ageing of the battery in the objective function (OF), therefore optimizing its lifetime operation intrinsically. To do this a cost for operation must be assigned to some parameter determining the use of the battery. This is generally done considering cycles as a function of DOD, in a non-linear formulation of the rainflow algorithm [DUG15] [XU18b], or considering a cost per ampere-hour (Ah) put through the battery [MAR17].

Because of the complex internal dynamics of a BSS, the more accurate models are highly non-linear and based on a combination of theoretical electrochemical models and statistically treated empirical data. This renders them unsuited for MILP integration. Therefore in this work, a constraint-based approach to modeling BSS degradation is followed. Additionally, the cycling resulting from the optimal BSS operation is analyzed in section 4.1.2.3.

2.1.2 Network modelling

When looking at real world scenarios, completely isolated buildings are the exception rather than the norm. In most settings, be it urban, sub-urban or rural, the individual units are connected, and their operation influences each other. This is the case when the energy inputs cannot be provided in infinite amounts, but rather are supplied through networks, or *grids*. These networks have limited carrying capacities, which directly limit the input power for each unit.

The most widespread networks are electrical grid and natural gas grid. In specific situations, district heating and district cooling solutions are an option for the district planner.

The carrying capacity of a line is determined by physical factors. In the case of electrical grids, the limiting variable is the current. This current will generate losses in the form of heat. If heat is generated faster than it can be dissipated, it can lead to line failure. Additionally operational constraints may be imposed which do not stem from the thermal behavior of the lines. The carrying capacity for the connections is usually calculated based on *diversity factors*, which assume low concurrency [BAY12]. This is done to avoid costly oversizing of the grids. Therefore in special situations with high concurrency, new additional loads and unpredictable local generation a grid may be overloaded. Other problems, such as voltage drop/pressure drop (for electricity/fluid networks), need to be addressed during the operation of the network. This can have an impact on the optimal operation of a node in the network.

The case of electrical grid modelling is central to the work of this thesis. Due to the complex behavior of AC networks, the approaches to modelling it mathematically are diverse, depending on the aspects on which the model focuses.

2.1.2.1 Power Flow analysis

Power flow analysis is the study of electricity distribution grids. It is applied for operational planning and real-time operation of electrical grids, as an exact calculation method which, assuming symmetrical loading, reflects the exact physical results in the grid.

The power grid can be modelled as a set of nodes, or *buses*, interconnected by a set of *lines* or *branches*. The topology and parameters of the branches do not affect the setting of the problem; they may however affect the solution process. Each node is character-

ized by four variables: active power injection, reactive power injection, and voltage magnitude and voltage angle. The nodes are classified by the subset of these variables that is known beforehand. This yields PQ nodes, where demand/injection is known but voltage is not; PV (not photovoltaic) nodes, where active power injection and voltage magnitude are known; and an additional *slack node*. The slack node serves two purposes: it sets an angle reference (its voltage angle is 0°) for all other nodes; and it serves as source/sink for possible power mismatches between demand and generation in the network. The state of the system is fully determined by the voltage of each node, in magnitude and phase, and the power injections/withdrawals at each node. With these values, the power (current) flowing through each line is determined.

The power flow (PF) equations (2-1) (2-2), which describe the power flow through a line connecting two nodes, are highly nonlinear. Additionally, the system equations form an overdetermined system of equations, so one bus is used as a reference from which the rest are determined.

$$P_{12} = |U_1||U_2|(G_{12}\cos(\theta_1 - \theta_2) + B_{12}\sin(\theta_1 - \theta_2)) \quad (2\text{-}1)$$

$$Q_{12} = |U_1||U_2|(G_{12}\sin(\theta_1 - \theta_2) - B_{12}\cos(\theta_1 - \theta_2)) \quad (2\text{-}2)$$

Explicit formulation of these equations results in complicated nonlinear models. Therefore different methods have been developed to simplify the calculations, adapt them to specific network topologies, or approximate the solution aiming at reduced computational strain. Due to the particular network structure, general PF calculation, and OPF calculation in particular, can have trouble arriving at the solution. Therefore specific methods have been developed for distribution networks, such as [LIU16] [FRA18] [DAL13]. Due to their nonlinear application, they are ruled out as an option for MILP modelling.

As an alternative, multiple linearizations of power flow analysis have been developed over the years. For more information and the specifics of some of the models, the author refers the reader to [AND17] [LIU19] [SHA17] [YUA18]. The main point of all of them is the large increase in the number of constraints and variables with the increase in network size. If applied to an already complex model such as the one used in this work, the magnitude of the problem can render it intractable.

One widespread approximation is the DC power flow (DCPF). By assuming a flat voltage over the whole network, purely inductive lines, and small angle differences between contiguous buses, the active power equation becomes much simpler (equation (2-3)). Reactive power flows are, however, ignored.

$$P_{12} = |U_1|^2 \, B_{12}(\theta_2 - \theta_1) \qquad (2\text{-}3)$$

The DC power flow model is used widely in instances where speed is required over accuracy [FRA12]. In principle it is not appropriate for distribution grids, as the base assumption of impedance being mostly inductive does not hold. However in the case of perfectly radial structures the power flows are easily traced, as generally any two nodes in the network are connected by only one possible path.

The application of DCPF has one advantage which makes it especially suited for the model at hand. Through the definition of a *Power Transfer Distribution Factor* (PTDF) matrix, the sensitivity of power flow through a line can be expressed as a linear combination of the power injections in all the nodes of the network. The PTDF matrix is calculated with grid parameters (impedances and connections) and is therefore independent of the state of the network.

The calculation proper is divided into three steps. First, the lines in the network are assigned a flow direction and an *incidence matrix* A is defined. A is size $L*N$, where L is the number of lines and N the number of nodes. It is built systematically by assigning a value to each element such that:

- If line l starts in node n, $A_{l,n}$ is 1;
- If line l ends in node n, $A_{l,n}$ is -1;
- If line l does not connect to node n, $A_{l,n}$ is 0;

Second, an L*L primitive admittance matrix is defined as Y_d in which each element of the diagonal is the line admittance of the corresponding line. Then the admittance matrix Y is calculated according to (2-4)

$$Y = A^T * Y_d * A \qquad (2\text{-}4)$$

With the DC approximation, the line admittances are approximated by line susceptances, so Y_d becomes B_d. Then the PTDF matrix is defined as (2-5)

$$PTDF = B_d * A * (A^T * B_d * A)^{-1} \quad (2\text{-}5)$$

Even though the calculation is convoluted, the interpretation is simple: element $PTDF_{l,n}$ represents the variation of power flow through line l due to an injection of power in node n. It can be thought of as a matrix of sensitivity of power flows to power injections.

Because of the PTDF being constant, linear and independent of system operation point, it is used in this work to incorporate line flows into the optimization structure as described in section 3.

2.2 Mathematical Fundamentals

2.2.1 Linear Programming

Linear Programming (LP) refers to the set of problem modelling and solution techniques that can be applied to optimization problems, which deal exclusively with linear functions. Given a certain optimization problem ((2-6)-(2-8))

$$\text{Maximize} \quad c(x) \quad (2\text{-}6)$$

$$\text{subject to} \quad h(x) \leq B \quad (2\text{-}7)$$

$$x \; unrestricted \quad (2\text{-}8)$$

Where $x \in \boldsymbol{R}^{n_x}, B \in \mathbf{R}^{n_x}$, and $c(x)$ and $h(x)$ are generic functions.

It can be considered a linear program if the condition of linearity applies to both objective function (2-6) and constraints (2-7), such that:

$$c(\alpha * x + \beta * y) = \alpha * c(x) + \beta * c(y) \quad (2\text{-}9)$$

$$h(\alpha * x + \beta * y) = \alpha * h(x) + \beta * h(y) \quad (2\text{-}10)$$

If this condition is satisfied, then the program can be rewritten in a matrix form as equations (2-11)-(2-12)).

$$\text{Maximize} \quad c^T x \quad (2\text{-}11)$$

$$\text{subject to} \quad Ax \leq B \quad (2\text{-}12)$$

Where c^T represents the vector of *cost parameters*, A is the *constraint matrix* and B is the *right-hand side* of the inequality. In a general sense, any inequality constraint can be reversed by negating; accordingly so for simplicity only right-hand-side inequalities will be referred to in the remaining explanations. The same reversal procedure applies to the transformation of a maximization problem into a minimization one.

The objective function (OF) ((2-11)) establishes a penalty (*cost*) for each variable, such that the modification of a variable affects the overall *OF* cost, either improving it or deteriorating it. The optimal solution is found, when the extreme value (minimum for minimization, maximum for maximization) of the OF that satisfies all the constraints, is found.

An important property of linear problems is that they are, by nature, *convex*. This implies a *convex feasible region*, which means any local optima are also global optima. This is of especial importance when comparing with heuristic optimization methods, which cannot guarantee global optimality for a given solution.

Another important concept in LP is the concept of *duality*. Any LP (*primal problem*) can be converted to an equivalent, *dual problem* that finds the OF value by finding the *most restrictive bound on the OF of the primal*. The most restrictive bound yields the optimum value of the OF. With this in mind, two theorems come into play: the *weak duality theorem* and the *strong duality theorem*.

Weak duality states that *the optimal value of the dual problem is equal to or larger than the optimal solution of the primal problem*. Strong duality states that *the optimal values of dual and primal are equal*. These two theorems are of vital importance for the solution method implemented in this work; as part of the problem is solved via its dual, the guarantee that the solution found is optimal comes from the duality theorems.

2.2.2 Mixed Integer Linear Programming

Mixed Integer Linear Programming (MILP) refers to optimization problems and solution methods such that the set of decision variables is composed by a subset of *integer* variables, and additionally a subset of *continuous* variables. In contrast with LP problems, MILP cannot be solved by methods like the simplex algorithm. The solution of such problems is complicated and usually follows a branch-and-bound routine.

This involves an initial relaxation of the integrality constraints, so that the problem becomes an LP. The relaxed LP problem is solved and integrality conditions are applied iteratively to the integer variables, checking for feasibility at every iteration. While these methods are capable in theory of finding the optimum, the process is very inefficient, as it forces the solver to test many candidate solutions that are not feasible until the optimum is found.

For this reason a solution routine known as Benders' Decomposition was developed to apply to certain MILP problems.

2.2.3 Benders Decomposition

Benders' Decomposition (BD) is a specific method aiming at efficiently solving certain large optimization problems. Although a generalized formulation exists for non-linear problems[LI11], this section will cover the formulation for linear problems, which has its roots in the original publication by Jacques F. Benders [BEN62]. The formulation for linear problems implemented in this work is a specific implementation derived by [VAN69].

The main premise of BD is that certain large problems are faster and/or require less resources to solve when broken up into parts. This decomposition results in smaller, simpler problems that are resolved iteratively until their optimal values converge. While the application is possible to any LP problem, only those with a certain internal structure result in efficient solutions. This structure is referred to as a *block-angular structure* (see section 3.1.2), and it is crucial for the successful application of BD.

In this section, the concept of BD is explained applied to the investment problem at hand.

Let our optimization problem be:

$$\text{Minimize} \quad c^T x + d^T y \tag{2-13}$$

$$\text{subject to} \quad Cx + Dy \leq a_s \tag{2-14}$$

$$Ax \leq d_x \tag{2-15}$$

$$By \leq d_y \tag{2-16}$$

$$x \in \{0,1\} \quad (2\text{-}17)$$

$$y \geq 0 \quad (2\text{-}18)$$

Where $y \in \mathbf{R}^{n_y}$,$x \in \boldsymbol{Z}^{n_x}$, each $c_i \in \mathbf{R}^{n_i}$, each $b_i \in \mathbf{R}^{n_i}$, each $A, B \in \mathbf{R}^{m_i \times n_i}$, and each $C, D \in \mathbf{R}^{m \times n_i}$.

The justification for the application of BD is the observation that the optimization of variables **x** and **y** are k *mostly* independent, and connected only via the *coupling constraints* from (2-13). Furthermore, variable subset **x** is observed to be a set of *complicating variables*, in the sense that fixing their value significantly simplifies the problem of optimizing the remaining variables.

The first step of the method is to reformulate original problem as *master problem* (MP) and *sub-problem* (SP). The MP is then presented as follows:

$$\text{Minimize} \quad z = c^T x + \theta \quad (2\text{-}19)$$

$$\text{s.t.} \quad Ax \leq d_x \quad (2\text{-}20)$$

$$x \in \boldsymbol{Z}^{n_x}, x \geq 0, x \leq 1 \quad (2\text{-}21)$$

Where **θ** is the *shadow variable* for the optimal value of the SP:

$$\text{Minimize} \quad w_s = d^T y_s \quad for\ s = 1, \dots, S \quad (2\text{-}22)$$

$$\text{s.t.} \quad Wy_s + T\bar{x} \leq h(w_s) \quad (2\text{-}23)$$

$$y \in \boldsymbol{R}^{n_y}, y \geq 0 \quad (2\text{-}24)$$

And

$$W = [B; D] \quad (2\text{-}25)$$

$$T = [0; C] \quad (2\text{-}26)$$

$$h(w_s) = [d_y; a_s] \qquad (2\text{-}27)$$

The MP will first optimize the x decision variables and relay the resulting values $\bar{x}$ and θ to the SP, which will solve the y decision variables taking the former as parameters. The SP solves the y using the value of θ as a lower bound (LB) for the objective value of w (Figure 2-3). The goal of the second stage problem is to find the expected value of the SP as upper bound (UB) estimator, and the gradient of the first stage variable with respect to the second stage objective.

The values of LB and UB should converge over the overall iteration process if the problem is convex. Every iteration their values are compared according to:

$$\left|\frac{UB - LB}{UB}\right| \leq \%\, required\ accuracy \qquad (2\text{-}28)$$

If the values of LB and UB hold (equation (2-28)), then the algorithm stops. If they don't hold, then an optimality cut is introduced into the MP, and a new iteration is started. Upon solution of the SP, three situations are possible:

- The SP is unbounded, and therefore the whole problem is unbounded.
- The SP is non-optimal ((2-28) does not hold).
- The SP is infeasible.

In the case of SP unboundedness, the algorithm stops, as the problem has no solution. If the SP solution is sub-optimal, a set of optimality cuts are added.

The MP after L optimality cuts are added has the form (2-29)

$$\text{Minimize} \quad z = c^T x + \theta \qquad (2\text{-}29)$$

$$\text{s.t.} \quad Ax \leq d_x \qquad (2\text{-}30)$$

$$\theta \geq e_l - E_l * x\, d_x \quad l = 1, \ldots, L \qquad (2\text{-}31)$$

$$x \in \boldsymbol{Z}^{n_x} \quad , x \geq 0 \quad , x \leq 1 \qquad (2\text{-}32)$$

The optimality cuts are generated via the dual of the sub-problem (DSP). This is formulated as (2-33) - (2-35):

$$\text{Maximize} \quad \pi^T[h(w) - T\bar{x}] \tag{2-33}$$

$$\text{s.t.} \quad \pi^T W \leq q \tag{2-34}$$

$$\text{s.t.} \quad \pi \geq 0 \leq q \tag{2-35}$$

By virtue of weak duality, (2-36) can be stated:

$$w \geq \pi^T[h(\omega_s) - T\overline{x}] \tag{2-36}$$

Which has the same form as (2-31). Therefore the definitions of e_l and E_l are given as (eq.9):

$$e_l \equiv \left(\pi^l\right)^T h(w_s) \tag{2-37}$$

$$E_l \equiv \left(\pi^l\right)^T T_s \tag{2-38}$$

It is the inclusion of these optimality cuts that drives the convergence of the solution.

Alternatively, if the SP is infeasible, different steps are undertaken. A set of feasibility cuts must be generated in order to eliminate candidate MP solutions that lead to an infeasible SP.

To generate feasibility cuts the SP is reformulated as (2-39):

$$\text{Minimize} \quad w_s' = e^T * v^+ + e^T * v^- \tag{2-39}$$

$$\text{s.t.} \quad Wy_s + Iv^+ - Iv^- = h_k - T_k x^v \tag{2-40}$$

$$v^+ \geq 0, v^- \geq 0, y \geq 0 \tag{2-41}$$

Where e^T is the identity vector, e^T is the identity matrix, and W, h, and T are defined as in (2-33). From here the dual of the new SP is formed and solved, yielding the duals

σ^{V} f. Since for a feasible solution, the value of W_S' is at most zero, the feasibility cut can be formulated as:

$$0 \geq d - Dx \tag{2-42}$$

Where

$$D_r = (\sigma^V)^T T_k \tag{2-43}$$

$$d_r = (\sigma^V)^T h_k \tag{2-44}$$

The first iteration of the MP solution can be skipped through the introduction of an initial guess, which can increase the execution speed substantially due to the inefficiency of the feasibility cut generation process.

Figure 2-3 shows the whole process in a schematic way.

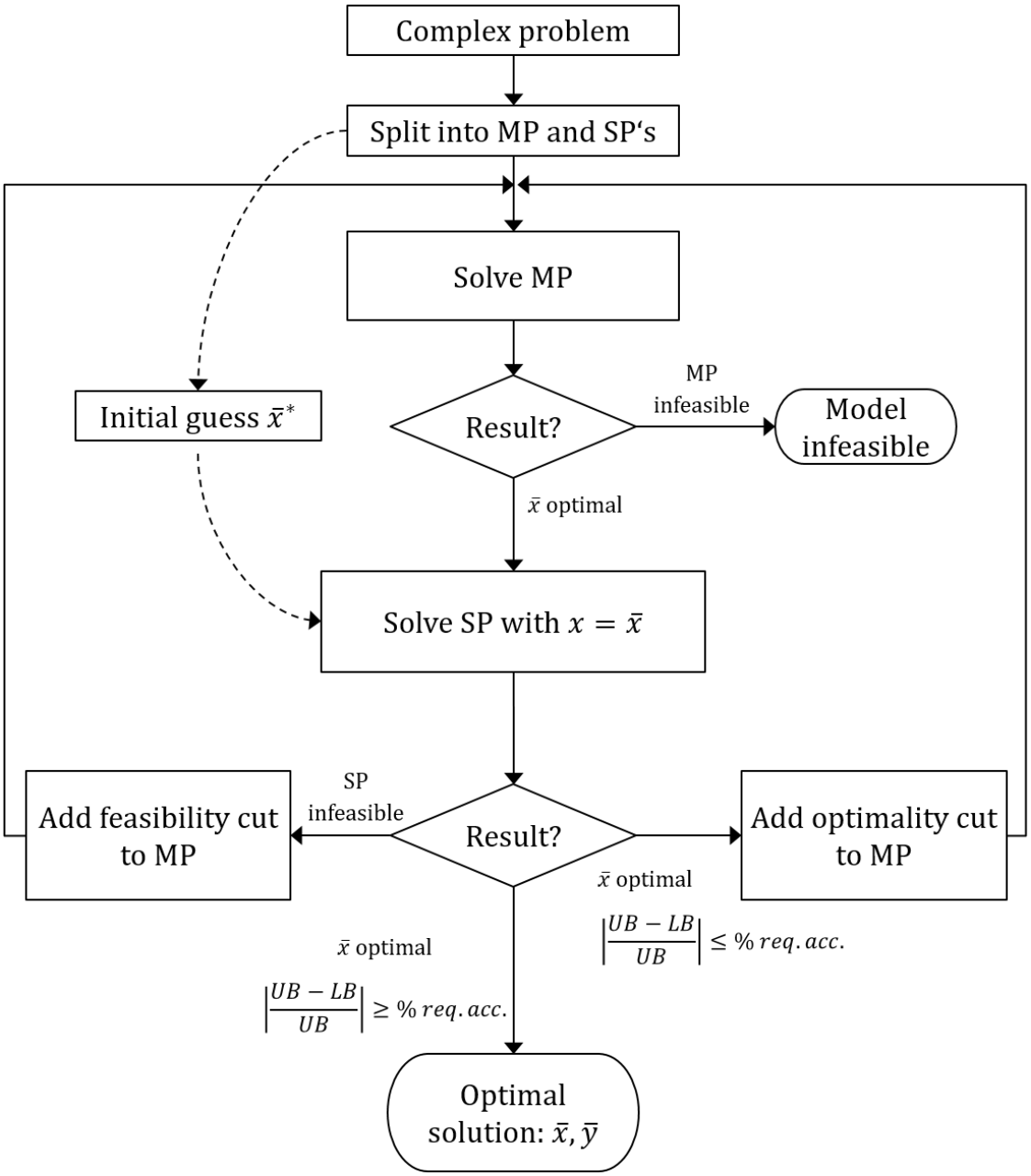

Figure 2-3: Benders’ Decomposition implementation algorithm.

3 Methods and Implementation

In this chapter, a detailed description of the methodology and developed tools is given. It includes the state of the art, describing the overall project in which this thesis is framed. From there, the contributions of the thesis to the described framework are explained.

3.1 State-of-the-art

The project in which the work of this thesis has been developed is a tool for multi-objective optimization of Distributed Energy Systems.

The optimization tool models a given neighborhood, where each building node acts as a demand/generation node. The individual buildings are modelled as *energy hubs*, in which certain energy inputs are converted, through the technologies available, into other types of energy, useful to cover the demand of each node. The tool allows for optimization on the basis of costs, CO_2 emissions, or a weighed combination of both. Therefore it entails the capability of a multi-criteria optimization. The connections between buildings are the *electric grid*, the modelling of which is one subject of this thesis.

3.1.1 Energy-hub model

An *energy hub* is a mathematical model of the energy transformations carried out by a unit (the *hub*) on a set of energy inputs to cover a set of energy outputs. The conversions are carried out by different technologies available for installation. An exemplary energy hub is modelled as shown in Figure 3-1 and equation (3-1).

Each term $\mathbf{C_{ij}}$ represents the conversion efficiency from input **i** to output **j**.

(3-1)

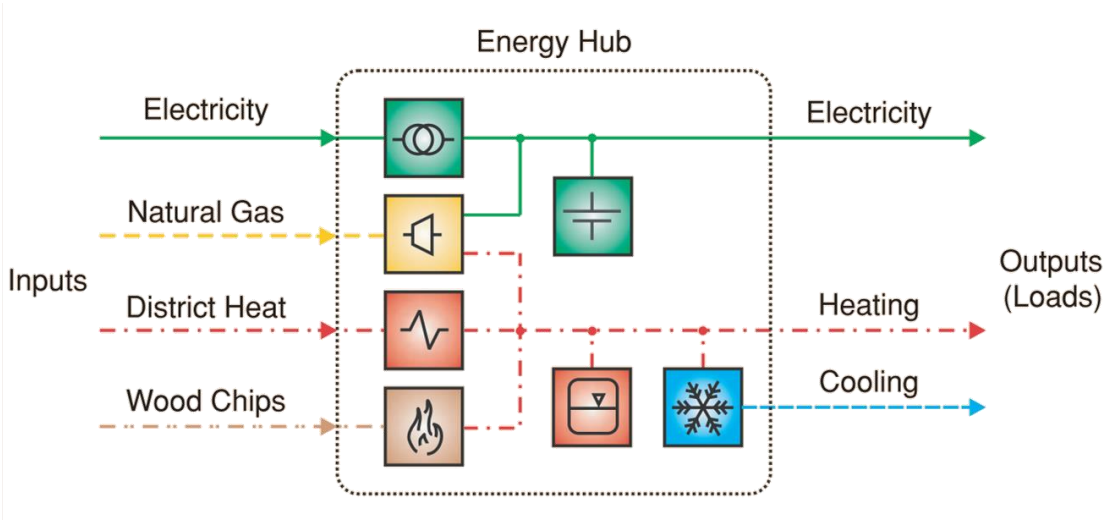

Figure 3-1: Exemplary Energy Hub model [GEI07].

In the case of inclusion of energy storages, the equation becomes (3-2), which includes the variation of energy stored in the system in a given time step **Δt.**

(3-2)

The energy hub formulation is well suited to large optimization problems due to its simplicity and scalability. The specific model used in this work is detailed in chapter 3.1.1.2.

3.1.1.1 Modelled technologies

The technologies considered are all largely available at consumer level. A comprehensive study of market-available technologies has been carried out, yielding a characterization of each technology based on the following parameters:

- Technology parameters
  - Energy inputs
  - Energy outputs
  - Conversion efficiencies (thermal, electrical, or both)
  - Power limits
  - Further technical constraints
- Financial parameters
  - Depreciation period
  - Capital costs

  - Installation costs
  - Fuel costs
  - Maintenance costs
  - Feed-in premium
- Emissions parameters
  - Equivalent CO_2 per kWh
  - Equivalent CO_2 for installation

The range of available technologies is displayed in Table 1, along with the corresponding input and output technologies.

Table 1: Available technologies

Conversion technology	Input	Output
PV	Solar irradiation	Electrical power
Thermal Solar	Solar irradiation	Heat
Electrical grid connection	Electrical power	Electrical power
Electrical heating	Electrical power	Heat
Heat pump (Air-Air, Air-Water, Ground-Air)	Electrical power/Gas	Heat
Gas condensing boiler	Gas	Heat
Combined heat and power (CHP)	Gas	Heat, Electrical power
Woodchip heating	Woodchip fuel	Heat
Pellet heating	Pellet fuel	Heat

Additionally, several renovation measure option are considered. This also falls in the category of energy efficiency *measures*, as this reduces heating energy demand. The renovation options are designed considering the different parts of the *building shell*. Different combinations of improvements on these parts yield the different renovation options. This is explained more in detail in section 3.1.1.2.

3.1.1.2 Building model

The building model is based on a comprehensive study of real world residential buildings. Each building is characterized by its demand curves, as well as parameters representing physical installations and/or properties. The building shell is modelled by heat transfer coefficients, representing the insulation of the building from the exterior. This has a direct relation with the thermal demand curves, which are generated according to the specific conditions of a building; e.g. if a building has a heated basement, the corresponding thermal demand curve will be influenced by the heat transfer coefficient between the basement and the ground. Environmental factors are also taken into account. For example, roof surface, angle and orientation are necessary to accurately calculate potential PV generation. Lastly, specific information regarding the possible installation of technologies, such as existing or possible gas connection, are also part of the building dataset.

The building shell, as pictured in Figure 3-2, is composed of the following elements:

- Roof
- Walls
- Basement/Cellar
- Windows

The partition allows more accuracy in the description of the building behavior, as heat losses can be modelled specifically for each insulation element. It allows as well for the modelling of renovation options.

The renovation options are improvements on the insulating properties of the building envelope. They result in reduced heat losses, and therefore reduced demand. The way they are carried out is not free however; not all combinations of improvements are allowed. This is not arbitrary, but is rather determined by building codes. The objective is to avoid fast degradation of the building proper. An example is the limit on the difference in thermal conductivity between windows and walls. If walls are more conductive than windows, condensation will happen on them, rather than on the windows. While condensation on windows is harmless, buildup of humidity on porous surfaces can cause degradation.

Therefore some constraints exist to the possible renovation measures; for example, an improvement on window insulation must not result in higher thermal conductivity of the walls (this would precipitate condensation on them, rather than on the windows).

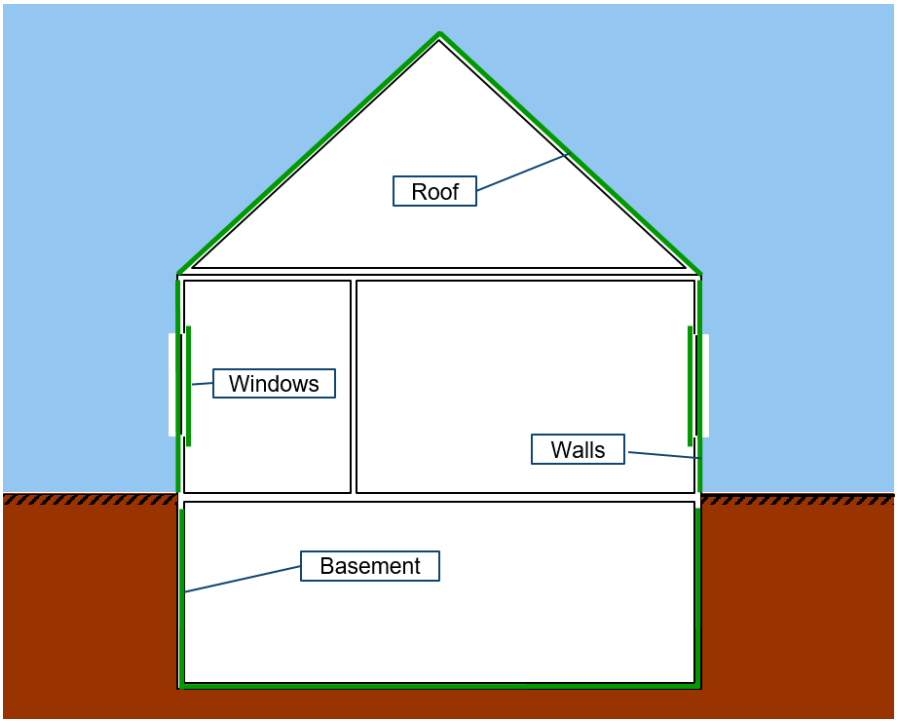

Figure 3-2: Model of a building shell.

3.1.2 MILP formulation

The optimization is carried out modelling the investment and operation decisions relative to the subject explained in Chapter 3.1.1 in an MILP formulation. The decisions are modeled with a set of integer variables and a set of continuous variables. The separation is understood as a causal conditioning of the continuous variables by the integers. The problem can be understood as a two-stage decision process, where initially a set of decisions is formulated, and then another set of decisions must be made, conditioned by the ones takes in the first stage. This simulates the system-building process: the first stage in this problem is the investment stage, where the decision must be made to invest in a portfolio of technologies. The second stage is the dimensioning and operation stage, in which the size and timely operation of each technology is decided.

The first stage is modelled with binary variables, a special subset of the integers. The second stage is modelled with continuous variables, and functions are linearized to result in an overall MILP problem.

The second stage of the problem becomes much easier to solve if the value of the first stage variables is fixed. Therefore the application of Benders Decomposition is warranted.

. In the MILP formulation the OF is defined as

$$Minimize\ CAPEX_{Fix} * x + CAPEX_{Var} * y_{dim} + OPEX * y_{op} \quad (3\text{-}3)$$

Variables represented by x are *investment variables*, which model the decision to adopt a certain technology or renovation measure. They are binary variables, representing the option to either invest (1) or not invest (0). Binary variables are by definition modelled as integer variables with values limited to {0,1}.

Variables represented by y_{dim} and y_{op} are respectively *dimensioning* and *operation variables*; for each available technology, they represent the installed power or operation power in each time step n_i, as presented in (equation) (vector of operation variables). In the case of storage systems, additional variables representing storage capacity and the state of charge (SOC) of the system at each time step n_i are necessary to fully model operation.

The parametrization of the problem is done with attention to the different factors being modelled. The real world data explained in section 3.1.1 is translated into specific parameters that appear in the objective function and constraints. The parameters can be then split into two categories.

Cost parameters are the coefficients of the objective function that multiply each variable in the objective function. In the formulation from Table 2, parameters in c_1 are the *fixed/investment cost*, while parameters $d_2$are the *variable/operation costs* associated to the sizing/operation decisions, respectively.

The sizing/operation costs d_2 represent the whole lifetime of the investment, even though only one year is considered in the operation optimization. To achieve this the CAPEX is annualized from the input cost parameters following equation (3-4) Annual increases in fuel/electricity costs are also taken into account, rendering a more realistic projection of the operation costs throughout the whole lifetime of the technology. The annuities are calculated as:

$$CAPEX_{Annuity} = C_{0t} * \frac{(1+r)^{n-1}}{(1+r)^n - 1} \quad (3\text{-}4)$$

Where C_{0t} is the fixed or variable investment costs term in year **0**, r is the yearly interest rate, g is projected the growth rate of the input costs, and n is the number of years of expected lifetime of the investment.

Every other parameter is grouped under the *constraint parameter* category. This includes upper and lower bounds for the variables, such as the PV installation limited by the available roof surface; conversion efficiencies relating input and output power for each technology; and all the building data covered in section 3.1.1.2. They form the basis of the constraint matrices. The constraints model the workings of the decision-making process, the logic of decisions, and the physical functioning of the technologies.

Constraints formulated with A (also stylized in Table 2 as MP for clarity) and d_x are related to investment decisions. In this model, they represent exclusivity between renovation options and possible limitations on the number of technologies to be installed. Constraints formulated with B (also stylized in Table 2 as SP for clarity) and d_y model the operation of technologies, including efficiencies and time-couplings caused by storage systems.

Constraints formulated with C, D, and a are called *coupling constraints*, and represent the conditioning of operation decisions caused by investment decisions. The first subset represents the limit on installed and operation power (Dimensioning & Operation variables) enforced by the respective investment decision (Investment variable). The second subset represents the change in thermal demand curve caused by improved insulation through renovation measures. This last subset is enforced using the *big M* method.

Additionally, every variable is bounded by two parameters (LB and UB), which restrict its values to possible and/or plausible limits. This is in general to avoid unreal values (e.g. negative powers) and to enforce model logic (decision variables as binary integers). These are not displayed in the model structure, as each pair of bounds for each variable is independent of other variables, and therefore does not affect the application of BD.

The application of BD is warranted by the possible division of the constraint set into the three mentioned subsets (variable bounds are included in A/B). The coupling constraints

are the complicating factor, as without them investment and operation would be completely independent and solvable separately. This distribution of constraint inequalities affects the solution process. As mentioned in previous sections, the success of the application of Benders Decomposition depends largely on an appropriate *problem structure* [BRA77]. Problem structure refers to the disposition of zero and non-zero elements in the constraint matrix. In essence, constraint matrices with many zero-values (high degree of sparsity) indicate low interdependency of the decision variables, while matrices with many non-zero elements (low degree of sparsity) indicate large interdependency between decision variables.

In the extreme case of independent subsystems (Figure 3-3), the complexity of the problem is substantially reduced, as the individual subsystems can be optimized independently, resting assured that the global optimization (minimization or maximization) is equivalent to the individual optimization of the sets of variables arranged in the subsystems.

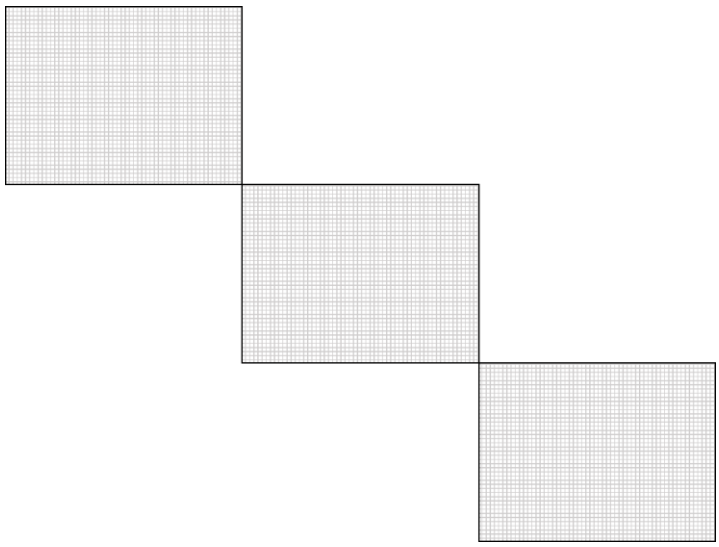

Figure 3-3: Independent problem structure [BRA77].

The case of a *block-angular* structure is that of a group of mostly independent subsystems, with a set of *coupling constraints* (). These coupling constraints are at the core of the application of BD, as they relate the integer investment variables with the continuous dimensioning and operation variables.

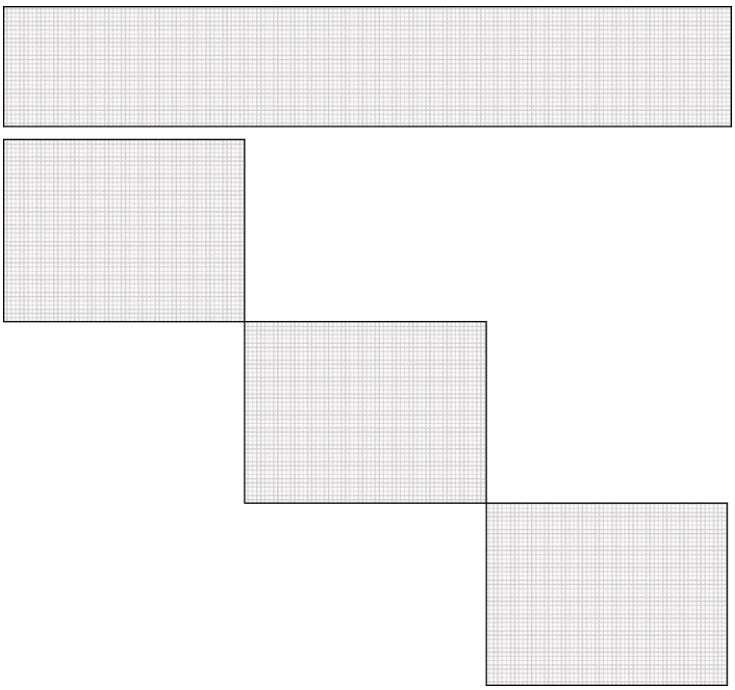

Figure 3-4: Block-angular problem structure [BRA77].

In this case, the problem can be understood as an *independent structure* of buildings that are optimized with no interdependencies. Each building however has a *block-angular* structure of integer and continuous variables representing the available technologies inside (Table 2).

Table 2: Single building optimization problem structure

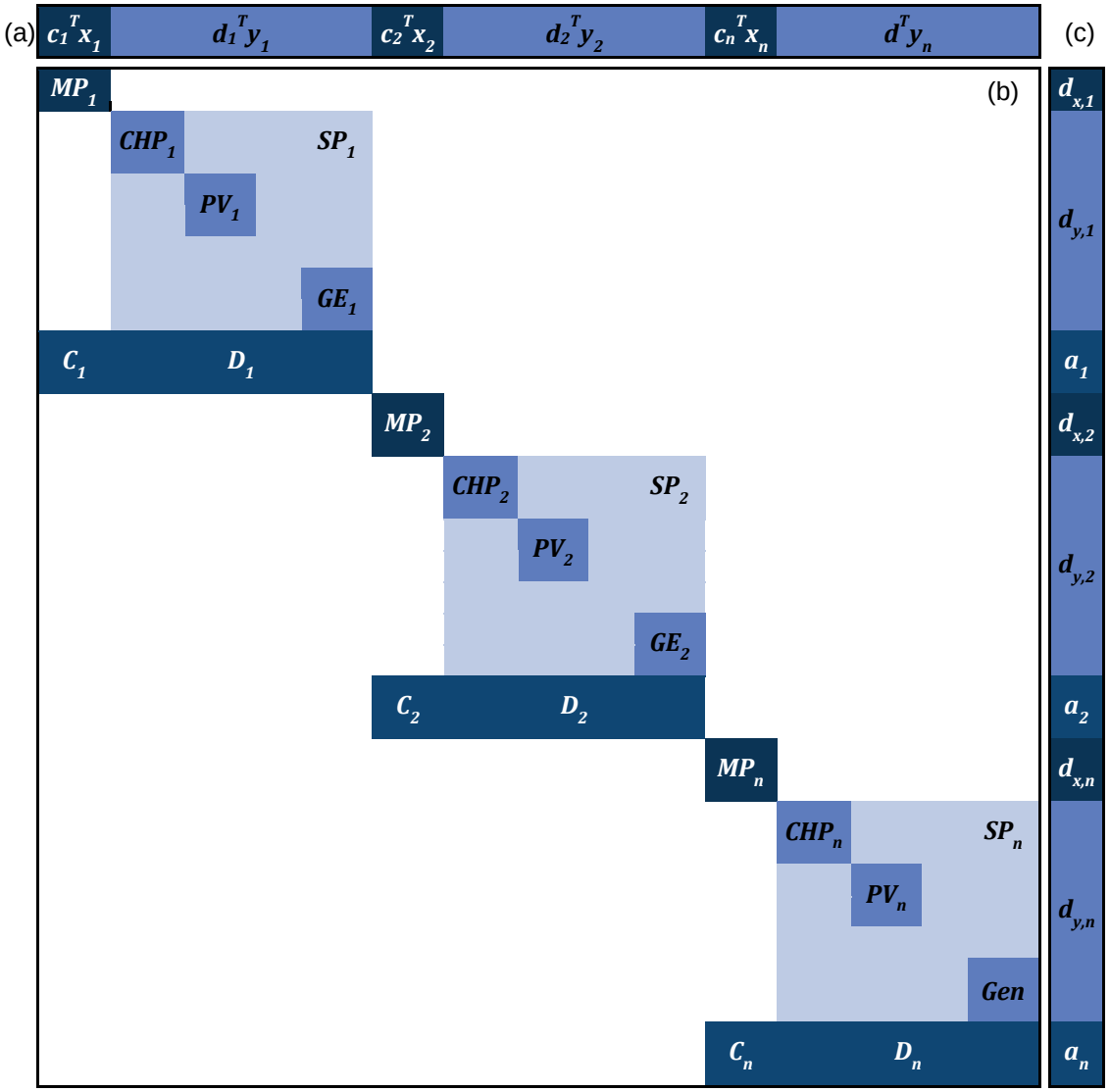

In section 3.3 the effect of including couplings between buildings is covered.

3.2 Battery Storage System model

The inclusion of energy storage adds a new dimension to the model. It involves incorporating new variables, constraints and parameters, and it strongly influences the behavior of other modelled technologies.

3.2.1 Mathematical model

The mathematical model is a generalized model of operation for any energy storage system. It can be adapted to inclusions of other energy storage systems into the model

(thermal, hydrogen, etc.) by modification of parameters and introduction of technology-specific operation constraints.

3.2.1.1 Variables

The variables defining the operation of the BSS are given in Table 3.

Table 3: Operation and dimensioning variables of BSS

Variable	Description	Name	Type	Limits
Charge power	Input power at time *t* [kW]	$x_t^{el_{in}}$	$\mathbb{R}$	[0,+∞)
Discharge power	Output power at time *t* [kW]	$x_t^{el_{out}}$	$\mathbb{R}$	[0,+∞)
State of charge	Energy stored at time *t* [kWh]	$x_t^{C\_SOC}$	$\mathbb{R}$	[0,+∞)
Installed capacity	Dimensioning of BSS [kWh]	C	$\mathbb{R}$	[0,+∞)
Installed power	Dimensioning of inverter [kW]	P	$\mathbb{R}$	[0,+∞)

It is worthy to note that the dimensioning of energy storages differs from generation technologies in that two variables define their installed capabilities. Without explicitly addressing it, the decisions of installed power and capacity are independent. In practice this is mostly the case: for lithium-ion storages, the range of capacity-to-power ratios available is vast; in the case of thermal or hydrogen storage, the capacity of a tank and the carrying capacity of pipelines are arbitrary and independent. Therefore, depending on the costs associated to each variable, some unreasonable solutions may arise. This is avoided by constraints explained in section 3.2.1.3.

3.2.1.2 Parameters

Table 4: BSS technology parameters

Parameter	Description	Name
Power cost	Annuity of inverter variable costs [€/kW]	c_{p_var}
Capacity cost	Annuity of storage variable costs [€/kW]	c_{cap_var}
Efficiency	BSS charge/discharge efficiency	ϑ_{el}
SOC limits	Limits on the State of Charge, used to avoid very high and very low SOC's that accelerate degradation	$SOC_{min}, SOC_{max},$
Duration limit	Limit on the maximum capacity/power ratio of the BSS [h], to avoid unreasonable solutions.	D

The parameters characterizing the BSS are all constant. In the case of efficiency, BSS and AC/DC converter efficiencies are considered lumped together, equal for charge and discharge, and constant. This is an approximation that avoids non-linearities in the constraint formulation.

The formulation of the OF costs for BSS decisions is calculated on the basis of certain input, real world cost parameters. These parameters, derived from previous extensive market search, are displayed in Table 5. They are formulated as linear functions, dependent on either installed power and/or installed storage capacity. The values are in the range of the ones used in the 2017 IRENA cost of Service tool [INT17].

Table 5: Battery Storage System cost functions

Parameter	Description	Function
Inverter capital costs	Cost of purchase of an inverter [€]	$105 * \mathrm{P_{inst}} + 0$
Installation cost function	Capital expenditure for the installation of the system (storage + inverter) [€]	$0 * \mathrm{P_{inst}} + 0 * C_{inst} + 750$
Storage costs function	Cost of purchase of storage [€]	$800 * \mathrm{C_{inst}} + 3000$

The OF parameters resulting from these input data are calculated according to chapter 3.1.2.

3.2.1.3 Constraints

The constraints governing the functioning of the Battery Storage System are given in equations (3-5) - (3-10). They follow standard energy storage formulations.

The basic operation principle is expressed in (3-5), namely: the energy stored at a time step t is the energy stored in the previous time step plus the difference of power injected/withdrawn in that time step. The state of charge is limited at all times by (3-6), modelling the measures incorporated by some BSSs to avoid the very high/very low SOCs that accelerate degradation. This forces the inclusion of (3-7) to avoid infeasibilities, as the battery is assumed to start its operation empty. Equations (3-8) and (3-9) limit the charge and discharge power, respectively. This allows for modelling of real limits (rating of the inverter) as well as more restrictive constraints designed to contain battery degradation. Finally, (3-10) limits the maximum capacity/power ratio; as the cost coefficients of power and capacity installations may vary, situations where the battery is over dimensioned with respect to the inverter.

$$x_t^{C\_SOC} = x_{t-1}^{C\_SOC} + \frac{x_t^{el_{in}} * \vartheta_{el} - x_t^{el_{out}} / \vartheta_{el}}{\frac{T}{8760}} \quad \forall\, t \in T \tag{3-5}$$

$$C * SOC_{min} \leq {x_t}^{C_{SOC}} \leq C * SOC_{max} \quad \forall\, t \in T | t \neq 0 \tag{3-6}$$

$${x_0}^{C\_SOC} = 0 \tag{3-7}$$

$$-P \leq {x_t}^{el_{in}} \;\; \forall t \in T \tag{3-8}$$

$${x_t}^{el_{out}} \leq P \quad \forall t \in T \tag{3-9}$$

$$C \;\leq D_{max} * P \tag{3-10}$$

It should be noted that cycling constraints are explicitly avoided in this work. The operation is expected to be relatively smooth, for the usage is self-consumption, as opposed to rapid signal following that could be seen in, for example, primary reserve provision.

With this model, the optimal integration of a BSS into a household energy hub can be obtained. However, it is worth noting that BSS control algorithms to optimize lifetime vs return on investment are currently being developed [SHI17]. In the model at hand no user-implemented BSS control algorithm further than the established variable limits is considered. This remains a potential future inclusion in the project.

3.3 Grid integration

The described model of isolated buildings is a first building block in the development of the model. However, in reality the external inputs are generally not available in an unrestricted way: those supplied through grids (as gas, electricity and district heating) are limited by the carrying capacity of these grids. In particular, the behavior of other users of the network affects the availability of the resource for the individual consumer. In practice, this translates as buildings connected to the same lines or pipelines having to strike a balance on the quantity of the limited resource each one of them draws.

Mathematically, this is modelled as constraints coupling buildings as described by network connections, establishing the carrying limits of these connections. In the case of fluid networks (heat/gas) the limit is the flow capacity of the network pipelines. In the case of electricity grid, it is the current limit of the lines. This limit can come from two factors.

The first one is the lines' capacity to dissipate heat: as long as the thermal losses in the line are lower than this limit, a line's temperature is stable. If the losses, however, are higher, the line slowly overheats. This has adverse effects on the operation of the line: increased resistance, sagging, and reduced insulation distances in overhead lines, and compromise of insulation in underground cables[MOR06].

The second one is the voltage drop over the line. As power flows through a non-ideal line ($Z > 0$), a voltage drop appears due to the impedance of the line. This voltage drop can be considerable in the situation of high power loading. The result can be voltage levels below the specified power quality standards as defined in [EUR04]

The limits on the lines are established as a function of the power flow through the line. However in both calculations this can be approximated as depending only on current. As thermal losses can be calculated as (3-11). Since a line will always operate close to nominal voltage due to voltage control mechanisms, the voltage drop can also be approximated as a function of the current (3-12), independent of the voltage level.

$$\Delta U = \bar{I}(R_l + jX_l) \qquad (3\text{-}11)$$

$$P_{loss} = \bar{I}^2 R_l \qquad (3\text{-}12)$$

This results in line limits being established from the more restrictive of the two values. The limits are expressed as a maximum rating in amperes. For some standard line types which are used in the model, the characteristics are shown in Table 6, according to [THU18].

Table 6: Distribution line characteristics used in the model [THU18].

Line type	R [ohm/km]	X [ohm/km]	C [nF/km]	Max I rating [kA]
NAYY 4x50 SE	0.642	0.083	210	0.1420
NAYY 4x120 SE	0.225	0.080	264	0.2420
NAYY 4x150 SE	0.208	0.080	261	0.2700

It is important to note that the values are calculated at 50Hz frequency. Additionally, the cable limits considered here are thermal limits for underground installation at which the insulation layer is compromised, as specified by standard [DIN05].

For the purpose of integrating the grid operation constraints, two methods were initially developed. The first one was an iterative calculation, including an extrinsic calculation of power flows. The second one is an integrated approach, with a simplified model of power flow calculations formulated explicitly in the MILP optimization problem.

3.3.1 Extrinsic power flow approach

An alternative way to calculate the impact of the grid on the optimal solution was devised using an external power flow analysis toolbox. The main idea is to calculate a relaxed optimization of the DERs first, and analyze which power flows result from this optimized, without considering the grid constraints. The solution to these power flow calculations would generate a bound vector for the power demands/injections to be relayed back to the optimization problem. The diagram of operation is detailed in Figure 3-5.

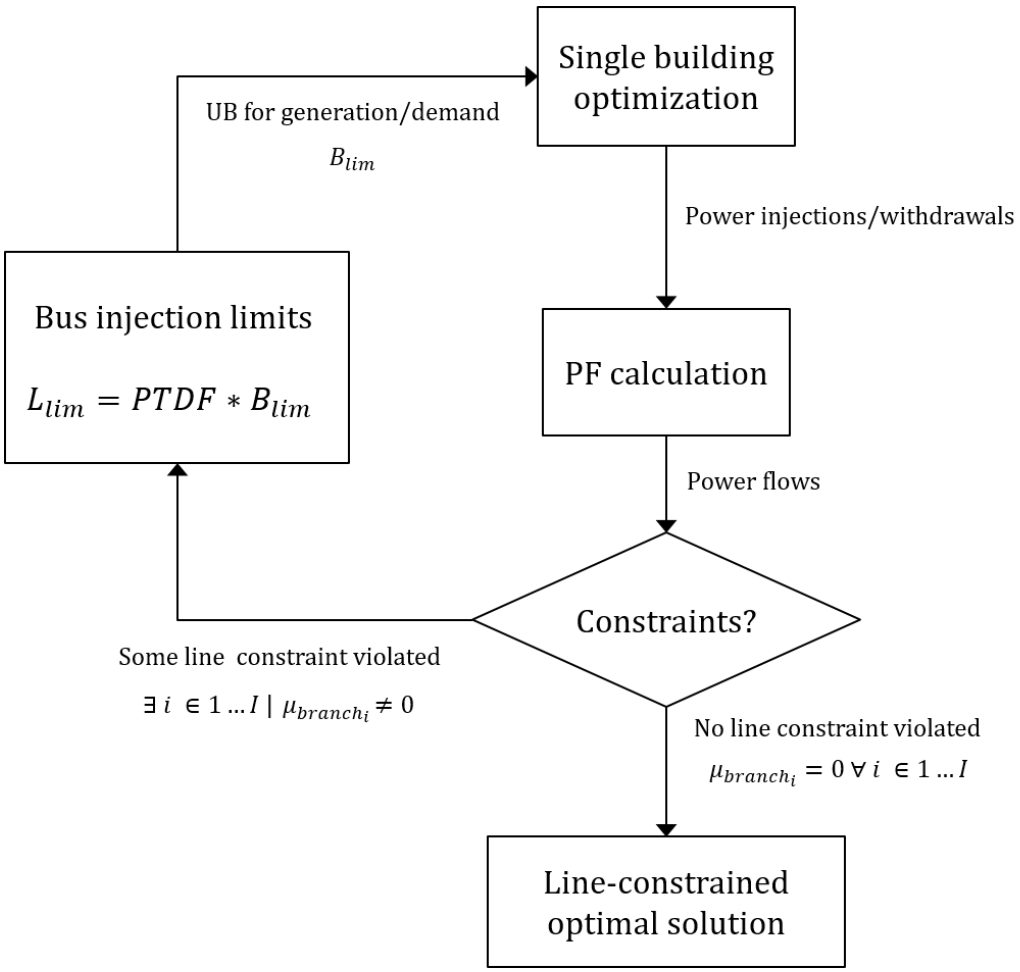

Figure 3-5 Power line restrictions via extrinsic power flow calculation.

The bus injection limits are established by solving equation (3-13), establishing symmetrical limits for bus injected/withdrawn power. In a generalized form this requires the calculation of the *left-side inverse*, as the PTDF matrix has dimensions $l * b$, where l is the number of lines and b is the number of buses in the network minus one (the slack bus), which need not be the same (equation (3-14)).

$$L_{lim} = PTDF * B_{lim} \tag{3-13}$$

$$(PTDF^T * PTDF)^{-1} PTDF^T * L_{lim} = B_{lim} \tag{3-14}$$

In the special case of a radial network, given (equation (3-15)), the solution simplifies to (equation (3-16)). This holds because in such networks, each bus can be uniquely associated to a line, except the feeder line, which connects with the slack bus at the other end.

$$b = l \tag{3-15}$$

$$PTDF^{-1} * L_{lim} = B_{lim} \tag{3-16}$$

While this methodology seems sound in principle, it was abandoned in favor of the one described in chapter 3.3.2 for a number of reasons. Firstly, the line flow limits are not considered in the MILP optimization; this negatively affects the guarantee of optimality provided by MILP. More importantly, it is inefficient; while the PF calculations take into account reactive power flows and are therefore accurate, the relay via PTDF matrix calculation ignores the impact of reactive power flows and voltage levels, yielding no more accuracy than the integrated method.

The final methodology implemented is described in chapter 3.3.2.

3.3.2 Integrated approach

The second method studied to include line limits in the optimization problem is the generation of additional constraints for the operation variables of the problem. This is what is referred to in this thesis as *integrated approach*. The basic idea behind this approach is to consider the whole neighborhood as a coupled structure, with grid inflows and outflows from each building coupled via line limit constraints. This allows for the application of BD to solve the problem, utilizing the same underlying routines from the original, single building optimization methodology.

The implementation requires, however, a restructured problem to apply BD. In essence, it requires all the original MP variables (investment decisions) to be grouped into one general MP, and the same to be done with the operation decisions. Therefore from the original independent structure of Table 2, the constraint matrices (blocks) are reordered resulting in the structure from Table 7. Additionally, constrains of the form of (3-17) (3-18) are generated through the use of the PTDF matrix.

$$\sum_{i=1}^{b} PTDF_{j,i}\left(P_g^i - P_d^i\right) \leq L_{lim,j} \quad \forall\, j \in 1 \dots L \tag{3-17}$$

$$\sum_{i=1}^{b} PTDF_{j,i}\left(P_d^i - P_g^i\right) \leq -L_{lim,j} \quad \forall\, j \in 1 \dots L \tag{3-18}$$

These establish the symmetrical limit $L_{lim,j}$ for each line **j**. By definition, the $PTDF_{j,i}$ factor denotes the variation of power flow through line **j** as a result of an injection of power in bus **I**, which is withdrawn at the slack bus.

Table 7: Integrated optimization problem structure

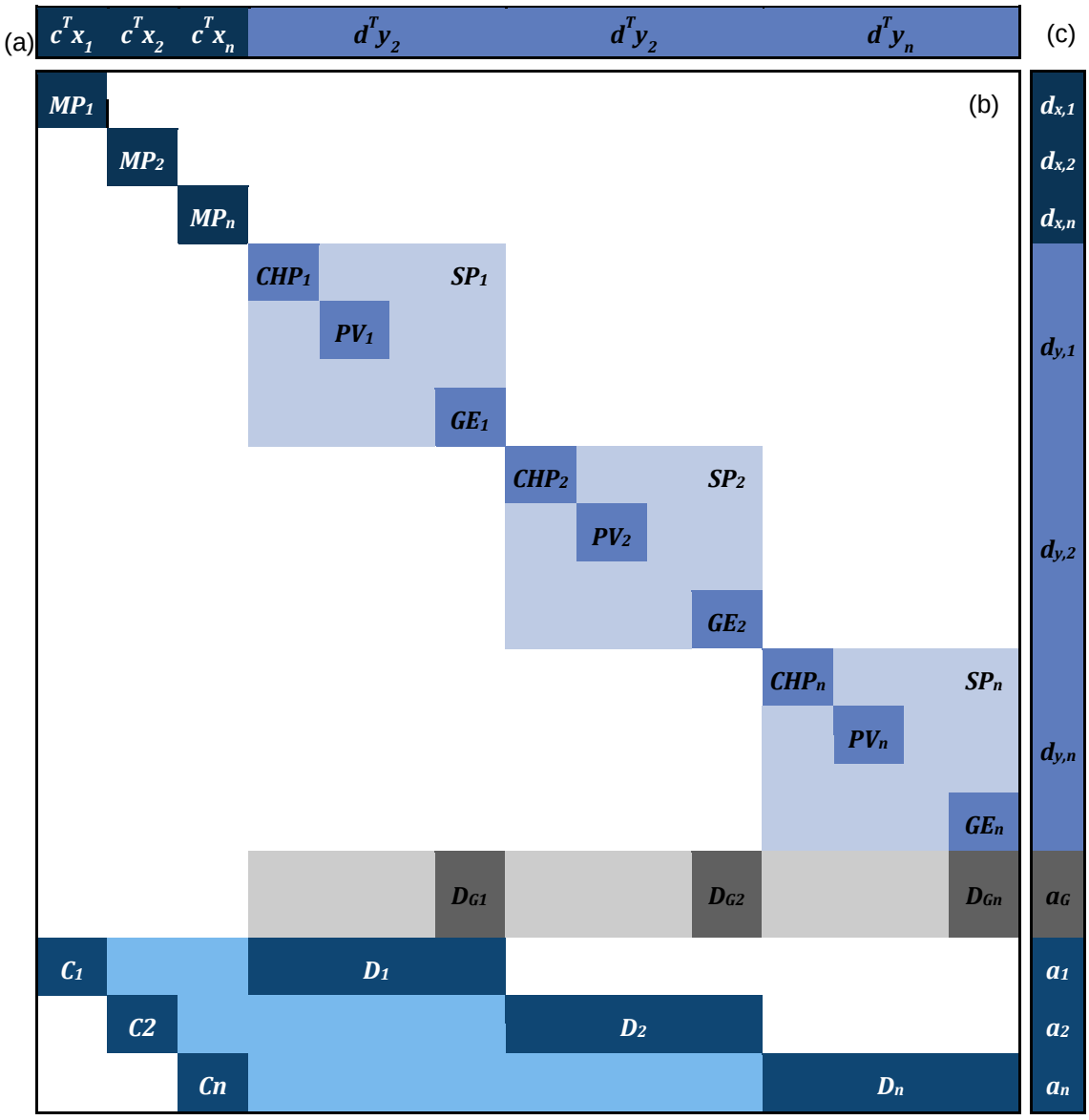

As is seen in Table 7, the grid constraint matrix D_G (grey) is a large sparse matrix where each $D_{G,i}$ is a block corresponding to the **i**th element of the left-hand side of the constraints from (3-17) (3-18).

The grid coupling constraints are merged together with the operational constraints of the technologies for each building to form the new sub-problem (SP). The master problem formed by simply combining the MPs from each building in the neighborhood, as

the investment decisions are completely decoupled. The coupling matrices are a re-structuring of the original ones, to line up each corresponding MP and SP properly, but no values are altered.

4 Exemplary studies

The integration of BSSs into DESs is analyzed through different use cases. The goal is to evaluate the benefits of BSSs for the two main actors involved in the distribution network; namely, the consumers and the grid operator, and to understand the possible asymmetries in costs/benefits for each one.

4.1 BSS for self-consumption optimization

The widespread installation of BSSs at a household level has been driven by several factors [BRA09]. In recent years Germany a growth in PV+BSS systems has been observed driven by a market incentive program implemented by the German Federal Government and the KfW banking group [KAI17]. This was intended primarily as a means to reduce the impact of distributed PV generation on the grid as a whole by promoting local consumption of generation. The alternative, injecting all excess power into the grid, can cause reverse power flows and inverted voltage profiles in distribution networks, both outcomes undesirable from the DSO's point of view.

The main hypothesis tested in this use case is whether BSS storages are actually economically viable when used exclusively as a means of improving consumption of self-generated power. To this end a specific test case was created.

4.1.1 Test case description

In general the optimization tool will take as an input a set of buildings, characterized as described in chapter 3.1.1.2. The number of buildings, as well as the roster of available investment options to choose from, define the complexity of the case. For this point in the study, having a set of buildings with sufficiently different demand profiles and characteristics is enough to reach significant results. Due to the absence of coupling between the buildings, the total number of buildings does not affect the results, so a simplified five building test case is devised

The test case is described physically in Figure 4-1. While the network connections are illustrated, they are not enforced via constraints for the purpose of this analysis. A general description of the buildings is given in Table 8.

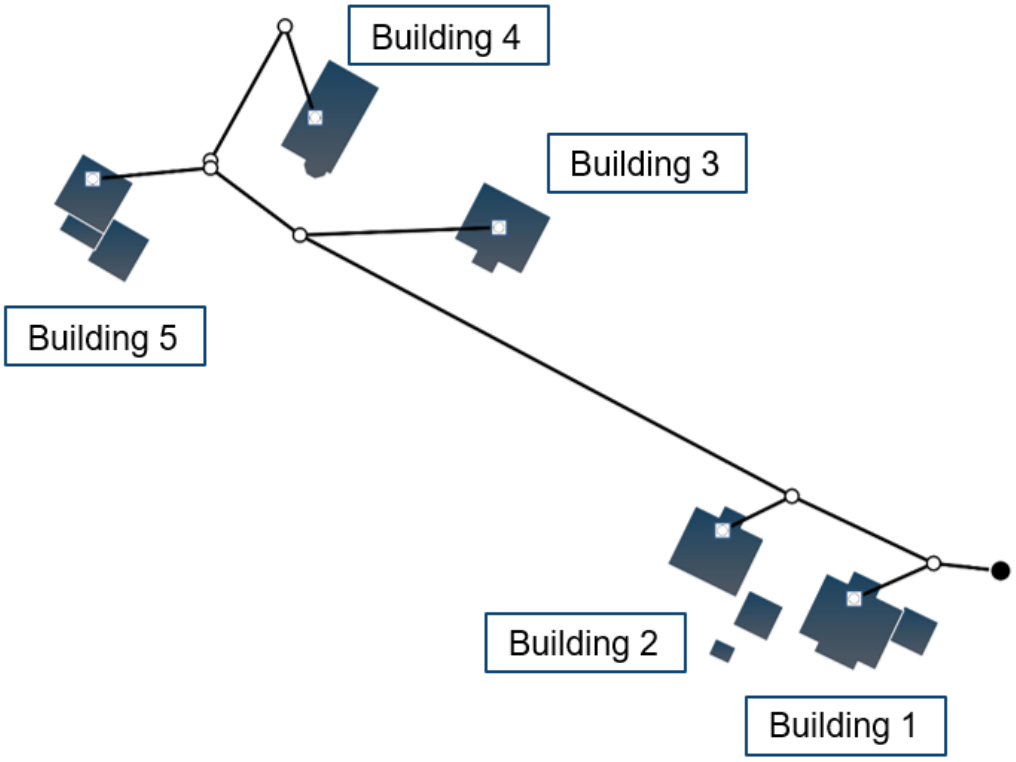

Figure 4-1: Schematic representation ofthe test case layout.

The buildings are modelled after real world data, and thus faithfully represent a generic cluster of suburban housing in Germany.

Table 8: Test Case 3 building description

Parameter	Residential units	Heated living area [m^2]	Yearly heat demand [kWh]	Yearly electricity demand [kWh]
Building 1	4	284.98	51574	10994
Building 2	1	228.15	36323	4170.1
Building 3	1	228.15	37600	3185.3
Building 4	1	197.93	32788	3829.8
Building 5	1	150.49	26221	1783.3

The available technologies are depicted in Table 9. For practical reasons, the roster is limited from all the options available in the model. This is done as a result of previous

runs, where the cheapest technologies come out as the chosen ones. It allows for faster executions, which simplify the model validation and result analysis process. Additionally, and for the same reason, none of the renovation measures are considered in the test case.

Table 9: Technologies enabled for investment in Test Case 3.

Conversion technology	Input energy	Output energy
PV	Solar irradiation	Electrical power
Electrical heating	Electrical power	Heat
Heat pump (AA, AW, GA)	Electrical power/Gas	Heat
Gas condensing boiler	Gas	Heat
Combined heat and power (CHP)	Gas	Heat, Electrical power
Lithium-ion Battery Storage System (BSS)	Electrical power	Electrical power

4.1.2 Impact of BSS technology

The impact of BSS installation is measured in this analysis through several metrics to test the hypothesis drawn out in chapter 4.1 are the following.

4.1.2.1 Performance metrics

Firstly, on the economic aspect, the most important metric is the *threshold cost of adoption*. This translates as the maximum cost which makes adoption of a technology cost-effective. It is of importance because it can be used in conjunction with market price projections, to predict the point of mass adoption for consumers.

Secondly, the *total cost at adoption* for each building is analyzed. This should always be lower than the total cost without the BSS; otherwise the solution would not be optimal.

Thirdly, from the technological side, the *installation and operation* are worthy of analysis. The sizing of the system, as well as the capacity/energy ratio, gives valuable insights. In addition, the operation of the BSS is of relevance for two reasons: firstly, it can validate

or disprove the hypothesis of smooth operation in self-consumption applications (as opposed to aggressive operation, typical of reserve provision); secondly, it allows for an accurate lifetime calculation through application of a cycle counting method. In this work the Rainflow algorithm is used. The capacity/energy ratio is used as an indicator for identifying unreasonable solutions.

4.1.2.2 Result analysis – Costs

The cost parameters of BSS technology play a decisive role in the optimality of the total system. Because the technology enables the storage energy not consumed immediately, and because of the difference between grid electricity cost and generator feed-in tariffs, it influences all electrical conversion within an energy hub. Therefore the impact of BSS cost parameters is non obvious, for it comes indirectly through complementing other installed technologies.

This section analyzes the impact of modifying the values of the storage costs function coefficients from Table 5. From this function (4-1) the fixed and variable costs of the BSS can be extracted.

$$K(C_{inst}) = CAPEX_{var} * C_{inst} + CAPEX_{fix} \quad (4\text{-}1)$$

The values tested are shown in Table 10 and Table 11.

Table 10: Sensitivity analysis values for fixed cost of BSS

Name	Base value	Variation over base value [rel]	Variation over base value [abs]	Final value	Units
$K_{fix,2}$	3000	-75%	-2250	750	[€]
$K_{fix,3}$	3000	-80%	-2400	600	[€]
$K_{fix,4}$	3000	-85%	-2550	450	[€]
$K_{fix,5}$	3000	-90%	-2700	300	[€]

Table 11: Sensitivity analysis values for variable cost of BSS

Name	Base value	Variation over base value [rel]	Variation over base value [abs]	Final value	Units
$K_{var,2}$	800	-75%	-600	200	[€/kWh]
$K_{var,3}$	800	-80%	-640	160	[€/kWh]
$K_{var,4}$	800	-85%	-680	120	[€/kWh]
$K_{var,5}$	800	-90%	-720	90	[€/kWh]

The results are displayed in Figure 4-2. The first clear point to extract is the fact that the original considered costs are too high for adoption at consumer level in our model. By lowering the costs substantially, it is seen that at 20% of the original cost (an 80% reduction) the first building adopts the technology. The other buildings follow suit as the cost decreases even more, reaching the *full adoption point* at 5% of the original cost. For clarity, when comparing the overall cost of each building from one BSS cost to another, values over 25% of original cost have been omitted, as they are equal to the result at 25% cost.

The results show a clear trend: the higher the electrical demand, the higher the price a consumer is willing to pay for an installation of a BSS. Take the difference between Building 1 and Building 2: Building 1, with a substantially higher energy demand, is able to make the investment profitable at 20% of base cost; Building 5 on the other hand barely makes a difference in its overall result, even when the BSS is 95% cheaper than the base cost. This is reasonable given that the gains do not come from the BSS itself, but rather from allowing more PV generation to be harnessed and less grid electricity to be consumed. Since its operational cost is null, it is essentially an investment problem: a building with a higher demand gives the investment more use; thus it distributes the cost of a BSS over more energy units, and is therefore willing to adopt at higher prices.

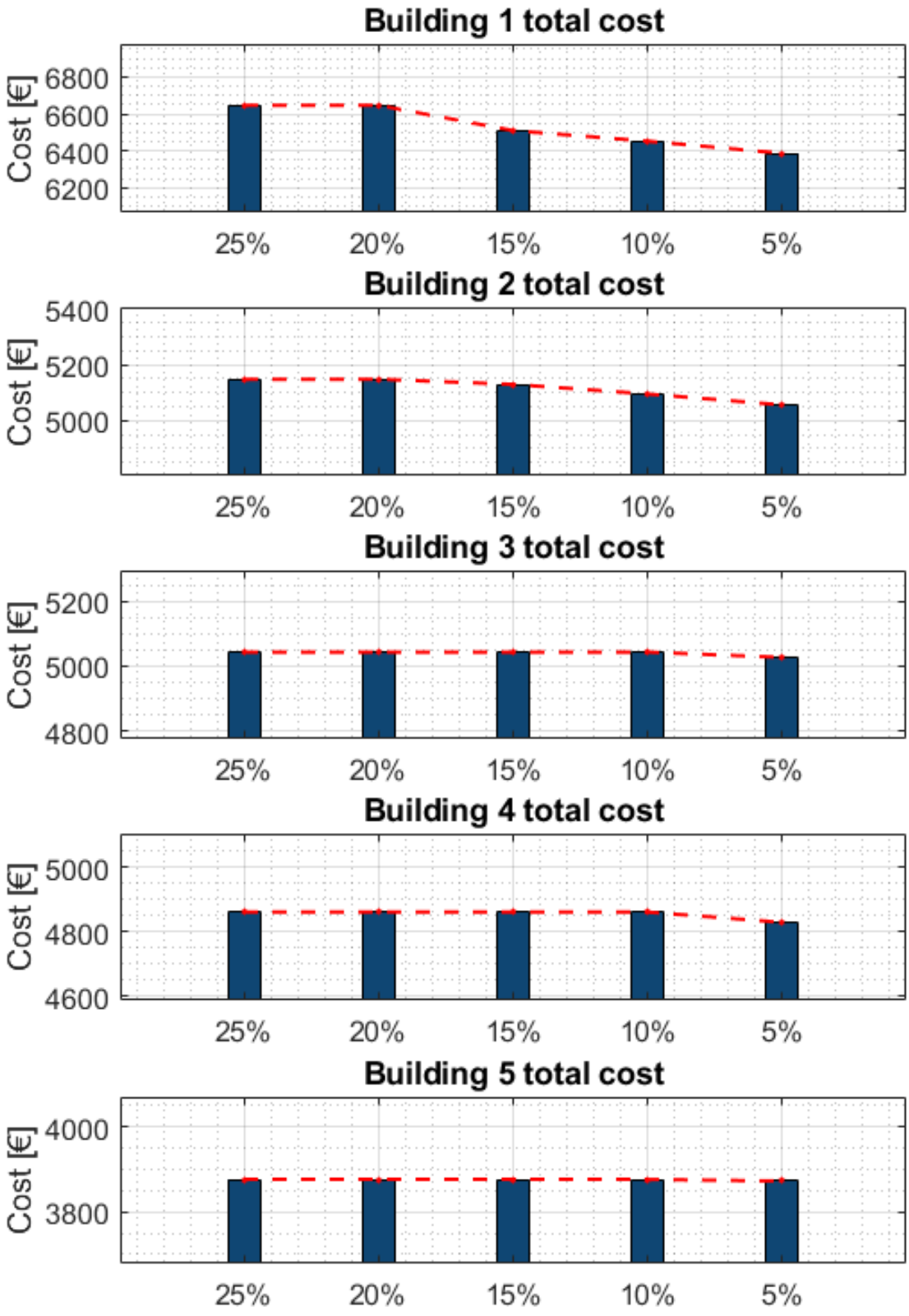

Figure 4-2: Total optimization cost for test case as function of BSS cost decrease.

4.1.2.3 Result analysis – BSS operation

From this point on, the analysis is carried out fixing the BSS cost at the values expressed in (4-2). From section 4.1.2.2, we obtained the cost function as (4-2).

$$K_{full}(C_{inst}, P_{inst}) = 42 * P_{inst} + (80 * C_{inst} + 300) + 750\ [€] \qquad (4\text{-}2)$$

These values were obtained subsequently lowering the costs until more than half of the buildings adopted the BSS technology, allowing for comparison between them. Table 12 shows the values of power and capacity installed under the assumed costs.

Table 12: BSS installation values

Building	Power [kW]	Capacity [kWh]	Cap/P ratio [h]
Building 1	5.55	16.66	3
Building 2	2.76	8.14	2.56
Building 3	0	0	-
Building 4	2.34	6.55	2.93
Building 5	0	0	-

As the results show, the capacity/power ratio stays slightly over the estimated 2-2.5h, which indicates the results are reasonable in terms of sizing.

In terms of operation, sample profiles from the three installed BSS operations are shown in Figure 4-3, Figure 4-4, and Figure 4-5.

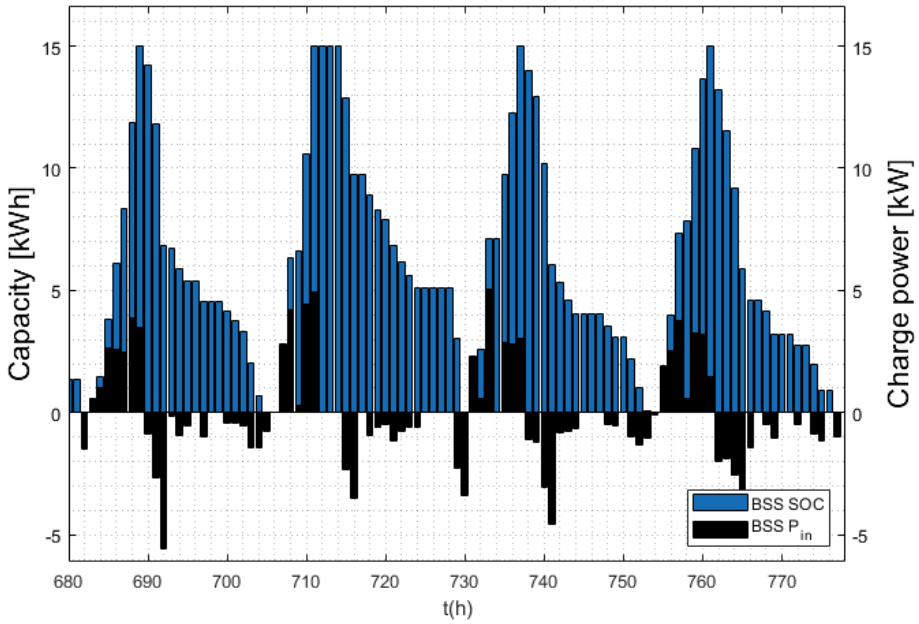

Figure 4-3: Exemplary BSS operation in peak demand winter days, building 1.

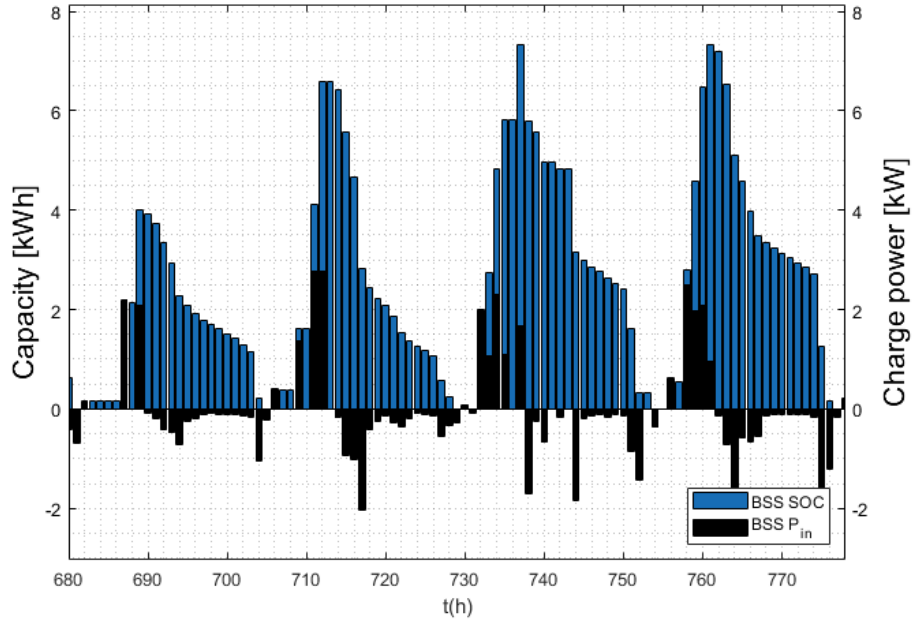

Figure 4-4: Exemplary BSS operation in peak demand winter days, building 2.

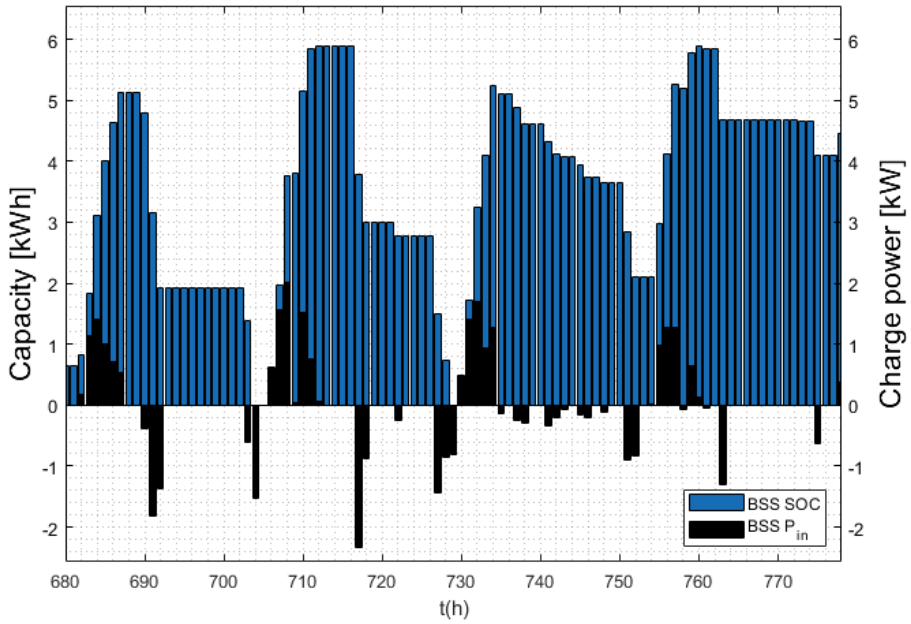

Figure 4-5: Exemplary BSS operation in peak demand winter days, building 4.

The yearly energy throughput is easily obtained by integrating either the charge power profiles or the discharge power profiles (As the system starts with 0% SOC and it would not be optimal to end the year with leftover charge, the magnitude of both integrals is equal).

In a discrete time operation, the total energy throughput is calculated as (4-3):

$$E = \sum_{t=1}^{T} (x_t^{el_{in}} - x_t^{el_{out}}) \Delta t \tag{4-3}$$

A rough approximation of the number of equivalent cycles is obtained by dividing the total energy throughput of each BSS by its installed capacity (4-4):

$$N_{eq,i} = \frac{E_i}{Cap_i} \quad \forall\, i \in 1 \dots B \tag{4-4}$$

The values obtained for each building are displayed in Table 13.

Table 13: Yearly BSS energy throughput

Building	Energy throughput[kWh]	Capacity [kWh]	Equivalent cycles
Building 1	2816.00	16.66	169.08
Building 2	1513.30	8.14	185.95
Building 3	0	0	-
Building 4	1116.28	6.55	170.41
Building 5	0	0	-

These results already give a sense of the relative smoothness of operation of the BSS.

However, the total equivalent cycle calculation described proves a very rough approximation. A more accurate counting comes from the application of the Rainflow algorithm. When applied to each buildings' installation, a DOD-dependent cycle count can be established. This allows for more accurate lifetime calculations if required.

Figure 4-6, Figure 4-7 and Figure 4-8 give a detailed cycle count for each of the three installations. From these data two conclusions can be inferred.

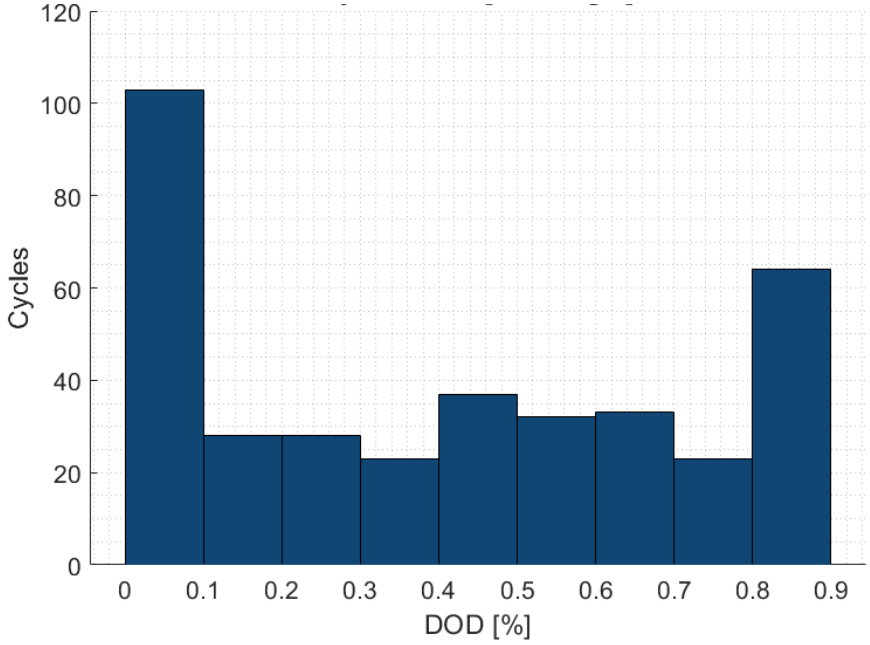

Figure 4-6: Rainflow cycle count based on DOD, Building 1.

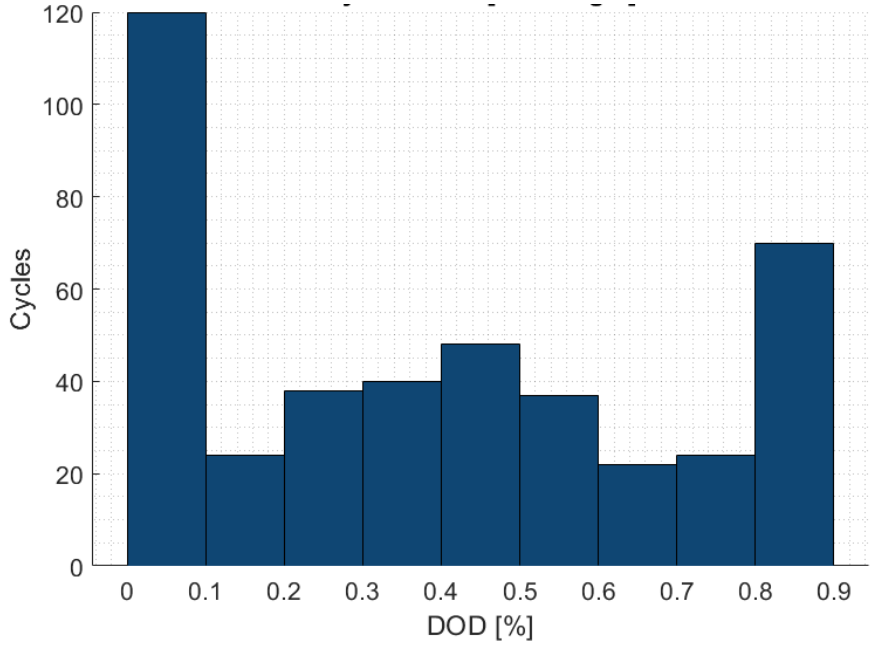

Figure 4-7: Rainflow cycle count based on DOD, Building 2.

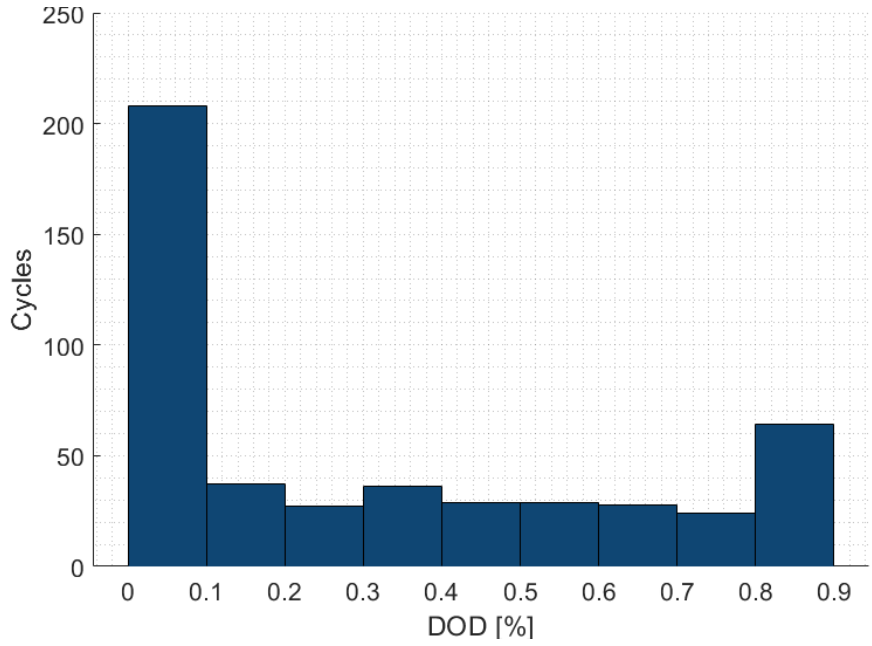

Figure 4-8: Rainflow cycle count based on DOD, Building 4.

The first is that, as assumed previously, the approximation of equivalent cycles from (4-4) is not accurate. In fact, a large portion of the cycling is made up of very shallow charge/discharge decisions. Therefore we can assume that the approximate equivalent cycle serves as an over-estimator of the actual cycling degradation of the BSS. It has the advantage of providing a conservative estimate, but it lacks accuracy.

4.1.2.4 Result analysis – Impact on PV installation

In addition the impact of the BSS on PV is of great interest, as it is hypothesized to be one of the sources of cost efficiency from the installation of BSSs. This impact is measured with the help of four metrics: PV power installed, operation profiles, and self-sufficiency ratio.

The installed PV power values can be observed in Table 14. The increase in installed power is clearly visible in the buildings that adopt a BSS. This increase is the main driving factor behind the energy (and cost) savings for the buildings, since it reduces the levelized cost of energy (LCOE) of the PV generation. The more power that can be harnessed translates into more savings, once the increase in installation costs is offset.

Table 14: Increase PV power installation with BSS

Building	PV power (no BSS)	PV power (BSS)	Variation	Variation
Building 1	8.64 kW	10.76 kW	2.12 kW	+24.5%
Building 2	3.20 kW	5.97 kW	2.77 kW	+86.6%
Building 3	1.76 kW	1.76 kW	0	-
Building 4	1.69 kW	3.86 kW	2.17 kW	+128.4%
Building 5	1.47 kW	1.47 kW	0	-

It is worth noting that the impact on building 1 is substantially lower than on the other BSS adopting buildings. This is because Building 1 has reached its maximum allowed installed PV power. This power is limited by the available roof area, assuming 8 m^2 of PV panels are capable of generating 1 kWp of electric power.

The impact on generated PV is predictable upon seeing the increase in installation. Since solar irradiation is equal in both scenarios, the generated PV power is always proportional, with a larger installation simply implying more area under the curve (Figure 4-9).

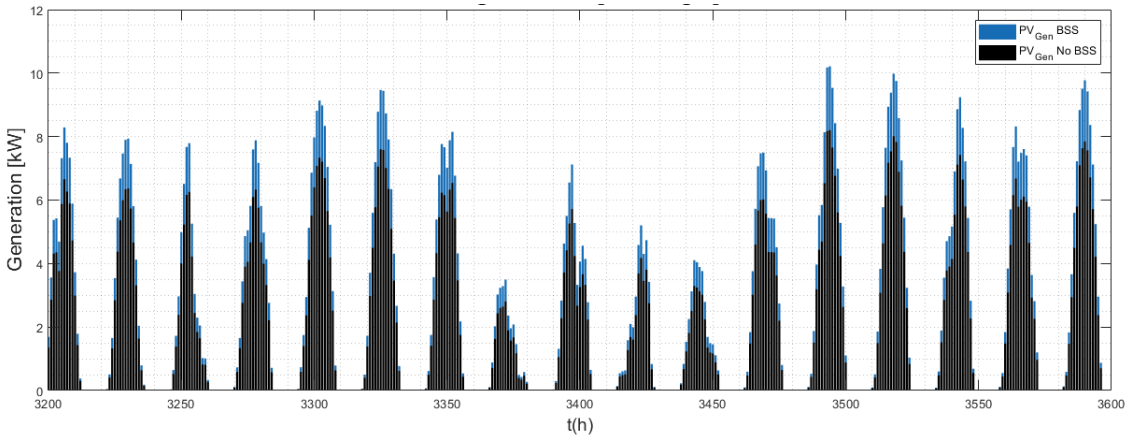

Figure 4-9: PV generation, summer days, Building 1.

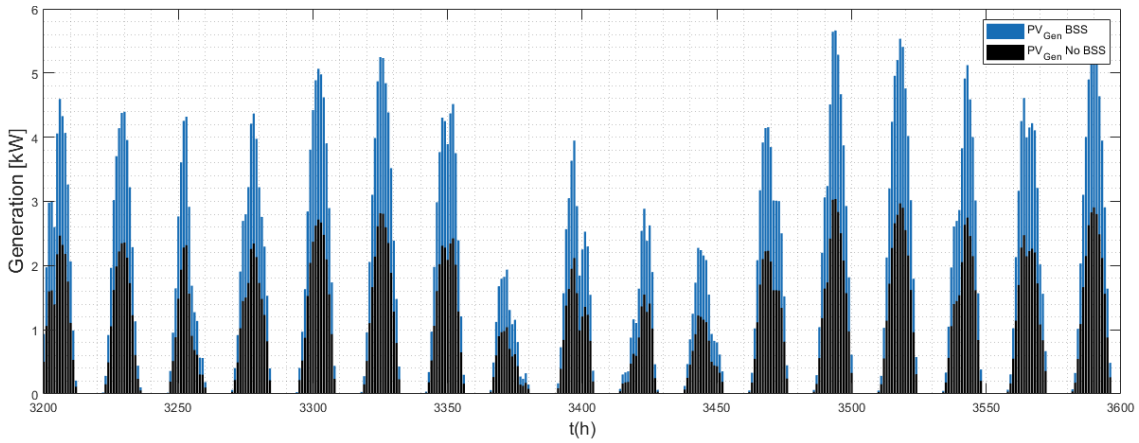

Figure 4-10: PV generation, summer days, Building 2.

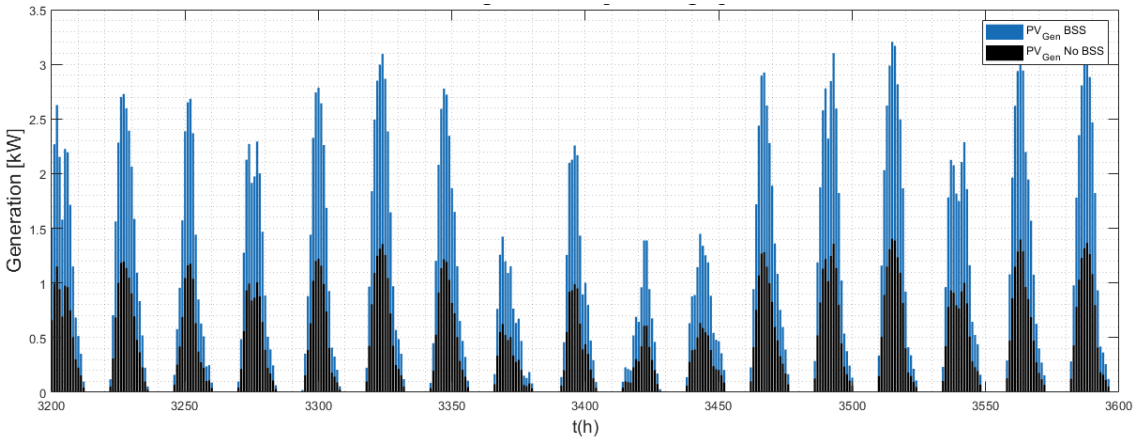

Figure 4-11: PV generation, summer days, Building 4.

This increase in generation should however be measured accounting for the local demand. In cases where local generation is higher than local demand, energy exports occur. When this is the case, circumstances may arise which compromise the functioning of the distribution grid, such as over voltages and reverse power flows. Therefore it is reasonable to install self-generation to a sizing which is roughly on par with demand.

To this end the Self-Sufficiency Ratio (SSR) is defined. As (4-5) shows, it is a simple calculation comparing the total PV generation to the total electrical load over a given time period.

$$SSR = \frac{\sum_{i=1}^{t} PV_{Gen,i}}{\sum_{i=1}^{t} D_{el,i}} \qquad (4\text{-}5)$$

A value lower than 1 denotes a *net importer* of electricity. A value of 1 would characterize a potentially self-sufficient household. A value over 1 denotes a *net exporter* of electricity.

It should be noted that it is a global measure, and not a time-specific one. This means that a value over one denotes a system that *could* be self-sufficient in terms of energy, but not necessarily is. While the total amount of energy generated can cover the total demand over that time period, the timing forces the system to export excess energy and import required energy when local demand and generation do not line up.

It is also important to note that SSR does not take into account the cost of energy, only the total amount of generation. Therefore when optimizing a system for CO_2 emissions for example, it can be a bad measure of emissions avoided [SUN18].

Lastly, the installation of other technologies can affect the calculation and value of the SSR. When electrical heating systems are in place, which draw electric power to cover heat demand, their consumption should also be considered in the calculation.

For the purpose of this analysis, the cost optimality is guaranteed by the optimization tool; therefore SSR is a good measure of BSS-PV synergy; and additional installations of electrically-powered heating systems are taken into account.

The values for SSR of the buildings with installed BSS are displayed in Table 15.

Table 15: Impact of BSS installation on SSR

Building	SSR (no BSS)	SSR (BSS)
Building 1	0.763	0.951
Building 2	0.746	1.39
Building 3	0.475	0.475
Building 4	0.351	0.801
Building 5	0.801	0.801

The results show diverse behaviors from the buildings that choose to install BSSs. Building 1 becomes almost a net exporter; however due to its nature (4 family house), the ratio of available roof area to electrical demand is lower than in single family homes. Building 2 is able to become a net energy exporter, even if at times it is importing power from the grid. Building 4 shows a clear increase in energy output.

These results become especially relevant when considering the limitations that grid operation imposes (see section 4.2.3).

4.1.2.5 Result analysis – Impact on imported grid electricity

The largest source of savings from the installation of the BSS come from the possibility to shift PV generation with null cost of operation to times when the households otherwise would be forced to rely on costly grid electricity. From the point of view of the consumer, this is the main point of interest. Therefore the impact of BSSs on the consumption of grid electricity should be analyzed.

To this end the total energy drawn over the course of a year is compared. The values are given in Table 16.

Table 16: Variation in yearly imported grid electricity.

Building	GE demand (no BSS)	GE demand (BSS)	Variation (abs)	Variation (rel)
Building 1	7267.7 kWh	4178.6 kWh	3080.2 kWh	-42.38%
Building 2	2978,9 kWh	1194,3 kWh	1784.7 kWh	-59.91%
Building 3	2384,4 kWh	2384,4 kWh	0	-
Building 4	3069,9 kWh	1596,9 kWh	1473.0 kWh	-47.98%
Building 5	1259.3 kWh	1259.3 kWh	0	-

As can be seen the reliance on grid electricity is greatly reduced in all adopters of BSSs. It is especially notable, as with previous results, in Building 2, where the solar installation is capable of covering most of its own demand on PV alone.

The operation curves of withdrawn grid power are also of interest. The usage of BSS allows for the peaks to be reduced .This is especially important for the consequences it brings when considering grid constraints (see section 4.2.1). It is clearly visible in Figure 4-12 , Figure 4-13 and Figure 4-14.

Figure 4-12: Grid electricity withdrawn, winter days, Building 1.

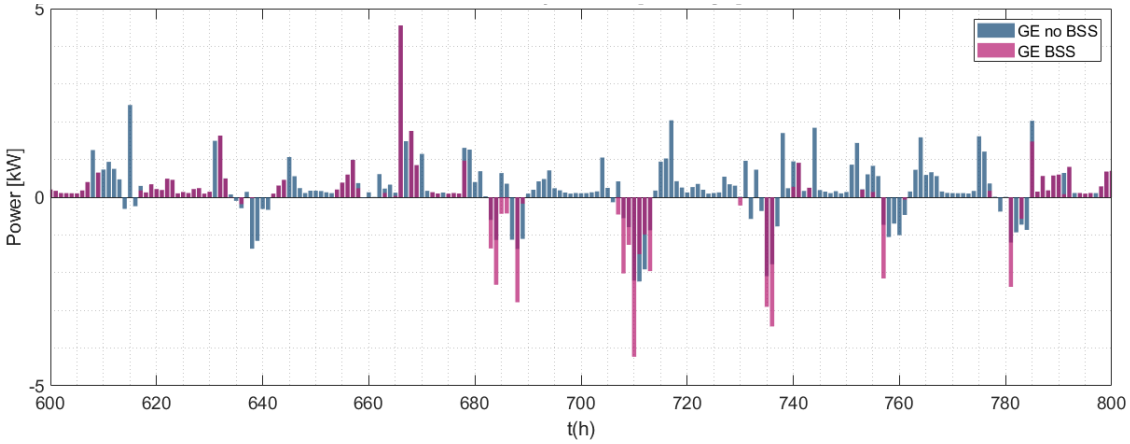

Figure 4-13: Grid electricity demand, winter days, Building 2.

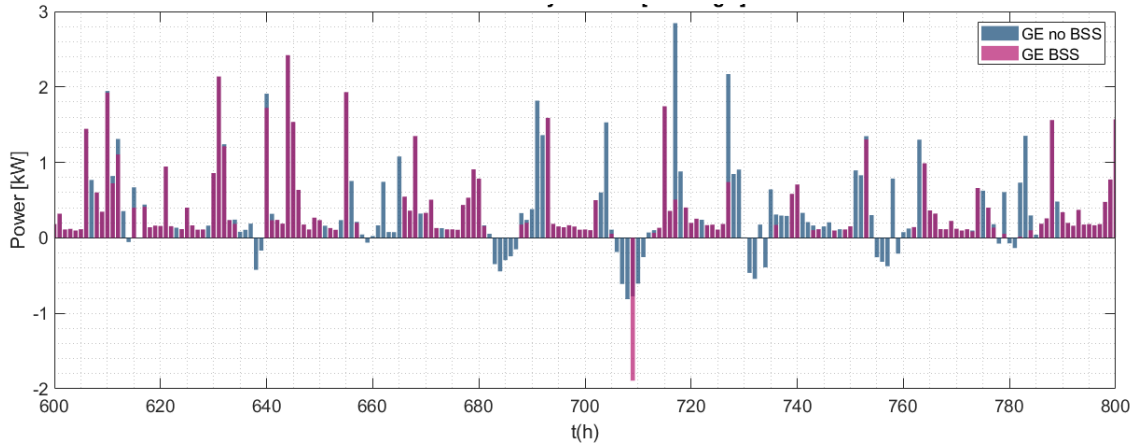

Figure 4-14: Grid electricity withdrawn, winter days, Building 4.

The operation clearly shows how, in periods of high demand and available PV generation, the power drawn from the grid is much less. However the BSS also indirectly enables large power injections into the grid. This is at the core of the dichotomy between user and grid operator interests when it comes to BSS investments: on the one hand, it allows for lowering of the demand, meaning less peak power drawn from the grid in general. On the other, it enables larger DER installations, which in turn inject more power into the grid. This point is analyzed further in Section 4.2.3.

4.2 Distributed BSS and grid congestion management

The second exemplary use case examined in this work is the potential of domestic battery storage systems to serve the DSOs for alleviation of grid congestions. These congestions are primarily caused by the consumers drawing large amounts of power simultaneously. This situation is unlikely to occur in current operation; since grid capacities are construed with sufficient safety margins and accounting for potential demand increases throughout the lifetime of the investment. It is however possible in a potential all-electrical system in the future. However the demand profile of any given household can change dramatically with the installation of DERs. In particular, the switch from a fuel-burning heating technology to an electric heating technology, such as electric water boilers and heat pumps causes the heat demand to effectively become electrical load. As seen in Table 8, the increase is not of a fraction, but rather of a multiple of the electric load.

What this implies for the DSO is a massive increase in loading of the distribution transformers and lines that feed into a given neighborhood. This can be seen in a real test

scenario applied to the test case in Figure 4-17. The case in point is an optimized installation of technologies for the neighborhood of the test case; however the technology roster is limited to electrically powered technologies. While this seems unreasonable at the light of previous obtained solutions, where gas-powered heating is a major part of the solutions, it is a realistic scenario in the case of an increase in cost of fuel due to, for example, a new carbon tax.

4.2.1 Impact of grid constraints

To analyze the role of BSS solutions in these situations, first the impact of grid constraints should be quantified. In this section the results of running the optimization routine under the condition of limited grid utilization are analyzed. The impact for the consumer, in cost, is quantified as the difference between the optimal costs without grid constraints (relaxed problem solution) and the costs with grid constraints (constrained solution).

To achieve line constriction, two options are available. The first, and more obvious one, is to define a much larger test case than the one described in 4.1.1. This is an easy solution, as the available dataset encompasses hundreds of buildings. However from the point of view of algorithm execution, the memory use and especially the long run times are limitations which must be contested with.

The other, less straight-forward approach is to reduce the carrying capacity of the elements of the distribution grid being simulated. This allows for a scaled-down analysis that maintains the thermal and electrical load characteristic curves, and all building features, to remain the same. For a given building that is part of a radial network, whether a line congestion occurs at its doorstep or at the neighborhood feeder main is indifferent. The effect both of these situations have on a consumer is that the power available to be withdrawn is limited, given that the DSO puts containment measures in place once the congestion is detected.

A different problem is how the effect of congestion is distributed among the different consumers connected to the network. This is covered more in detail in the result analysis in Section 4.2.1. As a basic rule, the further from the feeder a customer connection is, the more line sections are in the path between the two connection points. This allows for congestion to take place in more places, and forces the costumer to interact with all other customers connected along that path. This is illustrated in Figure 4-15.

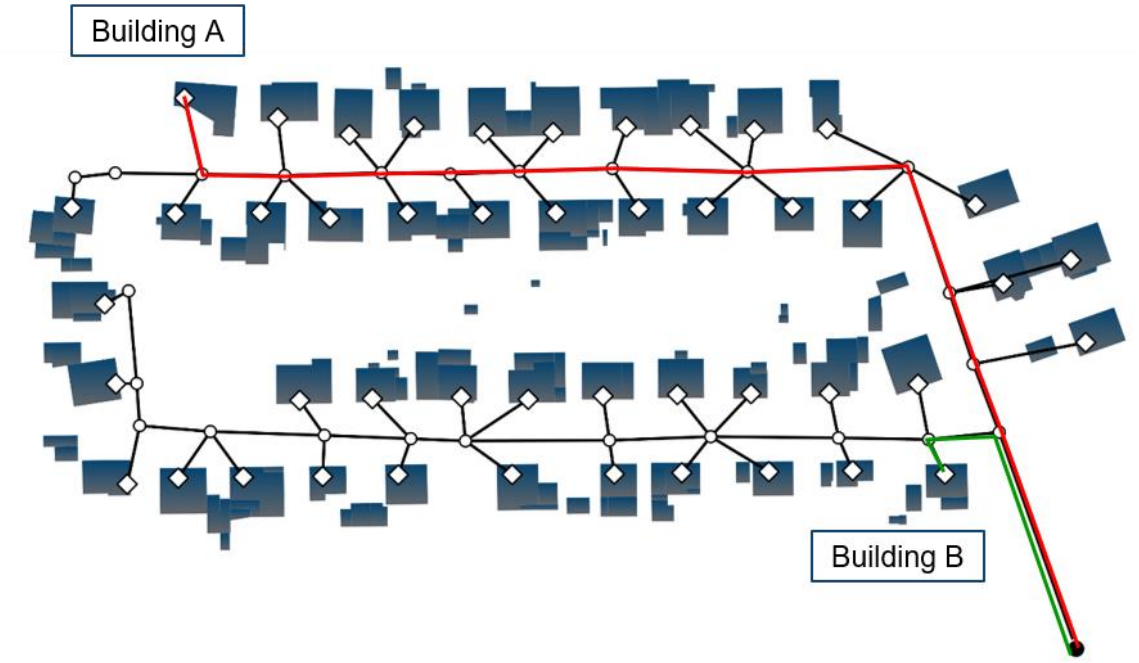

Figure 4-15: Comparison of paths from feeder to consumer: Building A (red), Building B (green)

In the figure, Building B is only affected by potential congestion in three sections of line; conversely, Building A is affected by 13 sections of line. This is also easily observable when looking at the PTDF matrix for a given network: the more non-zero elements in a column of a matrix, the more line limits are involved in restricting flows from/into the corresponding bus.

The expectation is, therefore, for the buildings further away (both in distance and in line length) from the feeder to be more affected by the modelled grid constraints when congestion is forced onto the test case.

The degree of congestion is determined by the *congestion factor* (CF): this is a parameter that is fixed as an input to restrict the capacity of the lines as seen by the building nodes in the integrated optimization routine. The CF is defined in equations (4-6) - (4-8) as:

$$\sum_{i=1}^{b} PTDF_{j,i}\left(P_g^i - P_d^i\right) \leq CF * L_{lim,j} \quad \forall\, j \in 1 \dots L \tag{4-6}$$

$$\sum_{i=1}^{b} PTDF_{j,i}\left(P_d^i - P_g^i\right) \leq CF * (-L_{lim,j}) \quad \forall\, j \in 1 \dots L \tag{4-7}$$

$$0 \leq CF \leq 1 \tag{4-8}$$

The CF can be seen as the percentage of a line usable, which effectively simulates a smaller line capacity. In normal operation, the lines rarely reach a total utilization higher than 25%, as seen from the result of the relaxed optimization. This entails that for line constraints to be active, the CF has to move at or below 25%. However CF factors that are too low can result in an infeasible problem.

With this information the value of CF is subsequently lowered searching for the window of values for which the grid constraints are active, and the problem is still feasible. At 15% CF the problem becomes infeasible, because there is no technical way to cover demand. Above 25% the line constraints are inactive. Therefore an analysis case is defined with value of CF 20%.

This value is reached after testing the power injections obtained without modelling the grid with the PTDF matrix generated from the test case (4-9).

$$PTDF_{Test\ Case} = \begin{pmatrix} 0 & 0 & 0 & -1 & 0 & 0 & -1 & 0 & 0 & 0 & 0 & 0 \\ 0 & 0 & 0 & -1 & 0 & -1 & -1 & 0 & 0 & 0 & 0 & 0 \\ -1 & -1 & -1 & -1 & -1 & -1 & -1 & -1 & 0 & -1 & -1 & -1 \\ 0 & -1 & -1 & -1 & -1 & -1 & -1 & -1 & 0 & 0 & -1 & -1 \\ 0 & 0 & -1 & -1 & -1 & -1 & -1 & -1 & 0 & 0 & 0 & -1 \\ 0 & 0 & 0 & -1 & -1 & -1 & -1 & -1 & 0 & 0 & 0 & 0 \\ 1 & 0 & 0 & 0 & 0 & 0 & 0 & 0 & 0 & 0 & 0 & 0 \\ 0 & 1 & 0 & 0 & 0 & 0 & 0 & 0 & 0 & 0 & 0 & 0 \\ 0 & 0 & 0 & 1 & 0 & 0 & 0 & 0 & 0 & 0 & 0 & 0 \\ 0 & 0 & 0 & 0 & 1 & 0 & 0 & 0 & 0 & 0 & 0 & 0 \\ 0 & 0 & 1 & 0 & 0 & 0 & 0 & 0 & 0 & 0 & 0 & 0 \end{pmatrix} \quad (4\text{-}9)$$

The PTDF in this test case shows one peculiarity: its elements are all 1, 0 or -1. This is due to the radial structure of the network: if power is injected in any node and drawn at the feeder, there is only one path connecting the two points. Therefore the power flow is not split between branches, which would render fractional elements.

The first analysis to consider is the impact of grid constraints in consumer cost.

4.2.1.1 Result analysis – Cost for customers

For cost analysis, the same test case as described in section 4.1.1 is used. The individual cost for each building is compared with and without grid constraints applied, as well as the distribution of costs among the buildings.

The basic expected impact of grid constraints can be summed up in two different actions. The first one is the shift from electric heating technologies to fuel-burning technologies. This is due to the extreme heating demand peaks occurring in the coldest days of winter. Since the cold temperatures apply to all buildings, a situation where all rely on electric heating causes the lines to overload repeatedly over a series of days (Figure 4-20). Therefore the solution comes from shifting some of the heating demand coverage to gas or biomass burning technologies. Alternatively a shift to more efficient electrical technologies such as ground heat pumps is an option, at an increase in CAPEX by the consumers.

The second one is the restriction on installed PV power and consequently on maximum PV power injected into the grid. This is the only technology capable of generating excess power in large quantities cost-efficiently, due in large part to the feed-in tariff in place. This is, there is an incentive to produce more power than is required instantaneously for it can be sold at a profit.

In this test case fuel burning technologies are included. Therefore some consumers adopt them when it suits, and the heating demand does not overload the grid. Thus no change in heating technologies is observed. The PV change is observed, as across the board all consumers install smaller PV systems. Table 17 presents the change in PV adoption decisions when line congestion restrictions are considered.

However even with visible changes in PV installation, the overall cost is barely affected.

Table 17: PV installation in presence of grid constraints

Building	No grid constraints [kWp]	Grid constraints [kWp]	Variation [kWp]	Variation [%]
Building 1	8.636	7.414	-1.222	-14.15%
Building 2	8.613	8.613	0	0%
Building 3	1.759	1.557	-0.202	-11.49%
Building 4	7.855	6.508	-1.347	-17.15%
Building 5	5.681	5.681	0	0

4.2.2 Impact of BSS on unconstrained power flows

The analysis of BSS utilization to mitigate line constraint violation starts with analysis the impact of the BSSs on the unconstrained line flows. There are two hypothesized ways the BSS may influence load flows: On the one hand, as the BSS allows for flatter demand profiles, it could be expected that individual households reduce their peak demand, relieving the grid of some of the pressure of the line flows from the feeder to the consumer. On the other hand, as shown in section 4.1.2.4, it enables larger installations of PV power. This in turn entails higher injections of locally generated power at peak points of generation, which could cause overloading in the direction consumer-feeder.

The two hypothesis can be easily tested applying the PTDF line flow calculations to the results obtained from the single building optimization runs, with buildings avoiding and adopting BSS installation, respectively. Figure 4-16 and Figure 4-17 show the results at the most interesting periods of the year, from the line flow point of view.

The first hypothesis holds generally, but does not apply to all points in time. In some time steps in fact, the BSS owners draw more power than they would without the BSS. The second hypothesis is also mostly true: the non-BSS household very rarely injects more power than it would with a BSS; however again we see some points in time where the opposite happens.

While the BSS allows the user for a certain degree of *time arbitrage* with respect to the power drawn from the grid, due to a constant pricing and no imposed shortages (i.e. no active grid constraints), there is no incentive to use the BSS for this purpose. It is always

more profitable to avoid storing grid energy in favor of maximizing usage of cheaper, self-generated PV.

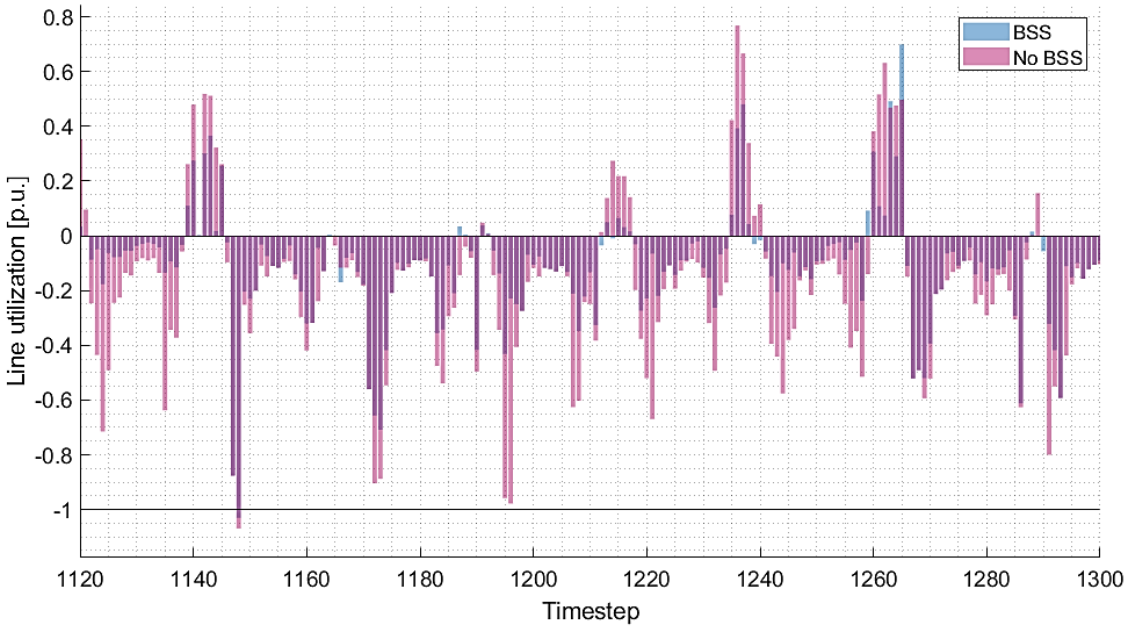

Figure 4-16: Feeder line utilization at 50% CF, winter days

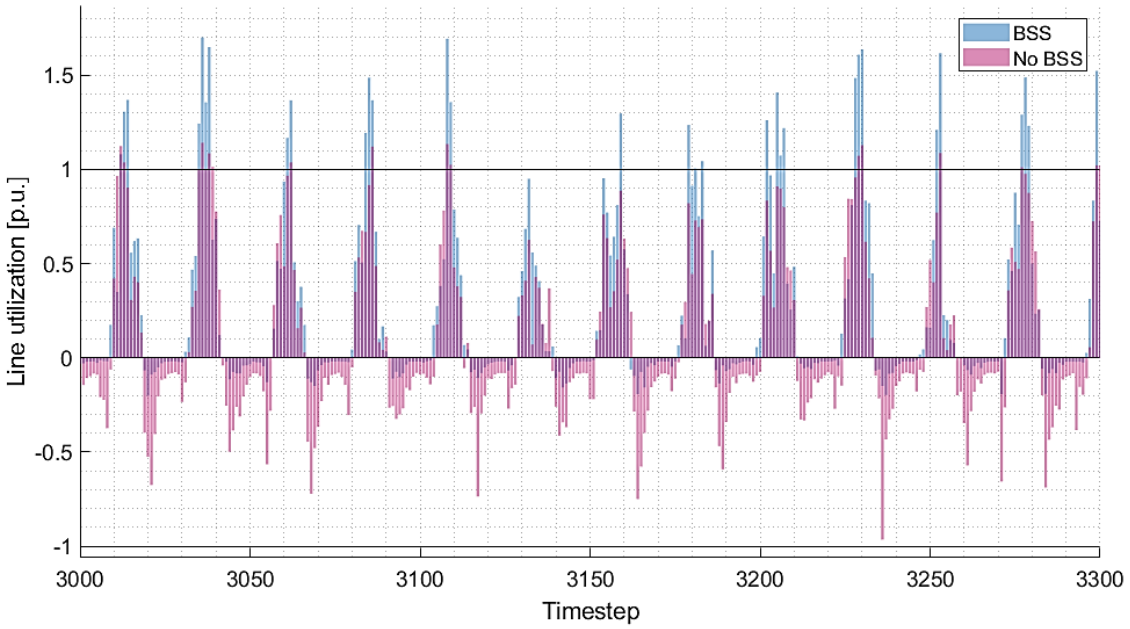

Figure 4-17: Feeder line utilization at 50% CF, summer days

Thus the results yield that the BSS user will not necessarily operate in a way that intrinsically alleviates congestions. In fact, the same behavior as the case without grid constraints is observed: an increase in PV injections generated by larger PV installations, enabled by BSSs.

Therefore the analysis of the role of BSSs in congestion alleviation must be done in a test case which enforces the power flow limits explicitly.

4.2.3 BSS operation in grid-constrained optimization

As shown in the previous section, for the BSS to operate in favor of the grid operation, the constraints must be enforced as part of the optimization problem. The formulation from section 3.3.2 is applied to TC3 with a restricted roster of technologies.

As seen in section 4.2.1 the consumers have a strong preference for fuel-burning DERs when it comes to covering heating demand. This is driven by low operation costs due to cheap fuel. In contrast electrical systems are generally more efficient, but powered with relatively expensive electricity. The modifications to TC3 force the system to operate only on electrically-powered technologies. This is intended to cause the maximum possible line flows by maximum injection/demand at each node. It also avoids the easy switch to fuel-burners, which are always selected over a combination of BSS and electrical heating.

The impact of grid constraints on BSS operation is far from intuitive. To illustrate a test case with forced congestion is analyzed over the next pages.

4.2.3.1 BSS installation

The limits the grid constraints impose on operation are first visible in the adoption pattern of the consumer households. The distribution of BSS capacity and power among the buildings is seen in Figure 4-18.

Two points stand out in these results. Firstly, the BSS adoption is not across the board. Rather, only two buildings end up adopting the systems, at a high individual cost. Secondly, even when the BSS is not being used exclusively for self-consumption purposes, the capacity to power ratio remains in the range of 3, similar to the results obtained when BSSs are adopted purely as a cost improvement measure.

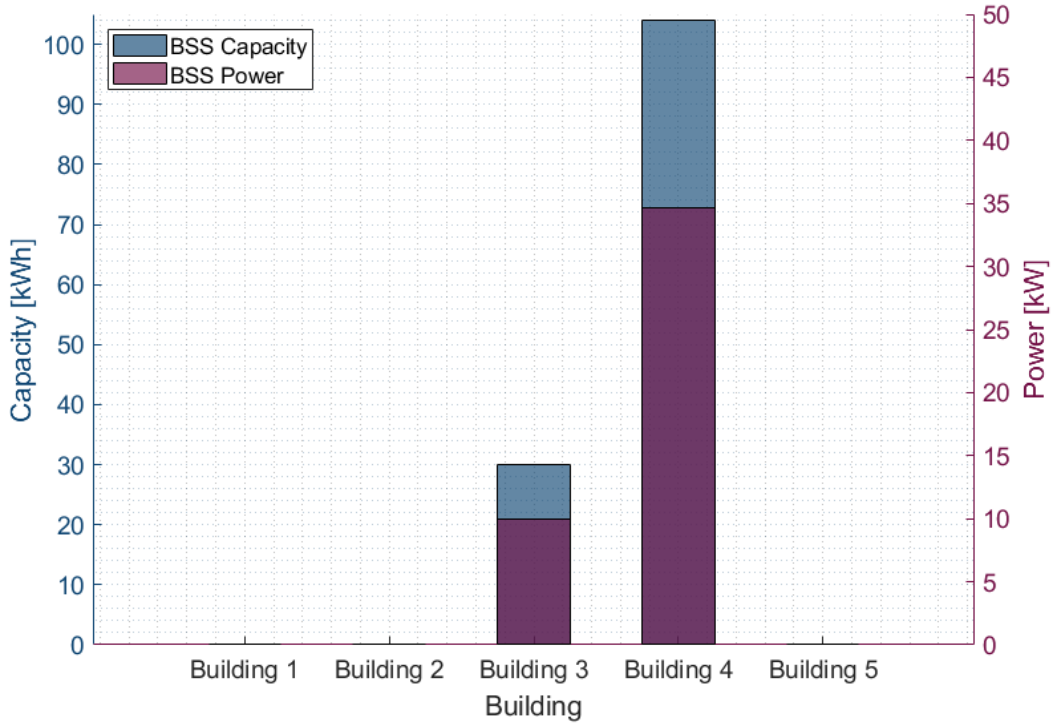

Figure 4-18: BSS installations in grid-constrained optimization

The installation of BSSs entails a severe cost increase for the buildings that are forced to adopt. Figure 4-19 shows the increase in cost the grid constraints cause for the whole system. The purple bars represent the cost of installing the required BSSs, and the blue bars the rest of the increases in cost brought by grid constrained operation. As can be seen, the installation of a BSS is extremely costly and accounts for most of the increase

in cost of the buildings that adopt it. In particular, in the case of Building 4, just the cost of the BSS is more than the overall unconstrained operation cost.

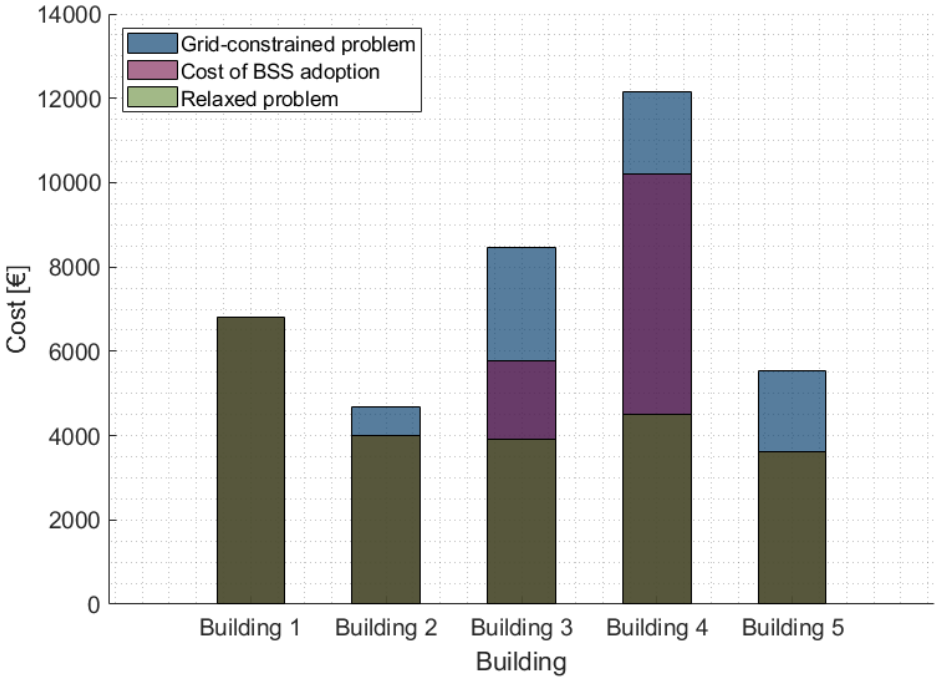

Figure 4-19: Increase in total cost caused by grid constraints

4.2.3.2 BSS operation

Although the circumstance that forces the adoption of BSSs is the insufficient supply of grid energy caused by line congestions, the BSS is still being used to maximize the PV generation that can be harnessed. Therefore the operation is not as straightforward as simply loading the BSS at low grid usage hours and discharging it at high usage hours.

The global optimum of operation has in fact an unintuitive distribution of operation decisions. To exemplify this, exemplary case mentioned in section 4.2.3 is analyzed at the point in time where lines would overload, when applying the results from the relaxed problem.

In the following analyses, first the line connecting to the feeder transformer is analyzed, as it is the only one where overloading is expected to arise. This is as a result of two factors. Firstly, the purely radial structure of the network means all flows outgoing from building nodes will inevitably come together at the sections of line they have in common. In this case, that section is the feeder line. Secondly, Building 1 from the test case has the closest connection to the feeder. Because it is a multi-family home with an important

part of the overall demand, the central lines past Building 1 will never overload before the feeder line, as the power flow through them will always be smaller and the line characteristics are the same. A special attention must be payed to the end connections: these are the consumer-end cables, and have lower loading capacities than the central branches of the grid. However their load flows are determined by the injections or demand of the building at the end node; therefore it is easy to characterize their behavior.

At 20% CF, the grid constraints are active on a limited set of time steps. Most of those time steps suffer line overloading because of an unusually high electricity demand, caused by abnormally low temperatures and across-the-board adoption of electric heating devices.

The other situation at which line overloading may arise is at points in time with high feed-in levels of local generation. This is occasionally the case during summer, where high PV generation peaks align with low demand levels. Since air conditioning is not being considered as an option for technology installation, the overall demand during summer is relatively low. Therefore we see some cases of reverse flow in the feeder line.

To precisely analyze the operation of generation and storage technologies at times of grid congestion, two specific sequences of time-steps are selected. The first one is a winter demand overloading, happening at the end days of January (Figure 4-20). The second one occurs in the beginning of May, and serves as an exemplar for the same situation happening along the other months of summer (Figure 4-21).

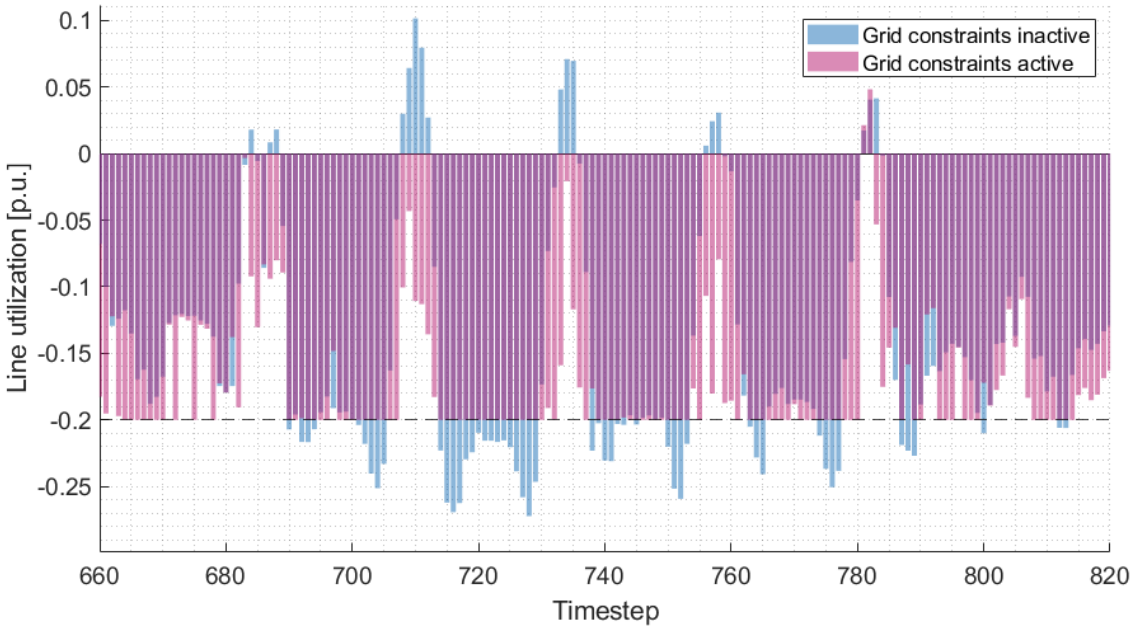

Figure 4-20: Feeder line utilization at 20% CF, critical winter days.

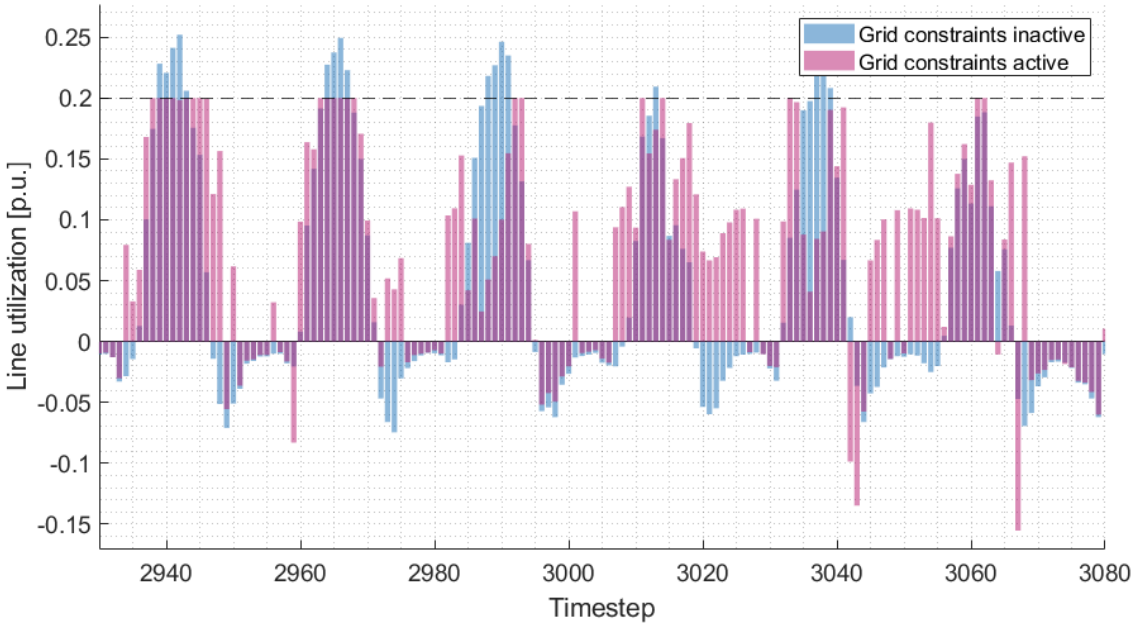

Figure 4-21: Feeder line utilization at 20% CF, critical summer days.

Upon a closer look on the demand-driven congestion, two distinct phenomena arise. The first one is the capping of plow in the direction of the consumers (negative in Figure 4-20). This is to be expected, as it is the objective of the line limit constraints. However the total energy required to meet thermal and electrical demand still comes from the grid. Therefore the consumption must be increased at some other time steps in order to store the

energy in the available storage devices. At the same time, changes in the installed technologies drive different behaviors, so the whole system operation must be analyzed closer.

To this end two time periods are studied in detail. Between time steps 708 and 713, the pairing of grid constraints causes the flow direction to reverse. Between time steps 714 to 732, the flow is capped and load shifting occurs.

The charging of the BSSs in Buildings 3 and 4 between the steps 708-713 is shown in Figure 4-22 and Figure 4-23.

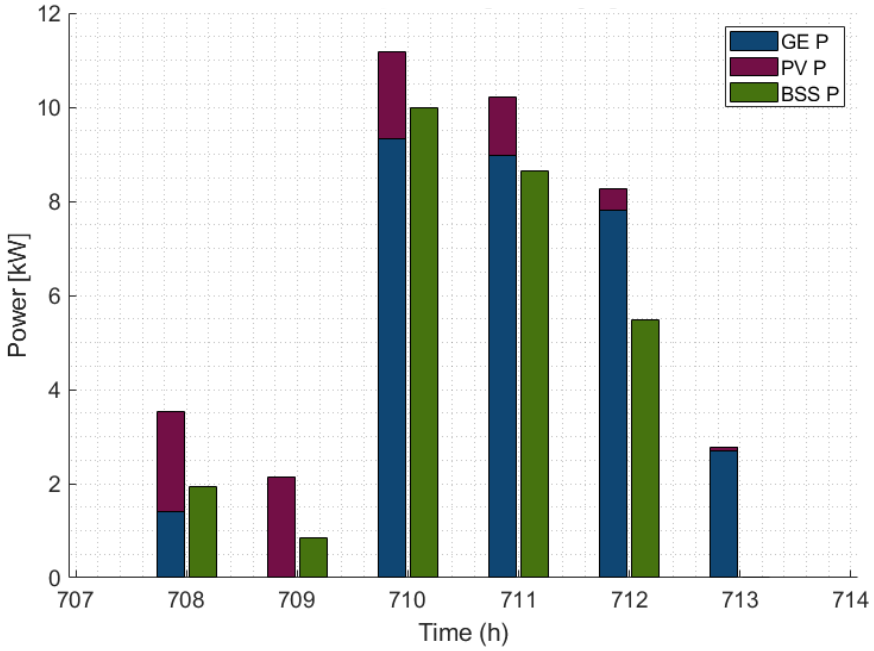

Figure 4-22: Building 3 BSS charging between time steps 708-713.

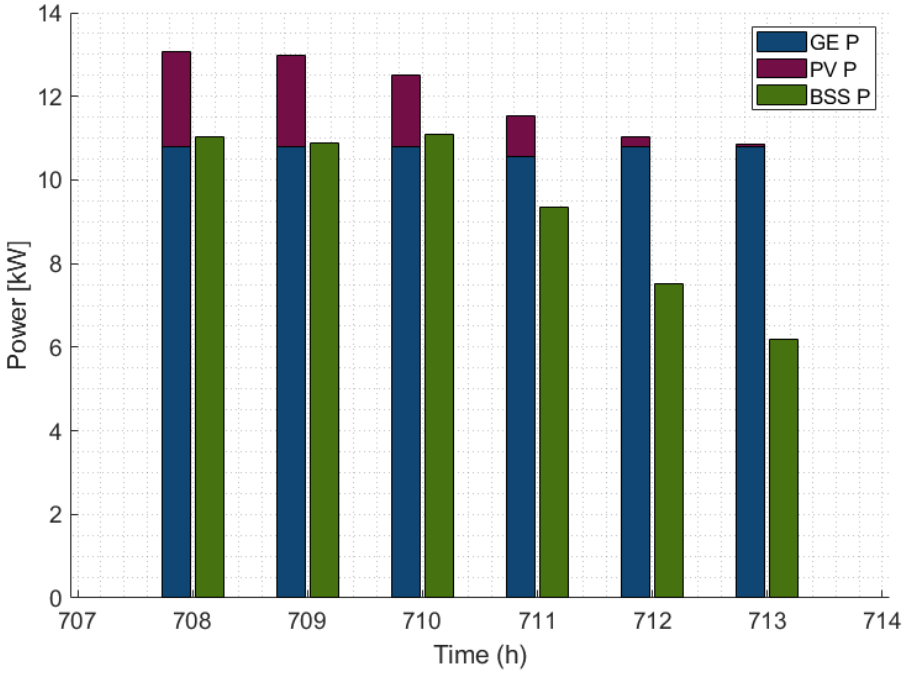

Figure 4-23: Building 4 BSS charging between time steps 708-713.

The stacked bars on the left indicate the grid power withdrawn and the PV power generated, while the green bars on the right indicate the BSS charge power. The difference is the demand being covered at each moment. This grants an insight into the actual operation of the system. In both buildings, at various time steps, the PV power is enough to cover demand, and the excess would in absence of a BSS be fed back into the grid. Therefore in these moments we see the whole grid import is charging the battery. In the remaining time steps the BSS charging power drops but still represents a substantial amount of the energy being fed into the household.

A detail that may pass unnoticed is the fact that, in Building 4, the grid power tops off at the same value in the moments of maximum battery charging. This is no coincidence; there is an implicit limit on the amount of power being drawn. At first sight it may seem that the maximum charge power of the BSS is causing this; while this is technically true, it is not the direct cause. Rather, it is the line limit of the connection from the house to the rest of the grid that is limiting the drawn power. In effect, when looking at the line flow in this particular section, several periods of line congestion are found (Figure 4-24).

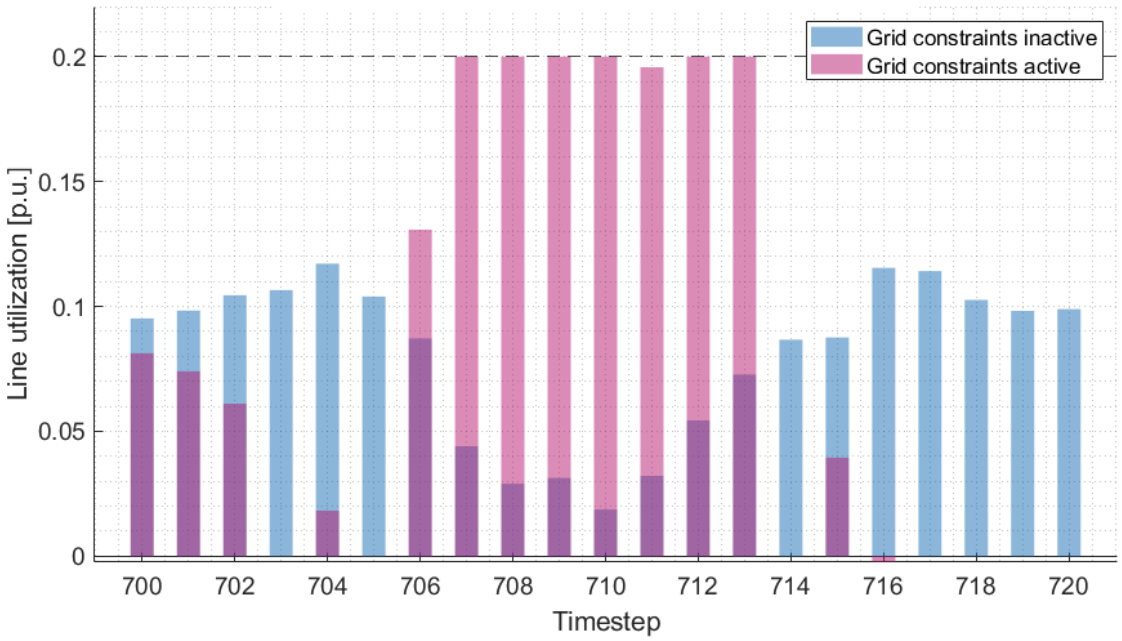

Figure 4-24: Building 4 connection line utilization between time steps 700-720.

Therefore, it can be deduced that the power limit from the battery is in fact a consequence of the power limit of the power line reaching the house. This is an important point to justify the location and sizing of the BSS in the whole system, which will be covered in section 5.

As can be seen in Figure 4-25, the grid electricity being fed into buildings 3 and 4 is composed of both external (non-local) and local generation: The stacked bars on the left representing excess PV generation and the stacked bars on the right representing the BSS charging power. It can be seen that at any of the BSS charging steps the system is still drawing power from the feeder to supply the BSS charging schedule. This explains the inversion of feeder line flow seen in Figure 4-20.

This BSS charging phase lasting from time step 706 to 713 is followed by a discharging phase at the moments of peak demand, between time steps 715 and 730 (Figure 4-20). During this discharging phase another unintuitive behavior is observed. While the BSS operation reaches its objective of limiting the overall power drawn from the feeder, the power flows between the buildings change substantially from the situation without grid constraints.

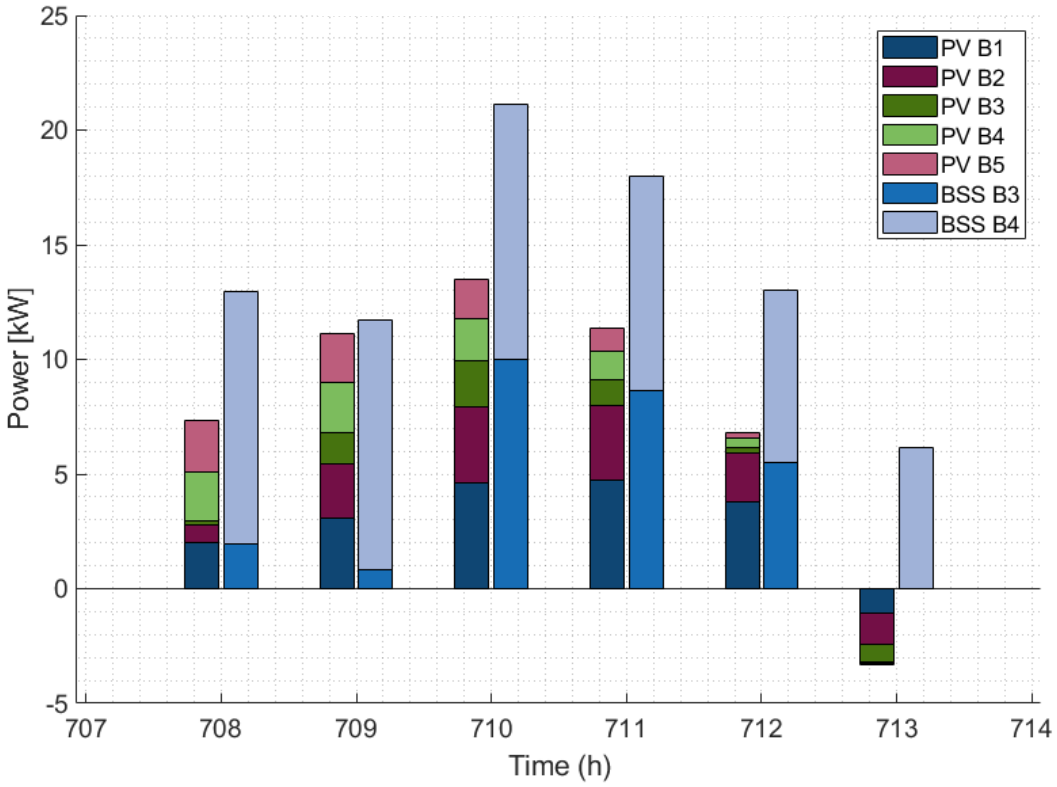

Figure 4-25: Comparison of system wide excess local PV generation with BSS charging power

At time steps 715-730, the power drawn from the grid at each building is displayed in Figure 4-26. The behavior of the buildings is seen to change in a very unequal way. The buildings with installed BSS operate the in such a way that their demand is neutralized (Building 3) or lowered (Building 4). Buildings 2 and 5 are able, because of the alleviated grid conditions, to operate freely, even increasing their consumption. This increase is due to a switch to cheaper, less efficient heating technologies (in this case a switch from Ground-Air heat pumps to Air-Air heat pumps). The increase in operational costs is (likely) to be offset by the decrease in CAPEX combined with the higher generation of PV enabled by larger PV installations (Table 18).

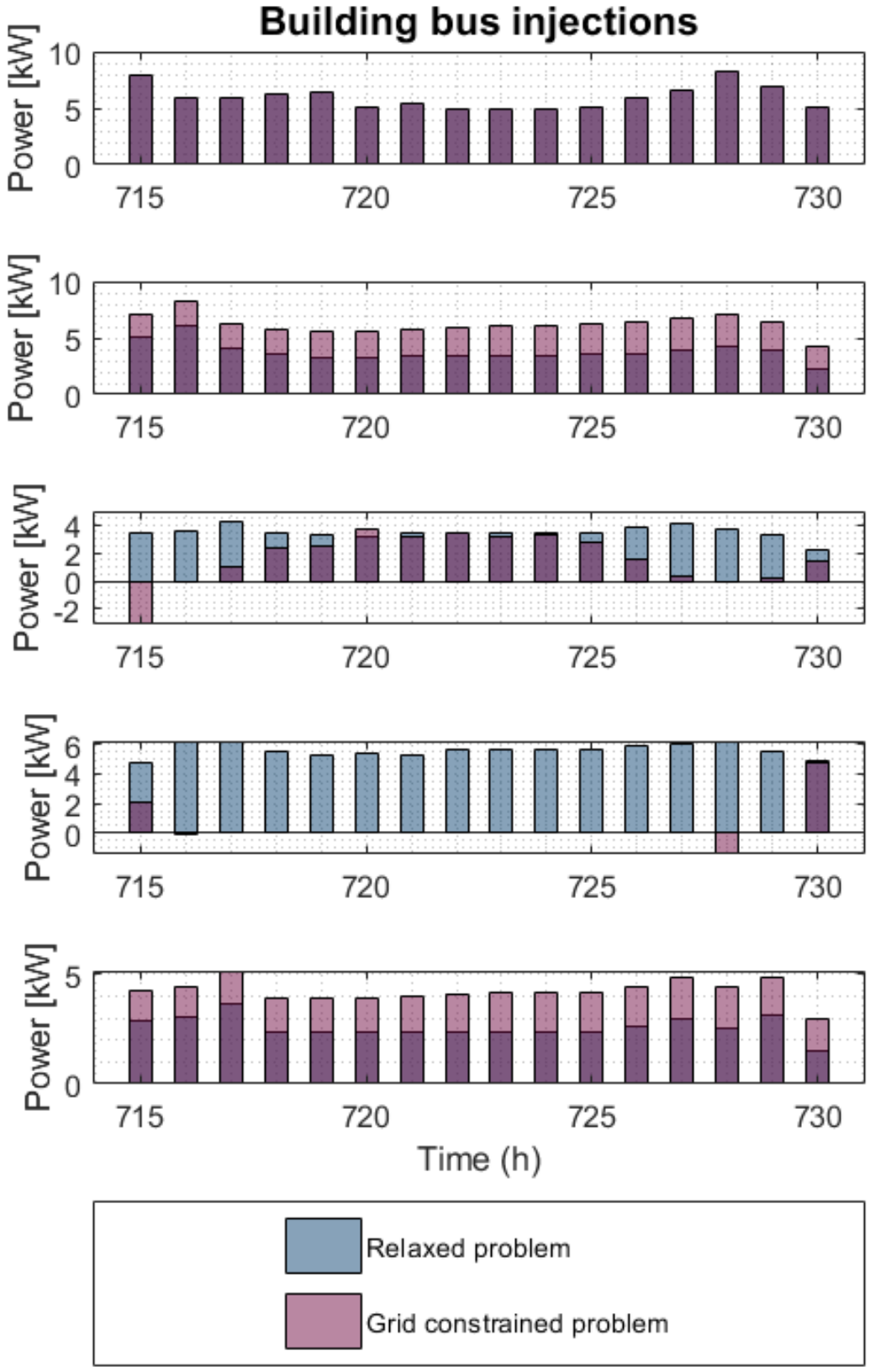
Building bus injections
Power [kW]
10
5
0
715
720
725
730
Power [kW]
10
5
0
715
720
725
730
Power [kW]
4
2
0
-2
715
720
725
730
Power [kW]
6
4
2
0
715
720
725
730
Power [kW]
5
0
715
720
725
730
Time (h)
Relaxed problem
Grid constrained problem

Figure 4-26: Grid injections at Buildings 1-5, CF20%, time steps 715-730.

Table 18: PV installation in combination with BSS

Building	No BSS [kWp]	BSS [kWp]	Variation [kWp]	Variation [%]
Building 1	10.758	10.758	0	0
Building 2	6.742	8.613	+1.871	+27.75%
Building 3	4.186	8.613	+4.427	+105.75%
Building 4	4.105	8.491	+4.385	+106.82%
Building 5	5.681	5.681	0	0

The increase in PV installation is considerable in the case of Building 3 and Building 4. Building 1 installs the maximum possible power based on the available roof surface. This is also the case for buildings 2 and 3, hence the same value for installed power.

The effect this increase in available PV generation is invisible from the point of view of the grid, as can be seen in Figure 4-21. The BSS are absorbing all the power that cannot be transmitted by the feeder line, as seen in Figure 4-27.

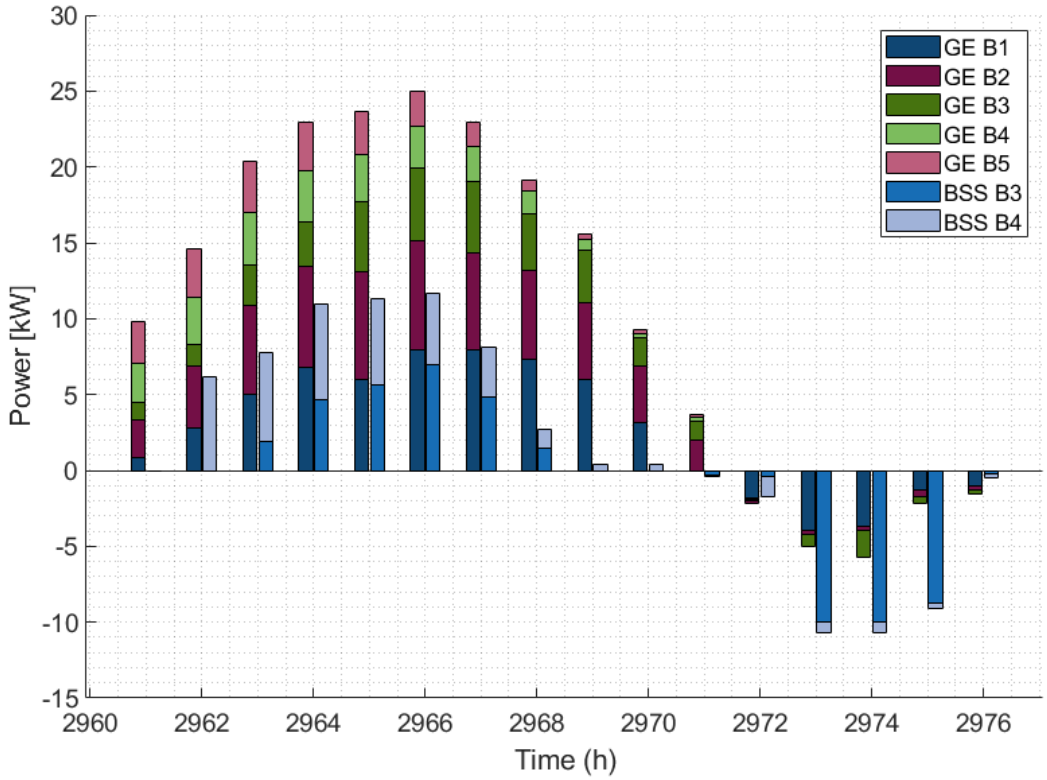

Figure 4-27: System wide grid injections and BSS power flows in critical summer days

The BSS are seen to dampen the injections of power into the grid, thus avoiding the overloading of the feeder line.

The overall installation and operation of the BSS in the test case points at the economies of scale present in this type of technology: effectively, the BSS in Building 4 is behaving as a quasi-central storage system for the neighborhood, and the BSS in Building 3 complements the operation: were it not for the limitation on the Building 3 grid connection, it seems all the BSS capacity and power needed would be lumped together at the same spot.

This is however an unrealistic solution: a BSS of the size suggested by the solution would be unreasonable in a single house. Furthermore, it should not be expected that one building shoulder the cost of providing flexibility for the whole neighborhood.

Because of the quasi-centralized operation it is very difficult to clarify whether the individual buildings are increasing their self-consumption, and when the operation decisions are a consequence of the limited grid constraints. For this reason a discussion on the applicability of this model is presented in section 5.

5 Summary and Outlook

5.1 Summary

The goal of this thesis was to analyze the roles BSSs can fulfill in a distributed energy system. To carry out this analysis, an existing MILP energy optimization tool for buildings was expanded with a model of the technology, as well as with a model of the electric grid lines connecting the buildings in the system. This allowed for testing of two initial hypotheses: the increase in self-consumed energy at the consumer end, and the potential use of BSS to alleviate line congestion problems at the low voltage distribution grid level.

The result regarding each hypothesis can be summed up as follows. For the self-consumption hypothesis, BSS adoption lead to larger optimal installations of PV generation, which in combination yield to a reduction in the consumers' dependence on grid-fed energy, thus increasing self-sufficiency. However by the same token, the consumers are able to sell off more of their PV generation to the grid. These results are bound by the costs of BSS: At current price levels, consumers will not find the adoption cost-efficient. With a considerable decrease in costs, as is expected in coming years, the situation of household BSSs may become commonplace.

When the two hypothesis are tested simultaneously, it is shown that BSS can be used effectively to manage line congestions at the distribution grid level. However the results also show that due to the economies of scale observed in BSS systems, when they are operated for line congestion alleviation, the optimal design is a centralized storage, rather than various distributed storages. Therefore a neighborhood-scale BSS can be a possible alternative to grid reinforcement, which can additionally serve to increase the self-consumption of the consumers in the quarter.

This ties back to the original motivation for this work, the integrated energy transition. To achieve the goals of increased efficiency in energy use, and increased sourcing of energy from renewable energy sources, centralized BSSs (or quarter-BSS) may be a useful tool for grid planning and operation.

5.2 Outlook

From the conclusion presented in the previous section, several further works may be of interest in continuing this line of research. The suggested aspects to study regard both the modelling and the implementation.

Upon analysis of the optimal solutions found, it is shown that the carrying capacity of the grid influences the allocation of DERs to the different buildings in the grid. The distribution of costs prescribed by the optimal solution is, however, not equitable for the involved customers. This is caused by differences in customer characteristics and behavior, which result in different marginal costs for improvement of the overall system cost. Whenever the network reaches operational limits, the optimal solution is reached by acting on the lowest marginal cost buildings first. This is of course not free of discrimination, so it is not to be implemented directly. In this regard, an analysis and comparison of centralized versus agent-based optimization may be warranted. A decentralized, agent based optimization model could be capable of considering the interests of each consumer individually, potentially yielding a more fair distribution of costs.

Another possible broadening of the model is to operate over stochastic, rather than deterministic input time series. This would involve a degree of uncertainty, in the face of which the flexibility provided by BSSs may prove valuable. A value of flexibility could then be established by comparing the solutions obtained from deterministic and stochastic models.

From the point of view of the implementation, an obstacle faced developing this work was the considerable increase in computation time and memory usage caused by the inclusion of BSS and grid models. Additional techniques, such as time series clustering, could be developed in order to reduce the temporal complexity of the operational planning. . This could improve both run time and memory use for the overall optimization.

References

[ABD18] Abdulla, K. et al.: Optimal Operation of Energy Storage Systems Considering Forecasts and Battery Degradation. In IEEE Transactions on Smart Grid, 2018, 9; S. 2086–2096.

[AND17] Andrey Bernstein and Emiliano Dall'Anese: NREL: Linear Power-Flow Models in Multiphase Distribution Networks: 7th IEEE International Conference on Innovative Smart Grid Technologies (ISGT Europe 2017), 2017.

[BAY12] Bayliss, C. R.; Hardy, B. J.: Transmission and Distribution Electrical Engineering. Elsevier, 2012.

[BEN62] Benders, J. F.: Partitioning procedures for solving mixed-variables programming problems. In Numerische Mathematik, 1962, 4; S. 238–252.

[BÖH09] Böhringer, C. et al.: EU climate policy up to 2020: An economic impact assessment. In Energy Economics, 2009, 31; S295-S305.

[BRA09] Braun, M. et al.: Photovoltaic self-consumption in Germany using lithium-ion storage to increase self-consumed photovoltaic energy. In (Sinke, W. Hrsg.): The compiled State-of-the-Art of PV Solar Technology and Deployment. 24th European Photovoltaic Solar Energy Conference Proceedings of the International Conference held in Hamburg, 21-25 September 2009, Munich, 2009.

[BRA15] Brahman, F.; Honarmand, M.; Jadid, S.: Optimal electrical and thermal energy management of a residential energy hub, integrating demand response and energy storage system. In Energy and Buildings, 2015, 90; S. 65–75.

[BRA77] Bradley, S. P.; Hax, A. C.; Magnanti, T. L.: Applied Mathematical Programming. Addison-Wesley Publishing Company, Reading, MA, 1977.

[BUN17]: Gesetzzur Einführung von Ausschreibungenfür Strom aus erneuerbaren Energien und zuweiteren Änderungen des Rechts der erneuerbaren Energien. EEG: Bundesgesetzblatt, 2017; S. 2258–2357.

[CUC16] Cucchiella, F.; D'Adamo, I.; Gastaldi, M.: Photovoltaic energy systems with battery storage for residential areas: an economic analysis. In Journal of Cleaner Production, 2016, 131; S. 460–474.

[DAL13] Dall'Anese, E.; Zhu, H.; Giannakis, G. B.: Distributed Optimal Power Flow for Smart Microgrids. In IEEE Transactions on Smart Grid, 2013, 4; S. 1464–1475.

[DAV15] Davidson, C.; Steinberg, D.; Margolis, R.: Exploring the market for third-party-owned residential photovoltaic systems: insights from lease and power-purchase agreement contract structures and costs in California. In Environmental Research Letters, 2015, 10; S. 24006.

[DEU18] Deutsche Energie-Agentur: Energy efficiency in the building stock-statistics and analyses, 2018.

[DI 16] Di Somma, M. et al.: Multi-objective operation optimization of a Distributed Energy System for a large-scale utility customer. In Applied Thermal Engineering, 2016, 101; S. 752–761.

[DIN05]:2005, DIN VDE 0276-603 Starkstromkabel – Teil 603: Energieverteilungskabel mit Nennspannungen U0/U 0,6/1 kV.

[DUG15] Duggal, I.; Venkatesh, B.: Short-Term Scheduling of Thermal Generators and Battery Storage With Depth of Discharge-Based Cost Model. In IEEE Transactions on Power Systems, 2015, 30; S. 2110–2118.

[END74] ENDO, T.: Damage Evaluation of Metals for Random or Varying Loading. In Proceedings of the 1974 Symposium on Mechanical Behavior of Materials, 1974, 1; S. 371–380.

[EUR04]:2004, Standard EN 50160.

[FAL16] Falke, T. et al.: Multi-objective optimization and simulation model for the design of distributed energy systems. In Applied Energy, 2016, 184; S. 1508–1516.

[FRA12] Frank, S.; Steponavice, I.; Rebennack, S.: Optimal power flow: a bibliographic survey I. In Energy Systems, 2012, 3; S. 221–258.

[FRA18] Franco, J. F.; Ochoa, L. F.; Romero, R.: AC OPF for Smart Distribution Networks: An Efficient and Robust Quadratic Approach. In IEEE Transactions on Smart Grid, 2018, 9; S. 4613–4623.

[GAB12] Gabash, A.; Li, P.: Active-Reactive Optimal Power Flow in Distribution Networks With Embedded Generation and Battery Storage. In IEEE Transactions on Power Systems, 2012, 27; S. 2026–2035.

[GAB13] Gabash, A.; Li, P.: Flexible Optimal Operation of Battery Storage Systems for Energy Supply Networks. In IEEE Transactions on Power Systems, 2013, 28; S. 2788–2797.

[GEI07] Geidl, M. et al.: Energy Hubs for the Future. In IEEE Power & Energy Magazine, 2007.

[GJE05] Gjengedal, T.: Large-scale wind power farms as power plants. In Wind Energy, 2005, 8; S. 361–373.

[GOL19] Goldie-Scot, L.: A Behind the Scenes Take on Lithium-ion Battery Prices. https://about.bnef.com/blog/behind-scenes-take-lithium-ion-battery-prices/.

[HAI13] Haikarainen, C.; Pettersson, F.; Saxén, H.: An MILP Model for Distributed Energy System Optimization. In Chemical Engineering Transactions, 2013, 35.

[HAR11] Harder, E.; Gibson, J. M.: The costs and benefits of large-scale solar photovoltaic power production in Abu Dhabi, United Arab Emirates. In Renewable Energy, 2011, 36; S. 789–796.

[IDA11] IDAE: Plan de Energías Renovables 2011-2020, Madrid, 2011.

[INT17] International Renewable Energy Agency (IRENA): Electricity storage and renewables: Costs and markets to 2030, 2017.

[KAI17] Kairies, K.-P. et al.: Analysis of Funded PV Battery Systems in Germany: Prices, Design Choices and Purchase Motivation, 2017.

[LI11] Li, X.; Tomasgard, A.; Barton, P. I.: Nonconvex Generalized Benders Decomposition for Stochastic Separable Mixed-Integer Nonlinear Programs. In Journal of Optimization Theory and Applications, 2011, 151; S. 425–454.

[LI16] Li, L. et al.: Economic and environmental optimization for distributed energy resource systems coupled with district energy networks. In Energy, 2016, 109; S. 947–960.

[LIU16] Liu, G. et al.: A MILP-based distribution optimal power flow model for microgrid operation: 2016 IEEE Power and Energy Society General Meeting (PESGM). IEEE, 2016 - 2016; S. 1–5.

[LIU19] Liu, K. et al.: Linear Power Flow Calculation of Distribution Networks With Distributed Generation. In IEEE Access, 2019, 7; S. 44686–44695.

[MAH18] Maheshwari, A.: Modelling, Aging and Optimal Operation of Lithium-ion Batteries. Ph.D, Delft/Turin, 2018.

[MAR17] Mariaud, A. et al.: Integrated optimisation of photovoltaic and battery storage systems for UK commercial buildings. In Applied Energy, 2017, 199; S. 466–478.

[MEH12] Mehleri, E. D. et al.: A mathematical programming approach for optimal design of distributed energy systems at the neighbourhood level. In Energy, 2012, 44; S. 96–104.

[MEH13] Mehleri, E. D. et al.: Optimal design and operation of distributed energy systems: Application to Greek residential sector. In Renewable Energy, 2013, 51; S. 331–342.

[MIL10] Millner, A.: Modeling Lithium Ion battery degradation in electric vehicles: 2010 IEEE Conference on Innovative Technologies for an Efficient and Reliable Electricity Supply. IEEE, 2010 - 2010; S. 349–356.

[MOG16] Moghaddam, I. G.; Saniei, M.; Mashhour, E.: A comprehensive model for self-scheduling an energy hub to supply cooling, heating and electrical demands of a building. In Energy, 2016, 94; S. 157–170.

[MOR06] Moreira, F. S.; Ohishi, T.; da Silva Filho, J. I.: Influence of the thermal limits of transmission lines in the economic dispatch: 2006 IEEE Power Engineering Society General Meeting. IEEE, 2006; 6 pp.

[MOR16] Morvaj, B.; Evins, R.; Carmeliet, J.: Optimization framework for distributed energy systems with integrated electrical grid constraints. In Applied Energy, 2016, 171; S. 296–313.

[MUE15] Muenzel, V. et al.: A Multi-Factor Battery Cycle Life Prediction Methodology for Optimal Battery Management. In (Kalyanaraman, S. et al. Hrsg.): Proceedings of the 2015 ACM Sixth International Conference on Future Energy Systems - e-Energy '15. ACM Press, New York, New York, USA, 2015; S. 57–66.

[MUS12] Musallam, M.; Johnson, C. M.: An Efficient Implementation of the Rainflow Counting Algorithm for Life Consumption Estimation. In IEEE Transactions on Reliability, 2012, 61; S. 978–986.

[OMU13] Omu, A.; Choudhary, R.; Boies, A.: Distributed energy resource system optimisation using mixed integer linear programming. In Energy Policy, 2013, 61; S. 249–266.

[SCH18] Schopfer, S.; Tiefenbeck, V.; Staake, T.: Economic assessment of photovoltaic battery systems based on household load profiles. In Applied Energy, 2018, 223; S. 229–248.

[SED16] Sedghi, M.; Ahmadian, A.; Aliakbar-Golkar, M.: Optimal Storage Planning in Active Distribution Network Considering Uncertainty of Wind Power Distributed Generation. In IEEE Transactions on Power Systems, 2016, 31; S. 304–316.

[SHA17] Shao, C. et al.: An MILP-Based Optimal Power Flow in Multicarrier Energy Systems. In IEEE Transactions on Sustainable Energy, 2017, 8; S. 239–248.

[SHI17] Shi, Y. et al.: Optimal Battery Control Under Cycle Aging Mechanisms in Pay for Performance Settings, 2017.

[STA14] Stadler, M. et al.: Optimizing Distributed Energy Resources and Building Retrofits with the Strategic DER-CAModel. In Applied Energy, 2014, 132; S. 557–567.

[SUN18] Sun, S. I. et al.: Self-sufficiency ratio: an insufficient metric for domestic PV-battery systems? In Energy Procedia, 2018, 151; S. 150–157.

[THU18] Thurner, L. et al.: pandapower - an Open Source Python Tool for Convenient Modeling, Analysis and Optimization of Electric Power Systems. In IEEE Transactions on Power Systems, 2018, 33; S. 6510–6521.

[VAN69] van Slyke, R. M.; Wets, R.: L-Shaped Linear Programs with Applications to Optimal Control and Stochastic Programming. In SIAM Journal on Applied Mathematics, 1969, 17; S. 638–663.

[WAN16] WANG, Y. et al.: Stochastic coordinated operation of wind and battery energy storage system considering battery degradation. In Journal of Modern Power Systems and Clean Energy, 2016, 4; S. 581–592.

[WIR19] Wirth, Harry | Fraunhofer ISE: Recent Facts about Photovoltaics in Germany, 2019.

[XU18a] Xu, B. et al.: Modeling of Lithium-Ion Battery Degradation for Cell Life Assessment. In IEEE Transactions on Smart Grid, 2018, 9; S. 1131–1140.

[XU18b] Xu, B. et al.: Factoring the Cycle Aging Cost of Batteries Participating in Electricity Markets. In IEEE Transactions on Power Systems, 2018, 33; S. 2248–2259.

[YUA18] Yuan, H. et al.: Novel Linearized Power Flow and Linearized OPF Models for Active Distribution Networks With Application in Distribution LMP. In IEEE Transactions on Smart Grid, 2018, 9; S. 438–448.

[ZHA15] Zhang, X. et al.: Optimal Expansion Planning of Energy Hub With Multiple Energy Infrastructures. In IEEE Transactions on Smart Grid, 2015, 6; S. 2302–2311.

List of abbreviations

AC	Alternate Current
Ah	Ampere-hour
BD	Benders' Decomposition
BSS	Battery Storage System
CAPEX	Capital Expenditure
CF	Congestion Factor
CHP	Combined Heat and Power
DC	Direct Current
DCPF	DC Power Flow
DER	Distributed Energy Resource
DG	Distributed Generation
DOD	Depth of Discharge
DSO	Distribution System Operator
DSP	Dual Sub-problem
EEG	Erneuerbare Energien Gesetz (German Law for Electricity from Renewable Energy Sources
EST	Energy Storage Technology
IFHT	Institute for High Voltage Technology
kW	Kilowatt
kWh	Kilowatt hour
kWp	Kilowatt peak
LB	Lower Bound
LP	Linear Programming
MILP	Mixed Integer Linear Programming
MP	Master Problem

MV	Medium Voltage
LP	Linear Programming
LV	Low Voltage
OF	Objective Function
OPEX	Operational Expenditure
OPF	Optimal Power Flow
P2G	Power-to-Gas
PV	Photovoltaic
RWTH	Rheinisch-Westfälische Technische Hochschule
SOC	State of Charge
SP	Sub-problem
UB	Upper Bound
VDEW	Verband der Elektrizitätswirtschaft

Annex I: Sustainable Development Goals

Introduction

This document is an annex to the Master Thesis by Gonzalo Falagan, titled “Analysis on the role of battery storage solutions in the optimal design of decentralized energy systems”. The annex provides a contextualization of the project within the overarching goals known as “*Sustainable Development Goals*” (SDG) set by the United Nations to be achieved by 2030.

The SDG are a framework for the social, economic and political development of humanity intended to promote equality and improved living conditions for every person regardless of their circumstances, and to guarantee these conditions for future generations. Within this framework the topic of energy supply takes a prime spot, as it connects exploitation of natural resources with direct improvement of living conditions and economic growth.

This annex develops the link between the project and selected SDG targets within the three main classes (social – economic – environmental). First the targets that more closely align with the goals of the thesis are identified; then, an attempt at quantifying the contribution of this work to the goals is identified.

Identified Goals

Economic aspect:

SDG 7: *“Ensure access to affordable, reliable, sustainable and modern energy for all”*

Target	Indicator
7.2. Increase substantially the share of renewable energy in the global energy mix	*7.2.1. Renewable energy share in the total final energy consumption*
7.3. Double the global rate of improvement in energy efficiency	*7.3.1. Energy intensity measured in terms of primary energy and GDP*

The alignment of SDG 7 with the goals of the thesis is self-evident: a tool devised to optimize energy efficiency and cost/emissions addresses targets 7.2 and 7.3 directly.

Social aspect:

SDG 12: *"Ensure sustainable consumption and production patterns"*

Target	Indicator
12.2. By 2030, achieve the sustainable management and efficient use of natural resources.	*12.2.1. Material footprint, material footprint per capita, and material footprint per GDP*

Economic optimization is an indirect way of optimizing resource allocation, as long as the pricing mechanism in place reflects the true cost of production (all externalities considered). For example, the choice to renovate a building versus installing a new boiler is a choice between the consumption of resources both in the present and in the future. The ability to assign not only economic but also emissions costs allows an efficient allocation of said resources.

Environmental aspect:

SDG 13: *"Take urgent action to combat climate change and its impacts"*

While the thesis does not directly and explicitly align with any of the explicit goals under SDG 13, it is clear that any effort aimed at increased renewable usage and to reduce greenhouse gas emissions

Methodology

The analysis on the contribution of this project to the SDGs can be performed from two perspectives. On the one hand, there is the impact of the *conclusions* of the project: this relates to the theoretical knowledge abstracted from the analyses carried out in the project. On the other hand, there is the impact of the analysis tool, the development of which this project belongs to. An approach to analysing both is presented in this section.

Theoretical conclusions:

Two main theoretical conclusions are drawn: battery storage systems improve self-consumption, and they allow for congestion management within distribution grids. These two effects serve as enablers of higher renewable generation on a localized level, additionally reducing transportation and consumption losses. The increase of renewable energy

generated by each building can be quantified in the analysis of sensitivity to battery cost: a correlation is observed between PV power installed and generated and the size of the battery involved. However, the optimality of a battery is not guaranteed for every building; this depends largely on the electricity consumption patterns, available space for generators, orientation, etc. Therefore extrapolating the increase in renewable generation is not as straightforward as scaling up the improvements observed in a few buildings to the pool of similar buildings in Germany. Rather, a more exhaustive analysis of hundreds of buildings should be conducted to establish statistically significant average values with which to extrapolate the bigger picture.

Another question that arises is the true cost of elements considered in the optimization: a very clear example is lithium, of which the mining process is notoriously polluting, which is required for lithium-ion batteries. The quantification of the environmental impact of such activity is, in the author's view, intractable due to the potentially infinite ramifications that need to be considered.

Overall, the conclusion is that the installation of home battery systems may improve the goals of energy efficiency and renewable generation locally, but it may just as well worsen other goals in other locations.

Optimization tool:

With regards to the implementation of an optimization tool, the impact of the tool would be limited by the application of the recommended measures. In this manner, one could estimate the impact as an enabler of the positive effects described in the previous point, with the advantage of possibly sparing time and resources dedicated to the case-by-case design required otherwise. Consequently, the cost-benefit analysis is plagued by the same problems of practical implementation described in the previous point.

Conclusion

The study carried out in the thesis aligns directly with the goals of improving energy efficiency and the fraction of energy generated from renewable sources. Indirectly it also affects more sustainable demand patterns and provides pathways to decarbonisation of part of the electrical sector.

In the view of the author however, the quantification of the impact through a cost-benefit analysis (CBA) has serious limitations in its implementation. Moreover, performing a conceptual meta-analysis of the CBA approach itself, the author finds that the negative impact a poorly performed CBA could have could potentially outweigh the benefit of the conclusions reached in the project. The author has seen countless instances of incorrect conclusions, reached through deficient research methodologies, being used as justification for questionable policies. Therefore the author recommends to abstain of such analysis unless the means and will to perform them thoroughly and rigorously are available.